PROBING GPCR ACTIVATION: FUNCTIONAL ANALYSIS OF THE N-TERMINUS AND EXTRACELLULAR LOOPS OF THE APELIN RECEPTOR

by

Nigel Antony Ian Chapman

Submitted in partial fulfilment of the requirements
for the degree of Master of Science

at

Dalhousie University
Halifax, Nova Scotia
August 2014

Dedication

For my parents, Jennifer and Anthony
my teachers, past and present,
and all who have encouraged and guided me along the way

Table of Contents

List of Tables

List of Figures

Abstract

The apelin receptor (AR or APJ) is a class A (rhodopsin-like) G-protein coupled receptor (GPCR) with wide distribution throughout the human body. Activation of AR by its cognate peptidic ligand, apelin, induces diverse physiological effects including vasoconstriction and dilation; strengthening of heart muscle contractility; angiogenesis; and, regulation of energy metabolism and fluid homeostasis. Recently, another endogenous peptidic activator of the AR, Toddler/ELABELA, was identified as having a crucial role in zebrafish embryonic development. The AR is also implicated in several pathologies, including cardiovascular disease, diabetes, obesity and cancer, making it a promising therapeutic target. Despite its established importance, the precise roles of AR signalling remain poorly understood. Moreover, little is known about the mechanism by which peptides activate the AR. Additional complexity arises because the AR is modulated by two endogenous peptide ligands, both of which appear to have multiple bioactive isoforms of varying length. This is compounded by the fact that the various apelin and Toddler/ELABELA isoforms are differently distributed and produce distinct cellular effects. This work aims to identify functionally critical amino acid residues on the extracellular face of the AR, as this region may contribute to the specificity and affinity of apelin binding, and to larger conformational changes preceding AR activation and internalization.

Alanine-substitution mutants of negatively charged and aromatic residues in the N-terminus and extracellular loops 1 and 2 of the AR were prepared. Apelin-13-induced activation of the wild-type (WT) AR and mutants was then evaluated in HEK293A cells using western blotting to measure extracellular-signal-regulated kinase (ERK) activation. These studies revealed several mutations of interest. In particular two N-terminal mutants, E20A and D23A, previously shown to have reduced apelin-binding affinity and internalization, exhibit maximal apelin-induced ERK activation comparable to the WT AR. This suggests that the binding affinity and ability of apelin to activate downstream signalling *via* the AR are two separate parameters. Lastly, one element of this work was the production and purification of recombinant apelin-36, to be used in future structural and functional studies of AR ligand-binding and activation.

List of Abbreviations Used

3xHA-AR: N-terminally triple haemagglutinin-tagged apelin receptor

AC: Adenylyl cyclase

AR: The apelin receptor

AT_1R: Angiotensin II receptor type 1

β_2AR: β_2 adrenergic receptor

BRET: Bioluminescence resonance energy transfer

BSA: Bovine serum albumin

CD: Circular dichroism

CHO: Chinese hamster ovary

CNS: Central nervous system

DMEM: Dulbecco's modified eagle's medium

DTT: Dithriothreitol

EC: Extracellular

EC_{50}: Half-maximal effective concentration

EGFP: Enhanced green fluorescent protein

EL: Extracellular loop

ELISA: Enzyme-linked immunosorbent assay

E_{max}: Maximal effect

ERK: Extracellular signal-regulated kinase

ESI+: Positive-mode electrospray ionization

FBS: Fetal bovine serum

FRET: Förster resonance energy transfer

G-protein: Guanosine nucleotide-binding protein

GAP: GTPase activating protein

GDP: Guanosine diphosphate

GRK: GPCR kinase

GTP: Guanosine triphosphate

HEK293A: Human embryonic kidney cell line, strain 293A

HIV-1: Human immunodeficiency virus-1

HUVEC: Human umbilical vein endothelial cell

IC: Intracellular

IL: Intracellular loop

IPTG: Isopropyl β-D-1-thiogalactopyranoside

JNK: c-Jun N-terminal kinase

K_d: Dissociation constant (binding affinity)

KO: Knockout

LDR: Linear dynamic range

NOS: Nitric oxide synthase

NS: Non-stimulated

OD_{600nm}: 600_{nm} optical density

P.O.I.: Protein of interest

PCR: Polymerase chain reaction

PCSK3: Proprotein convertase subtilisin kexin 3

PEI: Polyethylenimine

PKC: Protein kinase C

PLC-β: Phospholipase C-β

PM: Plasma membrane

pyr-apelin-13: Pyroglutamate-modified apelin-13

RET: Resonance energy transfer

RhoGEF: Rho guanosine nucleotide exchange factor

RIPA: Radioimmunoprecipitation assay

Rluc: *Renilla* luciferase

RP-HPLC: Reverse-phased high performance liquid chromatography

RVLM: Rostral ventrolateral medulla

SDS-PAGE: Sodium dodecyl sulphate-polyacrylamide gel electrophoresis

SUMO: Small ubiquitin-like modifier

TBS: Tris-buffered saline

TFA: Trifluoroacetic acid

TM: Transmembrane

UCP: Uncoupling protein

VP: Vasopressin

$V_{1A}R$: Vasopressin receptor type 1A

WT: Wild-type

Acknowledgments

Writing this thesis has given me some time to reflect on how many people I have to thank for my time here at Dalhousie. I have to thank you, because being here has transformed the way I think; it has helped to give me a sense of purpose and to see the depth and meaning in things that sometimes seem routine and mundane. I have learned, and am still learning, an abiding sense of patience, which, I slowly realize, is required not just for scientific practice, but in all aspects of my life. Here, I have found some confidence to work and live in my own way, study and use my education (a gift I cannot claim to have always fully appreciated or understood), and been given responsibility and independence. I have been working in a community of patient, sincere, self-disciplined, and idealistic people who have made me feel welcome from the very start, despite all the shades of hesitation, discouragement, stubbornness, and self-doubt that pursue the young and inexperienced grad student.

First and foremost I would like to thank my supervisor Dr. Jan Rainey. In inviting me to join his lab in 2011, and supporting me as a grad student since then, Jan gave me an opportunity that changed my life dramatically and that I could not thank him enough for. He has been supportive and encouraging from the very start, and taught me as much by his approach and attitude to his work as by his ideas and explanations about the scientific work itself. Especially when a kind of work is new, it can be difficult for me to see past the obstacles to the quality of what I am doing. In this respect, Jan has helped me a great deal, giving me space to figure things out on my own, but always encouraging me to see the merits of my work.

I would also like to thank my co-supervisor Dr. Denis Dupré, who has supervised the largest part of my experiments, and under whose guidance I have learned much of what I know about good experimental technique and the study of biochemistry and pharmacology in cell culture. Denis has also been a very inspiring presence in my time here at Dalhousie, and he too has been supportive and patient, doing bench-work alongside his students, and encouraging me to recognize my successes and pursue key experiments. Like Jan, he has seen me grow a lot as a scientist in the time since I arrived here, and I have him to thank, in large measure, for this growth.

During my time as a graduate student I have been struck again and again by the support and friendship of so many people working together "under the same roof" of the Tupper building, both within and beyond the Rainey and Dupré labs. In Jan's lab I have to thank so many members, both past and present, for guiding me, assisting me in my work, and making me feel welcome: Aaron Banks, Johnny Farah, Ryan Holstead, Kate Huang, Sam Kerzner, David Langelaan, Danielle LeBlanc, Ben Morash, Pascaline Ngweniform, Kathleen Orrell, Aditya Pandey, Robin Patterson, Tyler Reddy, Lesley Seto, Kyungsoo Shin, Muzaddid Sarker, Ellie Scott, Sara Sparavalo, Matthew Speckert, Bruce Stewart, Marie-Laurence Tremblay, Emily Truong, Nathan Weatherbee-Martin, and Lingling Xu. In Denis' lab I have to thank you for the same: Patrick Holland, Kelsie Gillies, Jaime Wertman, and Brent Young. In particular I want to thank David for the first training I received here; you welcomed me and helped me get prepared me for a lot of what was to come. I want to thank Adi and Kyung for their constant advice, support and encouragement. Working with you two has been a pleasure

and a great blessing. Marie and Robin, the same goes for you. Jaime, Brent, and Kelsie, you all really brightened my days and taught me a lot. Emily thank you for the help you gave me with my last experiments, which was so necessary. Bruce thank you for all the help you give us with our experiments and reagents, and for all the conversations we have had, about science, music, and life in general. It has been the best working with all of you and there's no way I could have done it without you, either experimentally or just mentally.

I also want to thank Dr. Neale Ridgway and Dr. Paul Linsdell, who were supportive and thoughtful guides in my committee meetings. Dr. Dobson, Mary and Joyce from the Dobson lab, our nearest neighbours, have given me and all of us in 10H a lot of advice and encouragement, as well as training and gracious sharing of equipment, along the way. I also want to thank Paul Briggs and Heidi MacKinnon for organizing the teaching labs, as well as Dr. Dobson and Dr. Singer and everyone who coordinates the experiential learning and honours programs, because this teaching experience has been a great gift for me as a graduate student.

And I want to thank my parents Jennifer and Anthony, who have given me so much and been so patient, even-tempered, wise, and supportive. The more I grow up, the more I realize this. Even if there were no other reason, I would know because of this that I have to work hard and do the best I can.

Thank you everyone!

Chapter 1: Introduction

Note: Portions of this chapter have been submitted for publication in the journal *Biochemistry and Cell Biology,* comprising a mini-review entitled "The apelin receptor: Physiology, pathology, cell signalling, and ligand modulation of a peptide-activated class A GPCR." (Submitted May 28th, 2014; accepted pending minor revisions July 29th, 2014)

The focus of my thesis project has been the apelin receptor (AR), and in particular its interaction with the peptide ligand, apelin. This chapter contains a general introduction of the G-protein coupled receptor (GPCR) superfamily to which the AR belongs; introduces the AR, reviewing the role of this GPCR in the physiology of health and disease; and states the goals of my research project. Chapter 2 presents my work to recombinantly express and purify the peptide ligand apelin-36 using *E. coli*. Chapter 3 focuses on my studies of AR activation, performed to identify functionally critical residues on the extracellular face of the receptor. In chapter 4, I conclude the thesis with a broad discussion of my findings, as well as future goals for the project.

1.1 G-Protein Coupled Receptors

1.1.1 Physiological Importance

G-protein coupled receptors (GPCRs) are a superfamily of membrane proteins predominantly present in the eukaryotic cell [1]. They are a highly diverse family, comprising, for example, more than 800 unique members in the human body [2; 3; 4], but share the same cardinal function – namely, transduction of an extracellular signal (the ligand) into an intracellular one, which is then propagated

further by intracellular signalling partners, and ultimately manifests in diverse and highly tunable physiological effects.

GPCRs classically transduce signals at the plasma membrane (PM), where they respond to a wide range of ligands, ranging from small molecules to peptides to proteins, from olfactory stimuli to photons of light [5]. The GPCR superfamily is subdivided into five families, named with reference to their hallmark receptor (rhodopsin-, secretin-, glutamate-, adhesion-, frizzled-like), of which the rhodopsin-like, or class A, GPCR family is by far the largest [4; 6]. Conserved among all GPCRs is their basic topology, comprising an extracellular N-terminal domain, an intracellular C-terminal domain, and seven α-helical transmembrane (TM) domains connected by six loops, three intracellular and three extracellular (ILs 1-3 and ELs 1-3, respectively) (Figure 1.1). In spite of this, individual GPCRs exhibit a high degree of ligand specificity and signalling diversity, which is all the more remarkable given the many fundamental structural features they all share. They are thus an example of nature using subtle variations on a complex theme to produce a vast array of useful, and sometimes detrimental, effects. Indeed, while their physiological importance alone would be enough to warrant intense study, their pathological relevance, combined with their potential to be modulated in a highly specific manner, has led them to become the target of ~25% of current drugs [7].

1.1.2 G-protein Signalling

The classical paradigm of GPCR signalling describes a two state (on/off) mechanism [8]. In its resting, or inactive form, the GPCR at the cell membrane is not

coupled to intracellular effectors. Upon ligand activation, the GPCR becomes associated with its canonical intracellular signalling partner, the trimeric guanosine nucleotide-binding protein (G-protein) [9]. This trimeric G-protein is comprised of the Gα subunit and the Gβγ heterodimer. There are numerous subtypes of the Gα, Gβ, and Gγ subunits, and each has unique signalling properties [10]. When a ligand binds the extracellular face of the GPCR, a small structural change at the binding site induces a larger structural change at the cytoplasmic face of the receptor, favouring association of the G-protein [9]. This association causes guanosine diphosphate (GDP) to be replaced by guanosine triphosphate (GTP) and, subsequently, dissociation of the activated Gα subunit from the Gβγ heterodimer [11]. From here Gα and Gβγ initiate signalling cascades (second messenger pathways) *via* direct interaction with, and regulation of, downstream effector molecules, including adenylyl cyclase (by $G\alpha_i$ and $G\alpha_s$), phospholipase C (by $G\alpha_{q/11}$), RhoGEFs (by $G\alpha_{12/13}$), and ion channels [10; 12; 13; 14; 15; 16; 17]. These second messengers then go on to regulate still more downstream effector molecules, propagating the signalling cascade, which eventually manifests as far-reaching cellular effects (*eg.* gene regulation, mitosis, apoptosis)[10]. The inactive, GDP-bound Gα subunit will eventually be regenerated by the inherent GTPase activity of Gα, or by the action of GTPase activating proteins (GAPs), which will accelerate termination of the signal [18].

The classical pathways downstream of GPCRs involve coupling to a heterotrimeric guanine nucleotide binding protein (G-protein), which, upon activation, goes on to regulate various cellular events. For a given GPCR, G-protein-

coupling preference is usually defined in terms of the Gα subunit, of which there are four main subfamilies: $G\alpha_s$, $G\alpha_{i/o,}$ $G\alpha_{q/11}$, and $G\alpha_{12/13}$ (Figure 1.2). Each family, in turn, is associated with a hallmark cellular effect: adenylyl cyclase (AC) activation for $G\alpha_s$; AC inhibition for $G\alpha_{i/o}$; phospholipase C-β (PLC-β) activation and increased intracellular [Ca^{2+}] for $G\alpha_{q/11}$; and, regulation of Rho GTPases, which are known for their role in regulating the actin cytoskeleton, for $G\alpha_{12/13}$ [19].

Although a helpful starting point, this simple picture belies the real situation. These classical pathways account for only a fraction of the many pathways activated downstream of GPCRs. Moreover, while they provide measurable endpoints for functional readouts of GPCR activation (*e.g.,* extracellular signal-regulated kinase (ERK) activation, changes in intracellular [Ca^{2+}] or [cAMP], etc.), these readouts can give few details about spatiotemporal cellular dynamics, pathway selectivity, degree of signal branching, divergence and re-convergence of various branches, and so on. In other words, with only a rough snapshot of a given downstream event, it is difficult to determine which upstream signalling events led to the signal being measured. Yet if we are to draw conclusions from our studies of GPCR signalling, it will be important to consider, as much as possible, the many details that contribute to the quality of a GPCR signal.

1.1.3 GPCR Desensitization and G-Protein-Independent Signalling

One of the key events to take place following activation of a GPCR by a ligand is receptor desensitization, which occurs *via* the recruitment of β-arrestin to the GPCR. The process is mediated by GPCR kinases (GRKs), which are recruited to, and

phosphorylate, the receptor in its ligand-stabilized active conformation. This phosphorylation of key intracellular serine and threonine residues creates interaction sites for β-arrestin, which will then bind the GPCR, occluding further interactions with the G-protein, and thereby preventing reactivation of the G-protein signalling cascade [20; 21]. Simultaneously, the recruitment of β-arrestin targets the GPCR for endocytosis *via* clathrin-coated pits, a process important for attenuation of the agonist-induced signal, as well as receptor resensitization and downregulation.

More recently, β-arrestin has been established as an important transducer of GPCR signals in its own right (Figure 1.3), and has been of central importance in the paradigm shift towards the concept of "non-canonical" or "G-protein-independent" signalling through GPCRs [20; 21; 22]. In this context, β-arrestin acts as a scaffold and adaptor protein for key second messengers, including Src family kinases and components of the extracellular signal-regulated kinase (ERK) and c-Jun N-terminal kinase (JNK) pathways [23]. Interestingly, for example, a study of the AT_1R revealed that G-protein- and β-arrestin-mediated signalling induce distinct spatiotemporal patterns of ERK activation (ERK → pERK) in HEK-293 cells [24]. More specifically, $G\alpha_{q/11}$ induces a transient spike in pERK localized in the nucleus (where it presumably regulates gene expression); conversely, β-arrestin, in complex with internalized angiotensin II receptor type 1 (AT_1R) and other proteins, induces a sustained cytosolic pool of pERK, which presumably has distinct signalling properties.

1.1.4 Biased Agonism at GPCRs

The discovery that receptors can transduce signals through means other than the classical G-protein mediated pathways has required a broadening of our understanding of GPCR function. In the past, GPCR ligands were neatly classified as agonists, antagonists, and inverse agonists, based solely on their effects on G-protein signalling [8]. That is, agonists were activators of G-proteins; antagonists blocked the effects of other ligands; and inverse agonists reduced even the basal G-protein activation mediated by *apo* (ligand-free) receptors. However, it has since become clear that a given ligand may be a "biased agonist", behaving, for instance, as an agonist towards one pathway (*e.g.* β-arrestin mediated ERK cascade), while acting as an inverse agonist towards another (*e.g.* $G\alpha_i$ mediated ERK cascade) [8; 20; 23; 25; 26]. The picture is modified further by the discovery of allosteric modulators, which bind sites other than the orthosteric ligand binding pocket, and can alter a GPCR's response profile to a given ligand [8]. These findings imply a much higher degree of complexity for GPCR signalling, bringing new challenges to studies of receptor systems, and calling into question previous assumptions about the interpretation of experimental data. On the other hand, the increased complexity promises to help explain the great specificity, versatility and dynamic range with which GPCRs signal. With a more nuanced understanding of biased agonism and allostery comes the potential to develop finely tuned pharmacological molecules that can maximize therapeutic benefits associated with a given signalling pathway, while minimizing adverse effects that may be associated with others [27].

1.1.5 Insufficiency of the Two-State Model of GPCR Activation

The developments discussed above make it clear that the classical two-state model of GPCR activation is insufficient to describe the complex and versatile behaviour of these systems. In particular, the 'signalling bias' observed for ligands that preferentially activate one pathway over another seems to require the existence of multiple 'active' receptor conformations, rather than a single active state [23; 24]. Such findings are corroborated by structural and thermodynamic studies that have elucidated the stepwise transition of rhodopsin from an inactive to an active conformation, providing evidence of several intermediate conformations along the way, each with a particular free energy, as well as transitional barriers to neighbouring conformations [28]. More recently, Kim *et al.* (2013) used ^{19}F NMR spectroscopy to observe the β_2 adrenergic receptor (β_2AR) in equilibrium across two distinct inactive conformations, an intermediate conformation, and a fully active conformation – the latter being observed only in the presence of a nanobody mimicking Gα_s [29].

Thus, gradually, the paradigm has shifted – away from a view of the GPCR as an 'on/off' switch waiting to be flipped on by cognate ligands of varying efficacies, and toward its description as a 'landscape of conformations' co-existing in thermodynamic equilibrium, with particular conformations being stabilized or destabilized by a given ligand [30]. Critically, each conformation may have different signalling properties, a consequence of the particular spatial positions of its amino acid residues, and of the resulting affinity of the GPCR for other molecules (*i.e.*

intracellular signalling partners, the lipid bilayer, orthosteric ligands, allosteric modulators, *etc*.) [8].

1.2 Overview of the Apelinergic System

The AR is a class A (rhodopsin-like) GPCR first identified in 1993 based on its sequence homology with the angiotensin II receptor (AT_1R) and dubbed APJ [31]. With the discovery that it was not activated by angiotensin II, and in the absence of an identified cognate ligand, the receptor was deemed an orphan GPCR. The AR retained this status until 1998, when its endogenous ligand, apelin, was first isolated from bovine stomach extracts [32]. In this study, the 77 amino acid protein preproapelin was identified as the precursor of bioactive apelin. Three shorter isoforms, apelin-36, -17, and -13 (nomenclature based on the number of C-terminal preproapelin amino acids retained), were hypothesized based on the presence of basic motifs in the peptide sequence suggestive of recognition sites for proteolytic cleavage (sequences in Table 1.1). Backing up this hypothesis, synthetic apelin-13, -17 and -36 peptides were all shown to activate the AR. Following up on this, our laboratory recently demonstrated the first enzymatic cleavage of proapelin to an active apelin isoform [33]. Specifically, proprotein convertase subtilisin kexin 3 (PCSK3 or furin) preferentially cleaves proapelin directly into apelin-13. It had been previously suggested that the longest cleavage product, apelin-36, is an intermediate for production of shorter isoforms [34]; our studies suggest that apelin processing may be more complex, with different isoforms being produced via disparate, as yet uncharacterized, mechanisms .

Both apelin and the AR are expressed across a wide range of eukaryotes, [33] including humans, and many relevant studies have been conducted in rodent or other animal models, as well as in cell or tissue culture. Consistently high levels of expression have been observed in the central nervous system (CNS), and both receptor and ligand are widely present throughout the peripheral tissues [35; 36; 37; 38; 39; 40]. The importance of apelinergic signalling is well established in areas as diverse as cardiovascular regulation, energy metabolism, fluid homeostasis, angiogenesis, human immunodeficiency virus-1 (HIV-1) infection, and the neuroendocrine stress response, among others [41; 42; 43]. Very recently, the AR has been shown to be activated by another endogenous ligand known as toddler or ELABELA, and in this capacity has been found to play a central role in embryonic development in zebrafish [44; 45].

Thus, various physiological and pathophysiological roles have been attributed to the apelinergic system, but the overarching theme of apelin-AR research to date is that of a complex and important regulator of physiology, the functions of which are only ambiguously characterized. The present section describes some of the main physiological and pathological roles of the AR, with a focus on the cell signalling pathways downstream of AR activation that may be involved in the varied and context-dependent behaviour of this GPCR. Finally, this introduction to the apelinergic system concludes with a comparison of the multiple endogenous ligands that regulate the AR, and how their distinct properties may influence the signals transmitted by this important receptor.

1.3 Physiology and Pathophysiology of the AR

Having given a general introduction to GPCR-mediated signal transduction, I now describe a number of the key normal physiological and pathological actions of the AR. Since AR-mediated signalling has not always been conclusively linked to any particular physiological processes, this is followed by a review of the primary cell signalling events mediated by the AR that have been characterized to date.

1.3.1 The AR in the Cardiovascular System

Some of the most compelling aspects of apelin-AR physiology, from a therapeutic perspective, are related to its effects in the cardiovascular system. Apelin is one of the most potent known inotropic agents [46], and doses in mice have been shown to increase myocardial contraction and reduce cardiac load without inducing pathological hypertrophy [47]. This GPCR is also involved in an apelin-independent response to mechanical stretch [48]. Notably, this response is pathological when the heart is experiencing chronic pressure overload, and AR knockout (KO) mice show reduced risk of cardiac hypertrophy under such conditions.

Apelin-AR signalling is also reported to have cardioprotective effects; for instance, administration of apelin-13 to glucose-deprived cultured cardiomyocytes had a significant inhibitory effect on apoptosis [49]. Likewise, myocardial apelin levels are reduced in patients with ischemic heart failure, and these lower levels are associated with greater mortality rates and less effective cardiac remodelling post-

injury [50]. Conversely, spontaneously hypertensive rats exhibit elevated apelin levels in the rostral ventrolateral medulla (RVLM) the region of the brainstem responsible for regulating blood pressure and other autonomic functions [51]. Microinjection of apelin into the RVLM caused chronic increases in mean arterial blood pressure and cardiac hypertrophy. In contrast to these CNS effects, peripherally administered apelin has typically been shown to decrease blood pressure [52; 53; 54; 55; 56; 57]. However, this is not without exception: for example, blood vessels denuded of epithelium show a vasoconstrictive response to apelin, directly opposite to the vasodilation observed in endothelium-intact vessels [37]. Similarly, studies of peripheral apelin adminstration in conscious rats have reported both increases and decreases in blood pressure [56; 58] – ambiguous results in comparison to the blood pressure decreases consistently observed in anesthetized rats, suggesting that the conscious state of the animal, or the different apelin isoforms being administered, may influence the vascular effects of AR signalling [41].

A study in sheep given a large systemic dose of apelin-13 led to a biphasic response in blood pressure, with an initial transient decrease in blood pressure immediately giving way to an increase in blood pressure. The dose also led to increased plasma concentrations of the vasoactive hormones vasopressin, adrenocorticotrophin, aldosterone, cortisol, atrial and brain natriuretic peptides, cyclic GMP and cyclic AMP [59].

The variety of apelin-AR effects summarized above emphasize the need to consider apelin-AR signalling in the context of whole organism physiology, as the

functional readouts chosen may reflect, for example, the organism's compensatory response to the effects of apelin-AR signalling, rather than the initial signalling itself. Overall the emerging picture of the AR and apelin in the cardiovascular system is one of complex and important regulators of the heart and vasculature. However, much more research is needed if we are to understand their subtle and often seemingly contradictory modes of action.

1.3.2 The AR in Energy Metabolism

Another key aspect of apelin and AR physiology, not least from a therapeutic perspective, is their influence on energy metabolism. Both the GPCR and its ligand are expressed in adipose tissue. Apelin is also secreted by adipose tissue. Similarly to other systems, apelin-AR signalling appears important in both normal and pathological processes. More specifically, both apelin and AR levels are elevated in the adipocytes of obese individuals, and apelin levels are also elevated in the plasma of these individuals [60]. However, these increases are only observed in cases where obesity coincides with elevated insulin (hyperinsulinaemia), indicating that obesity alone does not significantly affect apelin-AR signalling, and suggesting a co-regulatory role for these two hormonal peptides [60]. Further to this, administration of apelin-36 either to live mice or to isolated pancreatic islets inhibits glucose-stimulated insulin secretion [61]. Thus, it has been proposed that the AR may be present at the membrane of islet β-cells, with its activation by apelin leading to reduced insulin secretion, and to the resulting impairment of glucose elimination. Insulin, on the other hand, binds its receptors on adipocytes, and in

doing so induces apelin expression, thus providing a negative feedback mechanism for insulin's own production [61]. With respect to feeding behaviour, adipocyte apelin mRNA levels are significantly decreased (6.2-fold) in fasting mice, following the same trend observed for plasma insulin levels (5.4-fold reduction). In turn, levels of both return to normal after food intake [60].

There have been a number of studies suggesting the potential for apelin-AR-related therapy in metabolic disorders. Apelin-13 has been reported to increase pancreatic islet cell mass and β-cell insulin content in mice with type I diabetes, improving these two symptoms of the disease [62]. Likewise, administration of apelin alleviates the impaired insulin sensitivity of both apelin KO mice [63] and obese, hyperinsulinaemic mice [64]. Doses of apelin-13 in mice also induce elevated expression of mitochondrial uncoupling proteins 1 and 3, which are involved in the dissipation of the electron transport chain's proton gradient in the form of heat, rather than ATP production. It has been hypothesized that this action is responsible, at least in part, for the concurrent reduction in white adipose tissue and serum triglyceride concentrations that result from this apelin treatment [65].

Clearly, apelin and the AR have an important regulatory role in energy metabolism. Both are up-regulated in metabolic disorders, and their actions have until now generally been considered beneficial. However, further research is needed to establish in more depth both the causes and consequences of these altered expression patterns.

1.3.3 The AR in Fluid Homeostasis

A number of studies suggest that apelin-AR signalling has an important role in maintaining fluid homeostasis. As mentioned above, both ligand and receptor are present in high levels in the CNS. In particular, apelin-17 is highly present in the rat paraventricular nucleus and supraoptic nucleus of the hypothalamus [66], bodies of neurons that project into the pituitary gland, producing secretory hormones to be released into systemic circulation. Production of the antidiuretic hormone vasopressin is a hallmark action of these nuclei, and the co-localization of apelin with vasopressin here suggests a potential shared regulatory role of these peptides on fluid balance. For instance, one study observed a clear diuretic effect for apelin, opposing vasopressin's anti-diuresis and inducing decreased vasopressin expression [38]. Contrastingly, another reported anti-diuresis mediated by the AR, with AR knockout mice showing an inability to reduce urine volume in response to water deprivation [67]. Regarding drinking behaviour, some studies report increased water intake by water-replete animals in response to central apelin administration [68], whereas others report reduced intake [69], and still others report no effect [54]. Thus, apelin and the AR appear to be important physiological regulators of fluid homeostasis, but, as with their actions in other systems, further study is required to unravel the complexity of their signalling.

1.3.4 The AR in Angiogenesis

The actions of apelin through the AR have been shown to be angiogenic, both in normal physiology and in the pathology of cancer. The presence of both receptor and ligand is necessary for the normal development of frog and mouse heart vasculature, and their absence causes vessel disruption in a majority of embryos

[70]. On the other hand, apelin and the AR induce premature angiogenesis in Xenopus, and both are up-regulated in microvascular proliferations of malignant gliomas [71]. Recently, apelinergic signalling has been implicated in the growth of colon cancer, with apelin expression up-regulated in half of colon adenocarcinomas [72]. Moreover, both apelin and the AR are expressed in LoVo cells, a colorectal cancer cell line; in these cells, apelin-13 administration prevents apoptosis by inactivating a caspase pathway, while the antagonistic apelin-13 mutant F13A significantly reduces cellular proliferation [72]. The role of this system in tumour angiogenesis has led to identification of apelin and the AR as anticancer therapeutic targets or, at the very least, as potential diagnostic biomarkers.

1.3.5 Additional Physiological Actions

The physiological actions discussed above represent some of the most studied roles of apelin and the AR to date. However, the actions of this GPCR and its ligand are wide-ranging, and a number of other roles have been described (reviewed in [41]). These include, among others, a role for the AR as co-receptor with CD4 for HIV infection [73], which is inhibited by the various apelin isoforms [74], and an emerging picture of apelin and the AR as regulators of the stress response *via* the hypothalamic-pituitary axis [75]. Thus, while the physiological importance of apelin-AR signalling has been well established, much remains to be determined regarding its harmful and beneficial effects, and the actual mechanisms of signal transduction through the AR remain central and as yet unanswered questions.

1.4 Signal Transduction Pathways Coupled to the AR

As described in Section 1.1.1, the signalling cascades downstream of GPCR activation are highly complex. As a result, while physiological effects and signal transduction events may be characterized for a given GPCR, the links between these organism- and molecular-level phenomena are usually less well understood, and current knowledge of the AR is no exception. As described below, AR signalling is heterologous, with the receptor showing preference for multiple G-proteins, mediating different effects in different cell types, and being differentially modulated by its various endogenous ligands. Considering AR signalling in this light, it is less surprising that the AR is able to mediate so many different, sometimes seemingly contradictory, effects.

1.4.1 AR Coupling to $G\alpha_{i/o}$

The primary $G\alpha$ coupling preference of the AR is for $G\alpha_{i/o}$ (Figure 1.4) – in particular $G\alpha_{i1}$ and $G\alpha_{i2}$, but typically not $G\alpha_{i3}$ [76]. However, these interactions have been shown to vary with cell type; for instance, AR coupling to $G\alpha_{i3}$ is observed in human umbilical vein endothelial cells (HUVECs) [77]. Signal transduction *via* the AR in Chinese hamster ovary (CHO) cells has been linked to classical $G\alpha_{i/o}$-mediated downstream effects such as ERK and Akt activation and decreased cAMP production. Of note, this AR-mediated ERK phosphorylation appears not to be $G\beta\gamma$-dependent, despite such dependency being commonly observed for GPCRs [78].

1.4.2 AR Coupling to $G\alpha_{q/11}$ and/or Free $G\beta\gamma$ Subunits

In addition to its interaction with pertussis toxin-sensitive $G\alpha_{i/o}$ proteins, there is also evidence that the AR couples to pertussis toxin-insensitive G proteins, namely $G\alpha_{q/11}$ [46]. This is based on the finding that the contractile effects of the AR on cardiomyocytes are only partially attenuated by pertussis toxin, whereas addition of phospholipase C (PLC-β) and protein kinase C (PKC) inhibitors also significantly attenuated these effects. Similar attenuation was observed when Na^+/H^+ and Na^+/Ca^{2+} exchangers were inhibited. Thus, it has been proposed that the inotropic effects of apelin *via* the AR rely, at least in part, on $G\alpha_{q/11}$ coupling to the PLC-β -PKC pathway.

The vasodilatory effects of apelin-AR signalling appear to be mediated *via* nitrous oxide, as inhibition of nitric oxide synthase (NOS) prevents the apelin-induced decrease in blood pressure [55]. NOS is activated by calmodulin, which itself is activated by rising intracellular $[Ca^{2+}]$, a downstream product of the PLC-β -PKC cascade. Thus it is likely that these effects are mediated by the AR's activation of the PLC-β-PKC pathway, either through $G\alpha_{q/11}$, or through the free $G\beta\gamma$ subunits of the $G\alpha_{i/o}$ heterotrimer, or through a combination of both.

1.4.3 β-Arrestin-Dependent Internalization and G-Protein-Independent Signalling

The AR has been shown to internalize following association with β-arrestin [79; 80] in a clathrin-dependent manner [81]. Interestingly, the stretch activated response of the AR mentioned previously is both β-arrestin-dependent and G-protein-independent [48]. Administration of apelin-13 attenuates these harmful effects. This directly implies that mechanical force leads to the adoption of an AR

conformation capable of β-arrestin-mediated signalling that is distinct from the G-protein 'active' state conformation normally induced by apelin. Whether this stretch-induced conformation would be independently arrived at during β-arrestin-mediated internalization of the AR is not clear.

1.4.4 Summary of AR-Mediated Cell Signalling

The AR-mediated cell signalling events discussed above explain only a portion of the many physiological effects that occur in response to AR activation. To date, only a limited number of the AR's many cellular effects have been connected unambiguously to particular branches of the signalling cascade downstream of the GPCR. Moreover, it is likely that in many cases, the type and magnitude of downstream events are context-dependent, or vary with cell type, as was observed for the G_i coupling preference of the AR. This being said, one clear aspect of AR signalling is that the nature of the signal varies depending on the apelin isoform administered. Thus when studying the wide-ranging effects mediated by the AR under normal physiological and pathological conditions, it will be important to consider the distinct properties of the multiple endogenous ligands that activate it.

1.5 Comparison of the Properties of Endogenous AR Ligands

The following section describes some of the unique signalling properties that have been reported to date for the various endogenous apelin isoforms (Table 1.1) and highlights important aspects that remain to be characterized. As mentioned above, a second endogenous peptidic ligand of the AR, known as toddler/ELABELA,

was recently discovered [44; 45]. This new ligand appears to be an important regulator of the AR, and the study of it will likely provide significant insight into AR signalling. However, as toddler/ELABELA has so far only been implicated in zebrafish development, and as the focus of this thesis is limited to modulation of the AR by apelin isoforms, no further detail concerning this new AR ligand will be provided.

1.5.1 Apelin-Induced Signalling

The presence of multiple apelin isoforms in the body suggests an evolutionary purpose. In the initial report of apelin by Tatemoto *et al.* (1998), the potency of apelin-13, -17 and -36 peptides was directly compared. Notably, the two shorter isoforms had 8 to 60-fold higher activity than apelin-36 with respect to measurements of the AR-induced cellular acidification rate [32]. AR internalization post-activation in HEK cells, human neurons, and microvascular endothelial cells has been shown to vary depending on the apelin isoform, with apelin-36 inducing internalization – and a sustained β-arrestin association – more potently than apelin-13 [76]. This disparity is attributed to the different affinity of the receptor for each isoform; namely, apelin-13 dissociates more readily than apelin-36, and this rapid dissociation is accompanied by complete recycling of the AR to the cell surface within one hour. By contrast, apelin-36-associated AR remains sequestered in intracellular compartments, with no recycling even two hours after apelin administration [79; 82]. Subsequent studies have further highlighted differences in binding affinity (K_d) and potency (EC_{50}) for the different isoforms.

In addition, there are differences in the tissue distribution of these peptides. For example, apelin-36 seems to be the predominant isoform in the lung, testis, and uterus; conversely, both apelin-36 and pyr-apelin-13 (the pyroglutamate-modified form of apelin-13, a spontaneous modification (e.g. [33]) are present at high levels in the mammary gland [40]. By contrast, Pyr-apelin-13 has been the only isoform detected in the hypothalamus, and is the predominant form in rat brain extracts [38] and human cardiac tissue [37].

In human plasma, circulating apelin-13, Pyr-apelin-13, and apelin-17 have all been detected using antibody-based [35] or HPLC-based detection [36]. Recently, Zhen et al. [83] used mass spectrometry, a more reliable means than immunoassay for unambiguously distinguishing the isoforms, to demonstrate that Pyr-apelin-13 is the most prevalent isoform in human plasma. In an earlier study, Mesmin *et al.* [84] also used a mass spectrometry-based technique to identify apelin peptides in the bovine colostrum. Interestingly, they detected not only the expected 13, 17, and 36 residue isoforms, but also many other forms, including peptides lacking one or more C-terminal residues, to a total of 46 isoforms. Results such as these highlight the incompleteness of current knowledge about the distribution and function of the various apelin peptides.

In summary, both the tissue distribution of the various apelin isoforms, as well as their functional behaviour as activators of the AR, are distinct. Functionally, the shorter apelin isoforms have exhibited higher potency for certain downstream readouts and faster cell-surface recycling post-internalization, wheras the longer forms have exhibited higher affinity for the AR and increased intracellular retention

[76; 79; 82]. Though the effects of these distinct internalization patterns have not been studied in detail, it seems likely that they should confer unique, isoform-dependent cellular effects (*e.g.,* sustained cytosolic *vs*. transient nuclear ERK activation [24]). Moreover, despite, or perhaps because of, its lower affinity for the AR, apelin-13 is the more potent activator of $G\alpha_i$-mediated ERK phosphorylation [76]. Interestingly, while the affinities of the apelin-13-bound AR for $G\alpha_{i1}$ and $G\alpha_{i2}$ are roughly equivalent, apelin-36 induces the AR to couple preferentially to the $G\alpha_{i2}$ subunit [76]. Such differences suggest the existence of different conformations or timescales of 'activated' AR, which are differentially induced by the various apelin isoforms, and which may have physiological importance. There have been no studies probing for apelin-induced signalling bias towards specific downstream pathways (*e.g.,* G_i-mediated, β-arrestin-mediated), but it is a definite possibility that the different apelin isoforms direct the AR signal toward different branches of the downstream cascade.

Noting these unique properties of the apelin peptides, it is clear that although all isoforms share the same 12 C-terminal residues required for bioactivity [55] with correspondingly consistent structural properties [85; 86], the various peptides have different functional behaviour with respect to AR signalling. Compellingly, the conserved structural features of the apelin isoforms have been directly employed in design of peptide-based AR antagonists [87; 88], and agonists [89]. Nevertheless, to produce synthetic ligands capable of fine-tuning AR activity for therapeutic benefit, it will be necessary to better understand the apelin-AR interaction, and thereby determine how apelin N-termini of various lengths may act to modify the AR signal.

The majority of experiments presented in this thesis have focused on signalling induced by apelin-13, the shortest and most potent bioactive isoform of apelin that is thought to exist endogenously. We initially selected this isoform for our AR activation studies based on both its potency and the relative ease with which it can be produced by solid-phase peptide synthesis. In addition, this thesis reports production of the longer isoform, apelin-36, which is more difficult to produce synthetically, by recombinant expression in *E. coli*. The bioactivity of this apelin-36 peptide is confirmed herein, and its potency is compared to that of apelin-13.

1.5.2 Scope of Apelin Functionality

The variant properties of the multiple apelin isoforms – the different tissue distribution of these peptides, as well as the differences in affinity, potency, and internalization patterns that have been observed between the longer and shorter isoforms – all point to functionally important differences between them. Their presence in the body as endogenous regulators of the AR suggests that the receptor's activity can be fine-tuned to match cellular needs and achieve the highly diverse and complex signalling that has made the AR such an important target for study.

1.6 Summary of the Apelin Receptor System

It should now be clear that the AR is an important GPCR that mediates a wide array of normal physiological and pathological processes. With involvement in areas ranging from cardiovascular regulation, angiogenesis, and energy metabolism to

fluid homeostasis and the neuroendocrine stress response, AR signalling is implicated in several pathologies, including heart disease, diabetes, obesity, and cancer. Yet, while the importance of AR signalling is well established, relatively little is currently known about the way the receptor is activated by its multiple endogenous ligands, or about the downstream cellular signalling pathways that translate its activation into the diverse physiological effects that have made the AR such an important target of study. Future AR research should be both functional and structural in its scope, with particular focus given to the unique signalling properties of the different endogenous ligand isoforms of the AR and to functional and biophysical characterization of the apelin/toddler-AR interaction. Such studies will help unravel the mechanisms of the complex and context-dependent signalling behaviour of the AR, and will aid in the design of future therapies targeting this physiologically and pathologically important receptor.

1.7 Rationale and Objectives

Having introduced some of the wide range of physiological actions of apelin and the AR, as well as some details of the cell signalling pathways that mediate them, this section introduces the focus of this research on the AR, explaining the objectives and the experimental methods used to achieve them.

1.7.1 Probing the Binding Interaction Between the AR and Apelin

The principal goal of this research project has been to characterize the binding interaction between the AR and apelin – and in particular, to test the

hypothesis that the extracellular (EC) face of the AR is involved in apelin binding. Thus, an attempt has been made to identify key amino acid residues on the EC face of the receptor that are involved in apelin binding and AR activation.

Despite the established importance of the AR in normal physiology and pathology, research probing the structural/functional basis of the apelin-AR interaction has been limited, and little is known about the physical mechanism by which this ligand binds and activates its receptor. Yet understanding the apelin-AR interaction is important for several reasons. Most obviously, from a therapeutic perspective, identifying key interaction sites on the AR will aid in the development of novel synthetic ligands targeting this physiologically and pathologically important receptor. Moreover, the presence of multiple apelin isoforms suggests that each isoform may have unique signalling properties. As such, characterizing AR binding and activation by a given isoform will help us understand the isoform-dependence of the interaction. This can in turn be considered in the context of observed differences in the downstream signalling pathways. With this in mind, one aspect of the work described here involved production of recombinant apelin-36, to provide a sufficient and cost-effective supply of multiple apelin isoforms, to be used in future functional and structural studies. From a broader perspective, findings about the AR-apelin interaction can be considered alongside other GPCR-ligand systems, to help establish general features of ligand binding and GPCR activation, and to identify characteristics unique to apelin and the AR.

To date, several studies have identified key amino acids involved in the apelin-AR binding interaction and AR activation. Iturrioz *et al.* (2010) showed that

deletion or substitution of the C-terminal phenylalanine of apelin, despite having no effect on the coupling of the AR to $G\alpha_i$, yielded a ligand that could not induce AR internalization [90]. Moreover, they identified three key aromatic residues in the transmembrane (TM) domains of the AR (Figure 1.5): W152 in TM IV, and F255 and W259 in TM VI. Mutation of these residues, similarly to the C-terminal apelin mutations, had no effect on apelin binding affinity or $G\alpha_i$ activation, but nevertheless caused dramatically reduced receptor internalization (Figure 1.5). In a recent study from our lab, residues G42, G45, and N46 of the AR TM I were shown to play a critical structural role in disrupting the helical character of TM I, and mutation of these residues prevents proper trafficking of the AR to the cell membrane (Figure 1.5) [91].

However, reports so far have focused largely on apelin, or on the TM domains of AR; conversely, there has been little investigation of the involvement of the extracellular (EC) side of the AR in ligand-binding and receptor activation. Residues within the TM domains of GPCRs form what is often called the "binding pocket" for orthosteric ligands [92]. For GPCRs with soluble ligands, the TM domains embedded in the membrane are bundled together so as to exclude lipid molecules from the binding pocket [93], providing an aqueous environment for the ligand to enter, where it interacts with key residues in the TM domains. These interactions induce structural rearrangements in the binding pocket, which in turn lead to larger structural changes in the cytoplasmic domain, and associated effects, such as favouring the formation of the GPCR-G-protein complex [9]. Nevertheless, although ligand-induced activation requires eventual entry of the ligand into the TM binding

pocket, residues on the EC face also have functional importance for ligand binding and receptor activation. This being said, the rationale for studying this region of the AR is introduced below.

1.7.2 Rationale for Studying the Extracellular Face of the AR

This investigation of the apelin-AR interaction has focused on residues on the EC face of the AR for several reasons. Firstly, while the TM and intracellular (IC) domains of class A GPCRs are typically highly conserved, as a rule the N-terminus and extracellular loops (ELs) are varied and confer uniqueness to a given receptor. Thus while the TM domains of the AR and its closest relative, the AT_1R, share 40% sequence identity, the N-terminus and ELs of these GPCRs are more divergent, sharing only 18% sequence identity. Despite high TM identity between these receptors, angiotensin II does not activate the AR [31; 32]. We therefore propose that the selectivity of the AR for apelin may result from apelin's contact with residues in the less conserved N-terminus and ELs. Secondly, the involvement of this region makes sense spatially; the diffusing apelin most likely encounters these residues first before its C-terminus enters the TM binding cleft. Moreover, because apelin is highly cationic (pI for apelin-36: 12.85), we suspect binding affinity and specificity to be mediated by some of the numerous negatively charged aspartate and glutamate residues on the EC face of the AR. Due to their steric bulk and electronic properties, a number of aromatic residues in this region may also be involved.

There is literature precedent for the involvement of the AR EC face in binding apelin. One study by Zhou *et al.* (2003) reported the involvement of the N-terminus

of the AR in ligand-binding and receptor activation. Namely, they found that the second 10 residues of the N-terminus were important for the apelin-AR interaction: deletion of these residues led to a dramatic reduction in apelin-binding affinity (as measured by radioligand binding assay), and in apelin-induced Ca^{2+} mobilization and AR internalization. Moreover, two point mutations, E20A and D23A (Figure 1.5), had effects similar to the N-terminal deletion, greatly reducing apelin affinity and attenuating these two readouts of AR activation [94].

There is also precedent in other GPCRs for the involvement of the EC face in ligand binding. In a systematic analysis of EL2 of the vasopressin receptor ($V_{1a}R$), Conner *et al*. found that alanine substitution at four aromatic residues led to major disruption of ligand binding, with increases in mutant K_d values ranging from 200- to 2000-fold, relative to the WT $V_{1a}R$ [95]. For class A GPCRs in general, EL2 in particular has been highlighted for its functional importance in ligand binding. As revealed by X-ray crystallography, EL2 of rhodopsin folds to form two β-sheets, which twist together into a hairpin and dive downward into the TM binding pocket. This orientation is thought to occlude the binding pocket from premature solvent entry, preventing undue hydrolysis of 11-*cis*-retinal [93].

Conversely, in the β_2AR, EL2 contains a short α-helix, stabilized by a widely conserved disulfide bond to TM3 [96]. When this disulfide is disrupted, ligand-binding affinity is reduced 1000-fold [97]. Thus, it is thought that in these GPCRs, the α-helical EL2 is held away from the binding pocket, allowing entry of small diffusing ligands. The same helical motif in EL2 is present in the β_1AR [98].

These examples are not comprehensive, but, along with many others, they provide evidence of the variable nature of the EC face of GPCRs, and of the functional importance of this region in ligand binding and receptor activation. Because of this and the reasons outlined above, this region of the AR has been the focus in the present study of the apelin-AR binding interaction.

Table 1.1 Sequences of human apelin and Toddler/ELABELA, the endogenous peptide ligands of the AR. All isoforms of each ligand retain identical C-termini, and various lengths of peptide are presented based on biological detection or the presence of proposed dibasic proteolytic cleavage sites. Apelin-12 is most likely not produced endogenously, but is the shortest possible synthetic isoform that retains biological activity [55].

Apelin Peptide	**Sequence**
Preproapelin (Apelin-77)	MNLRLCVQALLLLWLSLTAVCGGSLMPLPDGNGLEDGNVRHLVQPRGSRNGPGPWQGGRRKF RRQ**RPRLSHKGPMPF**
Proapelin (Apelin-55)	GSLMPLPDGNGLEDGNVRHLVQPRGSRNGPGPWQGGRRKFRRQ**RPRLSHKGPMPF**
Apelin-36	LVQPRGSRNGPGPWQGGRRKFRRQ**RPRLSHKGPMPF**
Apelin-17	KFRRQ**RPRLSHKGPMPF**
Pyr-apelin-13	Pyr–**RPRLSHKGPMPF**
Apelin-13	Q**RPRLSHKGPMPF**
Apelin-12	**RPRLSHKGPMPF**
Toddler/ELABELA Peptide	**Sequence**
Preprotoddler (Toddler-54)	MRFQQFLFAFFIFIMSLLLISGQEPVNLTMRRKLRKHNCLQRR**CMPLHSRVPFP**
Protoddler (Toddler-32)	QEPVNLTMRRKLRKHNCLQRR**CMPLHSRVPFP**
Toddler-22[a]	KLRKHNCLQRR**CMPLHSRVPFP**
Toddler-11	**CMPLHSRVPFP**

[a] Toddler-22 is shown by analogy to apelin-17; zebrafish Toddler-21 and the corresponding apelin-16 isoform were shown to be active by Pauli *et al.* (2014), with divergent sequences in the N-terminal region compared to the human peptides.

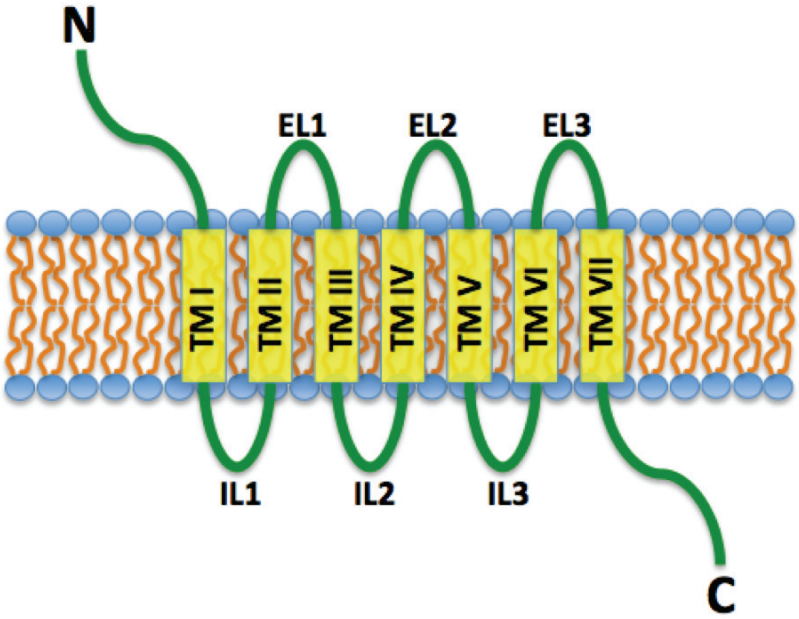

Figure 1.1 Schematic illustration of a GPCR embedded in the phospholipid bilayer. N and C indicate the N- and C-termini, respectively. ELs and ILs 1,2, and 3 correspond to the extracellular and intracellular loops, respectively. TMs I-VII correspond to the seven α-helical transmembrane segments.

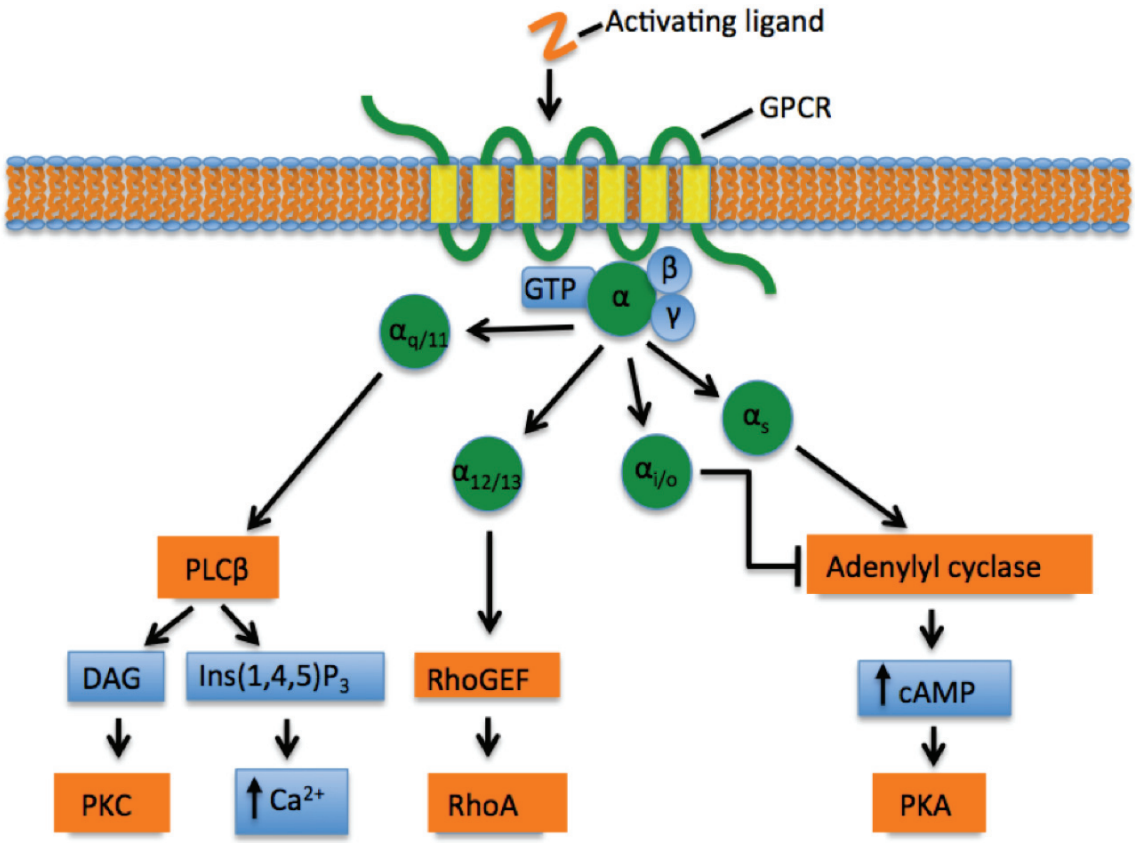

Figure 1.2 Canonical Gα-mediated signalling at GPCRs typically following ligand binding and activation. The heterotrimeric (i.e., αβγ trimer) G-protein coupling preference and downstream cellular effect of a GPCR is defined by the Gα subunit ($G\alpha_s$, $G\alpha_{i/o}$, $G\alpha_{q/11}$, and $G\alpha_{12/13}$). $G\alpha_s$ stimulates adenylyl cyclase, producing cAMP and inducing PKA (protein kinase A) activation; $G\alpha_{i/o}$ inhibits adenylyl cyclase activity; $G\alpha_{q/11}$ activates PLCβ, producing DAG (diacyl glycerol) and Ins(1,4,5)P_3 (inositol 1,4,5-triphosphate), causing an increase in intracellular [Ca^{2+}] and PKC activation; and, $G\alpha_{12/13}$ activates RhoGEF, causing activation of RhoA. Arrowheads indicate activation and blunted arrows indicate inhibition.

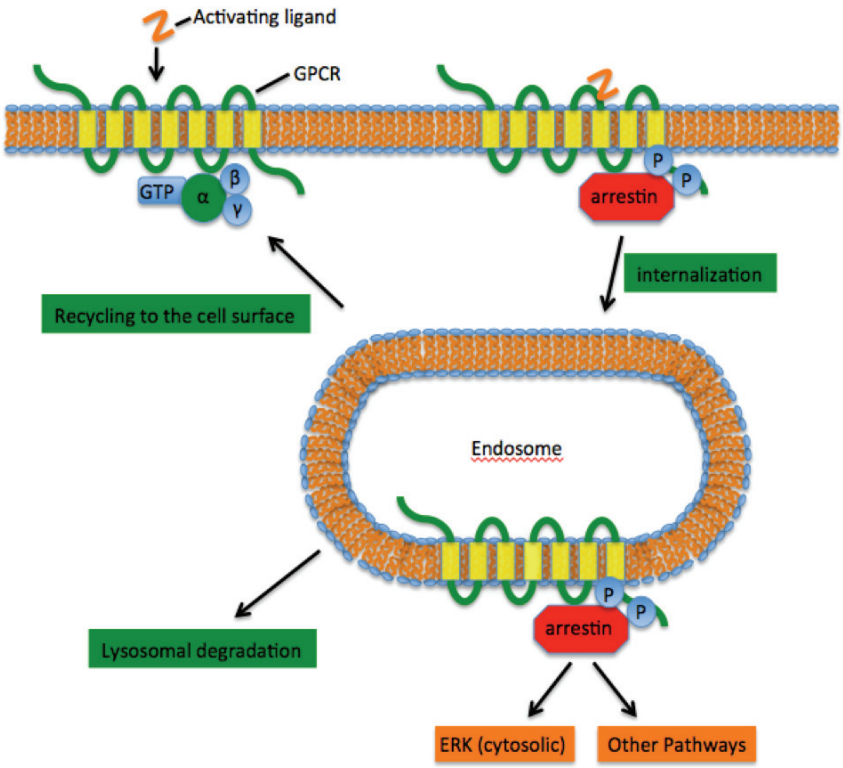

Figure 1.3 β-arrestin-mediated internalization and signalling at GPCRs. An activated GPCR is phosphorylated (circled P) by GRKs (GPCR kinases, not shown), leading to β-arrestin recruitment at the GPCR intracellular loops and C-terminus and occluding further G-protein binding and activation. This triggers internalization of the GPCR via endosome formation, in turn mediating activation of cytosolic ERK and other downstream signalling pathways. The internalized GPCR is eventually either recycled to the cell surface, or trafficked to a lysosome for degradation. Arrowheads indicate activation.

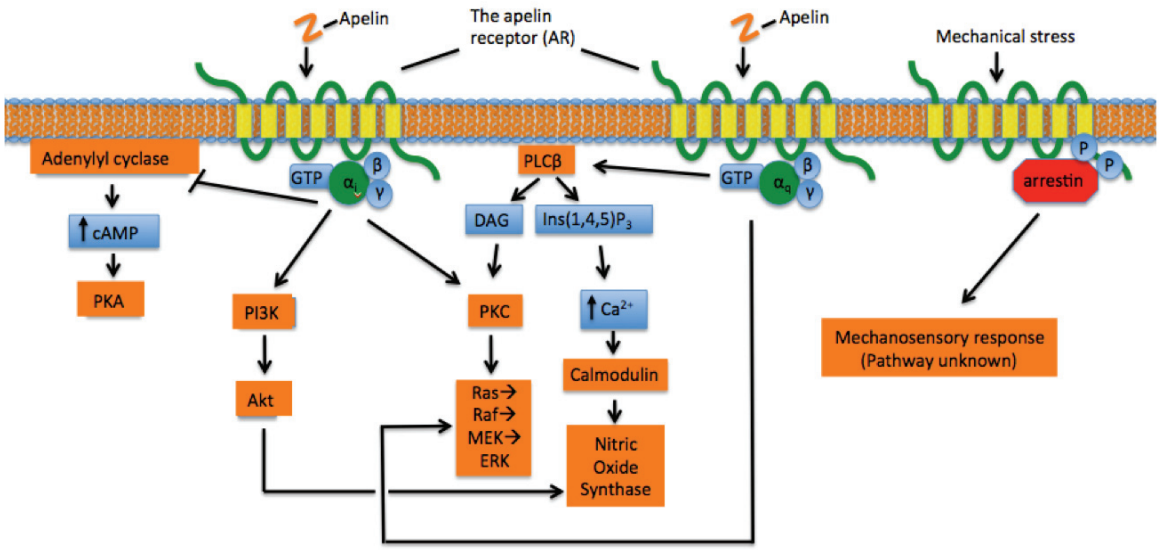

Figure 1.4 Overview of AR-mediated signalling pathways. Apelin-activated AR couples to $G\alpha_i$ and $G\alpha_q$. $G\alpha_i$ may inhibit adenylyl cyclase, reducing cAMP production and thereby inhibiting PKA activation; activate PI3K, leading to Akt activation; or, directly activate PKC, causing activation of the mitogenic ERK pathway. $G\alpha_q$ activates PLCβ, inducing DAG and Ins(1,4,5)P_3 production. DAG and Ins(1,4,5)P_3 activate the PKC cascade and the release of intracellular Ca^{2+}, respectively. Ca^{2+} release in turn activates calmodulin, which then activates nitric oxide synthase. Finally, the AR also mediates a mechanosensory response via a β-arrestin-dependent and G-protein-independent pathway. Arrowheads indicate activation and blunted arrows indicate inhibition.

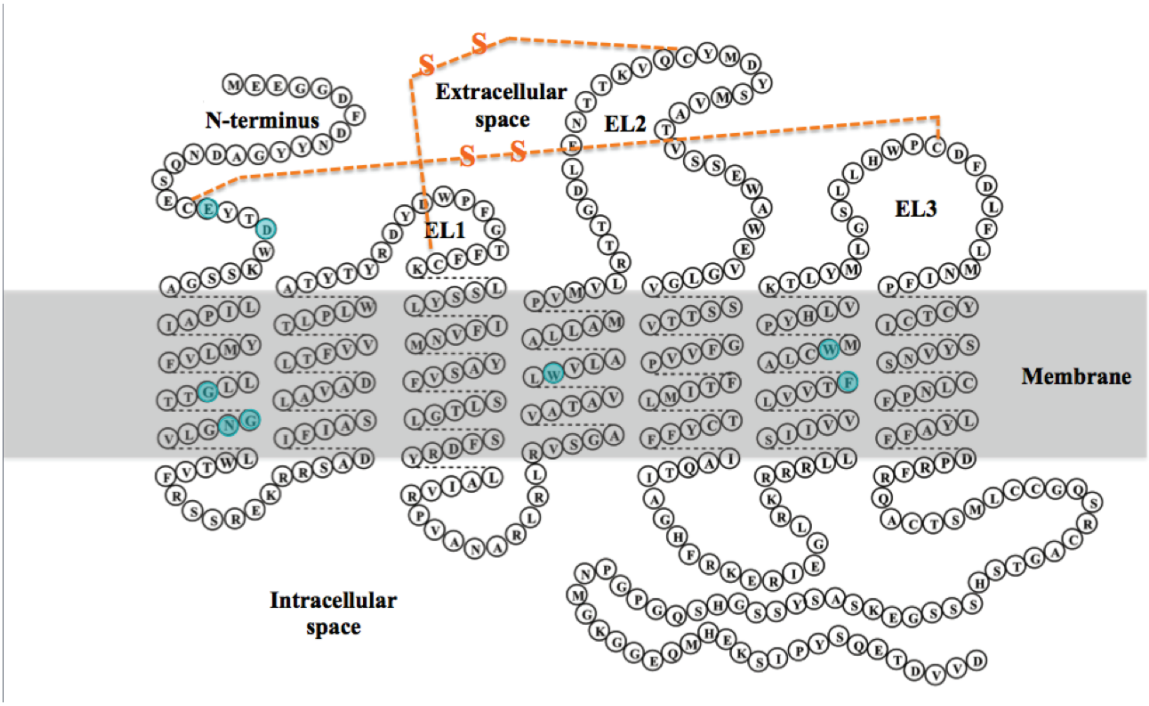

Figure 1.5 Schematic "snake-plot" representation of the AR, depicting previously identified functionally important residues [90; 91; 94]. The orange dotted lines represent putative disulfide bonds. Original AR snake-plot created by Aditya Pandey.

-

Chapter 2: Production and Purification of Recombinant Apelin-36

2.1 Introduction

As introduced in some depth in chapter 1, the peptide hormone apelin has wide-ranging tissue distribution and is a potent and selective activator of the AR. Numerous isoforms have been detected in the body, all of which retain the same 12 C-terminal residues critical for AR activation (Table 1.1). Apelin initially exists as a dimeric, 77 residue prepropeptide [32]. Preproapelin is cleaved to produce the monomeric, 55 residue proapelin. It is proposed that further proteolytic processing events yield apelin-36, apelin-17, and apelin-13 [32]. In addition, the N-terminal glutamine of apelin-13 spontaneously cyclizes, giving rise to the pyroglutaminated pyr-apelin-13 [33]. Synthetic apelin-12 has also been found to be bioactive, but this form may not exist *in vivo*, as it lacks an N-terminal dibasic cleavage motif, which may be required for proteolytic cleavage [32].

As introduced previously, the different isoforms have been shown to have different binding affinities and potencies for activating the AR [32; 76; 79], leading to differences in downstream signaling, receptor recycling/intracellular retention, etc., yet the details of these differences remain largely uncharacterized. In addition, there are the apparent differences in the tissue distribution of the peptides, which

strengthen the argument for important differences in the way the various apelin isoforms modulate AR activity.

There have been few studies directly comparing the properties of the different isoforms. For example, none has probed the potential for signaling bias by the isoforms towards different pathways downstream of the AR. Neither have the affinities, potencies, and recycling of the different isoforms been comprehensively compared. For example, although a few properties of apelin-13 and apelin-36 have been compared [76; 79], there has been no study investigating the signaling behaviour of the longer proapelin. Furthermore, while circular dichroism (CD) spectropolarimetry data and solution NMR structures of apelin-17 have been published [85], there is little structural information available for the other isoforms. The recombinant expression and purification of apelin-36 reported in this chapter will aid future studies investigating both structural and functional aspects of this AR ligand isoform.

The main requirement for functional studies of peptides is to produce a sufficient quantity (typically multi-milligram) of the peptide of interest, and this typically achieved by one of two methods: solid-phase peptide synthesis, or recombinant protein expression using a host organism. In the case of apelin-36, the size of the peptide is towards the upper limit of what can be efficiently produced by synthesis, and previous attempts to synthesize it in our laboratory proved unsuccessful. By contrast, recombinant expression in *E. coli* typically gives large yields, even for longer peptides and large proteins. Moreover, the *E. coli* expression system allows for easy and inexpensive incorporation of NMR-active ^{13}C and ^{15}N

isotopes for structural studies, through the use of minimal medium in which ^{13}C-glucose and ^{15}N-ammonium chloride are the respective carbon and nitrogen sources. In light of these advantages, an *E. coli* expression system was our choice for producing both labelled and unlabelled apelin-36.

Apelin-36 is a relatively small, disordered peptide, which may be prone to poor expression and/or degradation. To offset this, and to aid purification, the peptide was expressed with an N-terminal 6xHis-SUMO fusion tag (Figure 2.1). SUMO, or **S**mall **U**biquitin-like **Mo**difier is a small, globular protein that can be covalently attached to and detached from other proteins by SUMO ligases and SUMO proteases, respectively. By virtue of its size and structure, SUMO is soluble and stable, and recombinant SUMO is highly expressed in *E. coli*, and can confer these same properties onto its covalently bound protein partner [99]. The poly-His tag at its N-terminus allows for purification of a 6xHis-SUMO-tagged protein of interest (P.O.I.) *via* chromatography using an affinity resin containing divalent nickel or cobalt ions. In addition, the SUMO tag can be preferentially removed *in vitro* by the proteolytic action of 6xHis-SUMO protease. This enzyme recognizes the 3D structure of SUMO and cleaves it at a C-terminal recognition site, yielding an intact SUMO and a free P.O.I. with an unmodified N-terminus. The P.O.I. can then be isolated at high purity after another purification step, typically involving removal of the 6xHis-SUMO and 6xHis-SUMO protease by an additional incubation with Ni^{2+} or Co^{2+} affinity resin, or reverse-phase high performance liquid chromatography (RP-HPLC).

In this chapter I report the expression, purification, and cleavage of 6xHis-SUMO-apelin-36, followed by the isolation of pure apelin-36 (both enriched with NMR-active nuclei and at natural abundance), and the confirmation of its presence by mass spectrometry, and of its purity by analytical RP-HPLC. In chapter 3, I conclude this account with the demonstration that the purified peptide is bioactive and capable of activating the AR in human embryonic kidney (HEK) 293A cells.

2.2 Materials and Methods

2.2.1 Materials

pEDHC vector containing the SUMO gene was kindly supplied by the laboratory of Dr. Paul Liu. Phusion polymerase and reaction buffer for polymerase chain reaction (PCR) were purchased from New England Biolabs (NEB; Whitby, ON); dNTPs and DNA primers for amplification of the apelin-36 gene were purchased from Biobasic Inc. (Markham, ON). Ni^{2+}-NTA affinity agarose beads were purchased from Promega (Madison, WI). Acetonitrile, trifluoroacetic acid (TFA), dithriothreitol (DTT), ampicillin, isopropyl β-D-1-thiogalactopyranoside (IPTG), components of LB medium, and reagents for sodium dodecyl sulfate polyacrylamide gel electrophoresis (SDS-PAGE) were purchased from Fisher Scientific (Ottawa, ON). BLUeye prestained protein ladder was purchased from FroggaBio (Toronto, ON). Uniformly ^{13}C labelled glucose and ^{15}N labelled ammonium chloride were purchased from Cambridge Isotope Laboratories (Tewksbury, MA).

2.2.2. Cloning and Expression of 6xHis-SUMO-Apelin-36

The apelin-36 gene was amplified by PCR from a template pET23 plasmid containing the apelin-36 DNA sequence. The thermocycling reaction was performed according to the conditions specified in Table 2.1. The sequences of the forward and reverse primers used were 5'-GTACGCTCTTCAGGACTGGTGCAGCCGCGTGGC-3' and 5'-CATTGGATCCTTAGAACGGCATCGGGCCTTT-3', respectively. Following amplification, the PCR product was enzymatically digested using SapI and BamHI restriction endonucleases (NEB). The digested apelin-36 gene was then subcloned into a pEDHC expression vector using T4 DNA ligase (NEB), immediately downstream of the 6xHis-SUMO gene. The ligated product was transformed into DH5α replication strain *E. coli,* which were grown on LB agar plates selecting for ampicillin resistance. The SUMO-apelin-36-containing plasmid DNA was extracted, and the presence of the correct cloned fusion gene was confirmed by DNA sequencing (Genewiz; South Plainfield, NJ). Figure 2.1 shows the amino acid sequence of the translated fusion gene.

The plasmid was then transformed into BL21(DE3) expression strain *E. coli.*, which were grown in LB medium containing ampicillin (100 mg/L) to an optical density at 600 nm (OD_{600nm}) of 0.6, and then induced to express SUMO-apelin-36 by addition of 0.5 mM IPTG. Cells were incubated at 37 ˚C with shaking for three hours, then centrifuged (6000x*g*, 15 min) and prepared for P.O.I. purification.

For expression of the ^{13}C and ^{15}N labelled peptide, the same transformed BL21(DE3) *E. coli* were grown to an OD_{600nm} of 0.6 in LB medium; these cell

suspensions were centrifuged followed by collection of the cell pellets. Pellets were then transferred to one half equivalent volume of minimal medium (100 mM NaH_2PO_4 , 40 mM K_2HPO_4, 4 mM $MgSO_4$, 1.8 µM $FeSO_4$, 2 g/L uniformly ^{13}C labelled glucose, 1 g/L ^{15}N labelled ammonium chloride, 100 mg/mL ampicillin, pH 7.3). After 30 minutes, expression was again induced by adding 0.5 mM IPTG. Cells were incubated at 37 ˚C with shaking for three hours, after which the cell suspensions were centrifuged (6000x*g*, 15 min) and prepared for P.O.I. purification.

2.2.3 Initial Purification of Apelin-36

Cell pellets were resuspended in lysis buffer (50mM NaH_2PO_4, 300 mM NaCl, 10 mM imidazole, pH 8.0), frozen, thawed, and lysed by sonication. Subsequently DNAase (3 mM) was added, and the suspensions were incubated at 37˚ for 30 min, then centrifuged (6000xg, 30 min). The lysate supernatant was then loaded onto a Ni-NTA affinity purification column, pre-equilibrated with lysis buffer. The column was washed with 4 column volumes of wash buffer (50mM NaH_2PO_4, 300 mM NaCl, 20 mM imidazole, pH 8.0), and then the column-bound protein was collected as a separate fraction upon the addition of elution buffer (50mM NaH_2PO_4, 300 mM NaCl, 300 mM imidazole, pH 8.0). Column flow-through, wash, and elution fractions were analyzed by SDS-PAGE (15% acrylamide), resolved at 170 V for 70 minutes, and visualized using Coomassie Blue stain. Elution fractions were then combined in a single 50 mL falcon tube.

2.2.4 Expression and Purification of 6xHis-SUMO Protease

A pEDHC plasmid containing the 6xHis-SUMO protease gene was obtained from the lab of Dr. Paul Liu, and transformed into BL21(DE3) expression strain *E. coli.*, which were grown in LB medium containing ampicillin (100 mg/L) to an OD_{600nm} of 0.6, and then induced to express 6xHis-SUMO protease by addition of 0.5 mM IPTG. Optimal expression was achieved after two hours of incubation with shaking at 37 ˚C, and the cells were centrifuged (6000x*g*, 15 min) and prepared for purification. The cells were then lysed, and 6xHis-SUMO protease was purified by Ni-NTA affinity chromatography according to the same protocol as 6xHis-SUMO-apelin-36. The presence and approximate concentration of the pure protease were verified by SDS-PAGE, and the protease was stored at -20 ˚C in Ni^{2+}-NTA elution buffer and 50% glycerol.

2.2.5 Cleavage and Final Purification of Apelin-36

The Ni-NTA purified 6xHis-SUMO-apelin-36 was cleaved by the addition of 100 µL recombinantly expressed 6xHis-SUMOprotease and 1 mM dithiothreitol, with incubation at 37˚C for 2 hours. The cleavage product was then lyophilized and resuspended in H_20. This sample was then separated by semi-preparative RP-HPLC (Cosmosil C_{18} column, 5 µm particle, 10 mm x 250 mm (Nacalai Tesque, Kyoto, Japan)) with a non-linear gradient from 2-100% acetonitrile in H_2O, both containing 0.1% trifluoroacetic acid (2-50% acetonitrile from 2-27 min; 50-100% acetonitrile from 27-33 min). Peaks were collected and samples were analyzed by positive mode electrospray ionization (ESI+) mass spectrometry (Dalhousie Mass Spec Lab; Halifax, NS). The purity of this sample was assessed by analytical RP-HPLC (AAPPTec Spirit Peptide C_{18} column, 5 µm particle, 4.6 mm x 250 mm (AAPPTec,

Louisville, KY)) with a linear gradient from 2-100% acetonitrile in H_2O with 0.1% trifluoroacetic acid. The pure apelin-36 fraction was lyophilized and stored at -20 ˚C.

2.3 Results and Discussion

PCR amplification and subcloning of the apelin-36 gene into the pEDHC vector were successful, and apelin-36 was inserted immediately downstream of the 6xHis-SUMO gene, as confirmed by DNA sequencing (Genewiz, South Plainfield; NJ). A schematic of 6xHis-SUMO-apelin-36, as well as the amino acid sequence of the fusion protein, are shown in Figure 2.1. Expression of 6xHis-SUMO-apelin-36 (both enriched with NMR-active nuclei and at natural abundance) was successfully induced with isopropyl β-D-1-thiogalactopyranoside, and initial purification by Ni^{2+}-NTA affinity chromatography was verified by SDS-PAGE (Figure 2.2). This was followed by enzymatic cleavage with the recombinantly expressed and purified SUMO protease, during which most of the fusion protein was successfully cleaved, as shown in Figure 2.3. It is likely that a more complete cleavage can be achieved with a longer incubation and/or the addition of more protease. The crude cleaved apelin-36 was subsequently purified by RP-HPLC (Figure 2.4), to a final yield of ~2.5 mg per L of nutrition-rich (non-minimal) culture medium. Figure 2.5 shows an analytical RP-HPLC chromatogram of the purified, natural abundance apelin-36, demonstrating ~91% purity. The identities of natural abundance and NMR-active isotope-enriched apelin-36 were confirmed by mass spectrometry, indicating masses of 4195.1 Da and 4434.2 Da, respectively (Figures 2.6 and 2.7). According to the ExPasy protein pI/Mw tool, the expected monoisotopic mass of natural

abundance apelin-36 is 4193.29 Da. This discrepancy of 1.9 Da between our experimental mass and the expected mass (which is monoisotopic and assumes that the more abundant ^{12}C isotope will be incorporated 100% of the time) is explained by the statistical likelihood that apelin-36 (chemical formula: $C_{184}H_{297}N_{69}O_{43}S_1$) will incorporate approximately two ^{13}C atoms per molecule, corresponding to a mass increase of 2 Da. The expected mass of 100% ^{13}C- and ^{15}N-enriched apelin-36 is 4444.00 Da, indicating that the labelled peptide incorporated NMR-active ^{13}C and ^{15}N isotopes with approximately 96% efficiency.

Thus, the expression of apelin-36 as a 6xHis-SUMO-fusion protein allowed for successful isolation of the pure apelin-36 peptide. Because SUMO protease cleaves the SUMO C-terminus with high efficiency and specificity, and also can be produced recombinantly in *E. coli*, this protocol provides an efficient and inexpensive means to obtain recombinant peptides in high purity. Of note, the protocol can be applied to produce and purify the remaining bioactive apelin isoforms, as well as the various toddler/ELA isoforms for future comparisons of the signalling properties of these AR ligands.

Table 2.1 The reaction composition and thermocycling conditions used for PCR amplification of apelin-36.

Reaction composition	
Total volume (μL)	50
Buffer	1x Phusion HF buffer
Template DNA (ng)	1
[Primers] (μM)	0.5
Final [Mg^{2+}] (mM)	2
[DNTPs] (μM)	200
Polymerase type and amount	Phusion polymerase, 1 unit
Cycling conditions	
Initial denaturation	98 °C, 30 sec
Number of cycles	25
Melting step	98 °C, 10 sec
Annealing step	60 °C, 30 sec
Extension step	72 °C, 1 min
Final Extension	72 °C, 15 min

Table 2.2 Parent masses of apelin-36 (natural abundance), corresponding to individual multiply charged mass spectrometry peaks shown in Figure 2.6. Each parent mass is calculated by multiplying the peak value by the corresponding charge, then subtracting the value of that charge to correct for the addition of protons.

Actual Peak	Charge	Isotopic Mass (Da)
420.5	10+	4195.0
467.1	9+	4194.9
525.4	8+	4195.2
600.3	7+	4195.1
700.2	6+	4195.2

Table 2.3 Parent masses of apelin-36 (^{13}C- and ^{15}N-enriched), corresponding to individual multiply charged mass spectrometry peaks shown in Figure 2.6. Each parent mass is calculated by multiplying the peak value by the corresponding charge, then subtracting the value of that charge to correct for the addition of protons.

Actual Peak	Charge	Isotopic Mass (Da)
444.3	10+	4433.0
493.7	9+	4434.3
555.3	8+	4434.4
634.5	7+	4434.5
740.1	6+	4434.6

MGHHHHHHGSDSEVNQEAKPEVKPEVKPETHINLKVSDGSS
EIFFKIKKTTPLRRLMEAFAKRQGKGMDSLRFLYDGIRIQADQ
TPEDLDMEDNDIIEAHREQIGGLVQPRGSRNGPGPWQGGR
RKFRRQRPRLSHKGPMPF

Figure 2.1 Schematic representation and amino acid sequence (open reading frame translated from Table 2.2) of 6xHis-SUMO-apelin-36. The 6xHis, SUMO, and apelin-36 elements of the sequence are colour-coded to match the schematic representation.

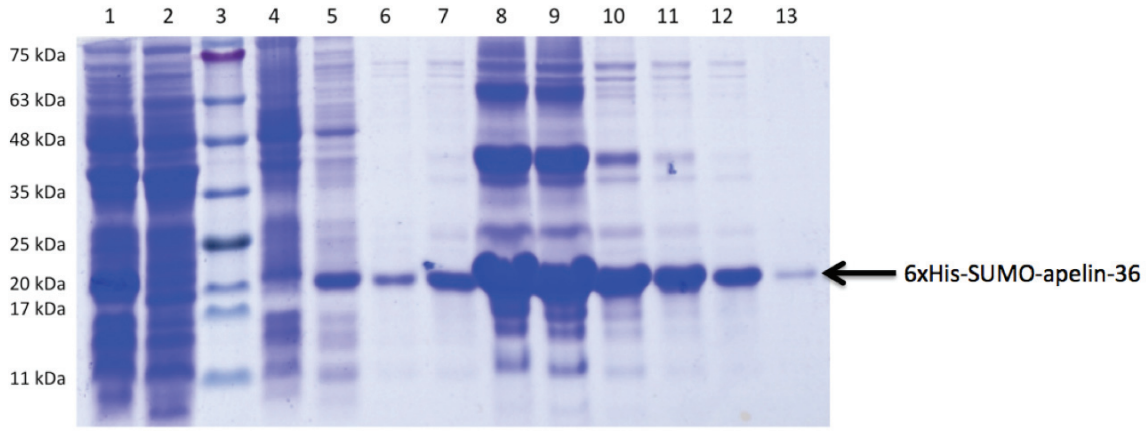

Figure 2.2 SDS-PAGE analysis demonstrating successful expression and initial Ni^{2+}-NTA affinity purification of 6xHis-SUMO-apelin-36. The BLUeye prestained protein ladder (Froggabio) is shown in lane 3. Lanes 1 and 2 contain BL-21 (DE3) *E. coli* cell pellets, 3 hours after induction with 0.5 mM IPTG (1) and without induction (2). Lanes 4, 5, and 6 show the Ni^{2+}-NTA column flow-through, and fractions from two 10 mL washes (20 mM imidazole), respectively. Lanes 7-12 contain samples from 6 x 1 mL elutions, and lane 13 contains a sample from a final 7 mL elution. All elutions were performed at 300 mM imidazole. SDS-PAGE was performed using a 15% acrylamide gel, with electrophoresis at 170 V for 70 minutes. Bands were visualized using Coomassie Blue stain.

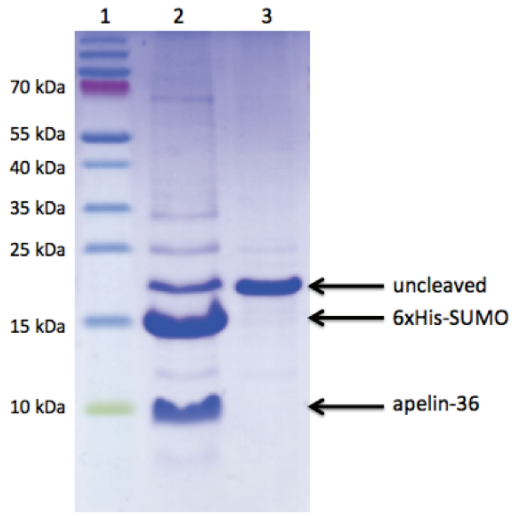

Figure 2.3 SDS-PAGE analysis demonstrating successful enzymatic cleavage of 6xHis-SUMO-apelin-36 by SUMO protease. The PageRuler prestained protein ladder (Bio-Rad) is shown in lane 1. Cleaved 6xHis-SUMO-apelin-36 is shown in lane 2, and the uncleaved sample is shown in lane 3. 6xHis-SUMO-apelin-36 Ni^{2+}-NTA elution fractions were combined and incubated for 4 hours at RT with 100 µL recombinant 6xHis-SUMOprotease and 1 mM DTT in Ni^{2+}-NTA elution buffer. SDS-PAGE was performed using a 15% acrylamide gel, with electrophoresis at 170 V for 70 minutes. Bands were visualized using Coomassie Blue stain.

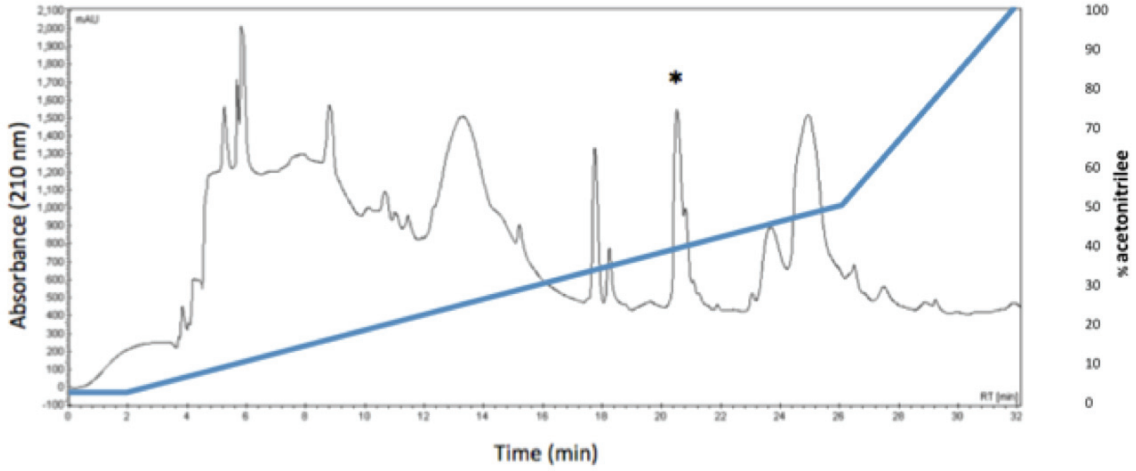

Figure 2.4 Reversed-phase HPLC purification of crude apelin-36. HPLC was carried out using a C_{18} column (5µm particle, 10 mm × 250 mm Cosmosil semi-preparative column, Nacalai Tesque) with a water:acetonitrile solvent gradient progressing from 2% to 100% acetonitrile over 35 min. The peak at ~20.5 min (marked with "*") (~38% acetonitrile; excluding shoulder) corresponds to apelin-36. The blue line indicates the gradient of increasing acetonitrile.

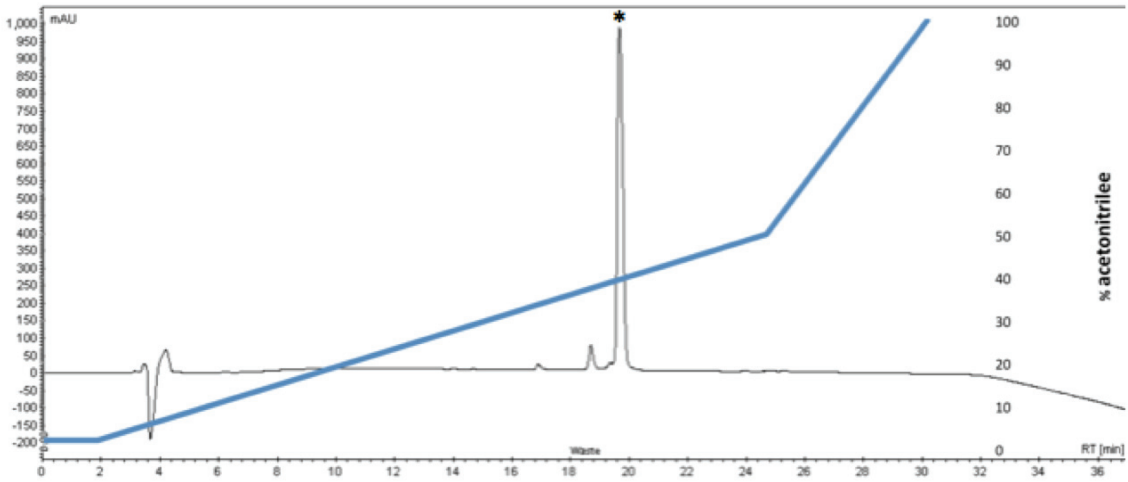

Figure 2.5 Reversed-phase HPLC analysis of purified apelin-36. HPLC was carried out using a C_{18} column (5µm particle, 4.6 mm × 250 mm Spirit Peptide column, AAPPTec) with a water:acetonitrile solvent gradient progressing from 2% to 100% acetonitrile over 35 min. The major peak corresponds to apelin-36 and elutes at ~20 min (~37% acetonitrile). Quantification of peaks indicated ~91% sample purity. The chromatogram was processed by blank-subtraction, and peak areas determined by integration, in Varian's Galaxie software.

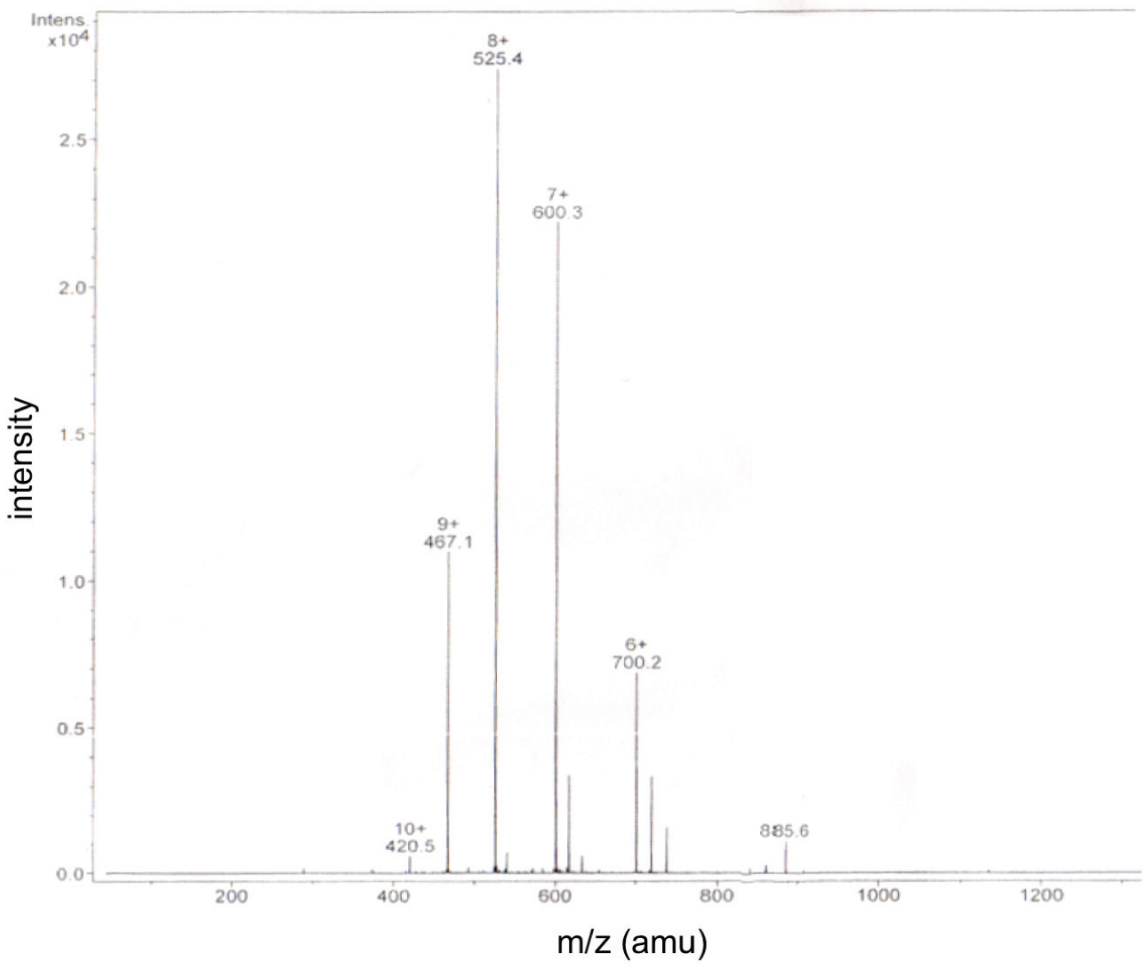

Figure 2.6 Positive mode electrospray ionization mass spectrometry analysis of the unlabelled apelin-36. All multiply charged peaks correspond to unlabelled apelin-36 (see Table 2.2) (m/z range = 4194.9 – 4195.2 amu; expected monoisotopic mass apelin-36 is 4193.29 amu (ExPasy Mw/pI tool)).

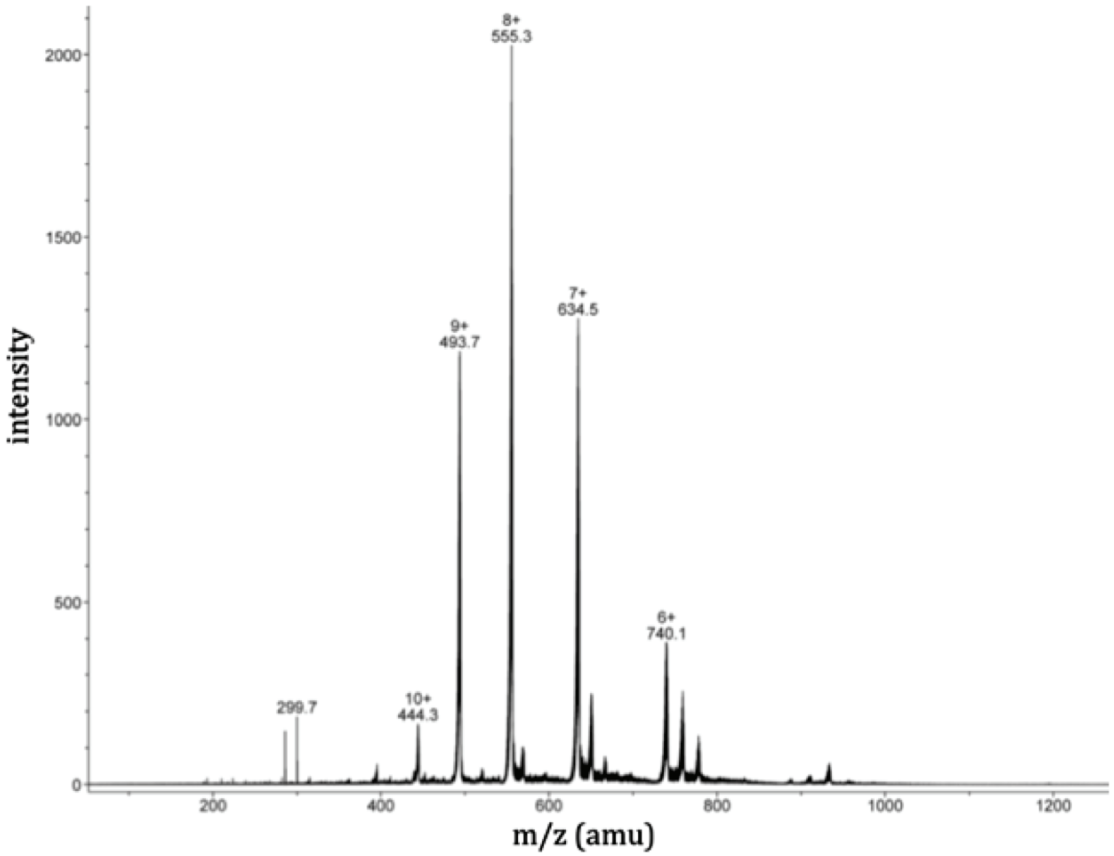

Figure 2.7 Positive mode electrospray ionization mass spectrometry analysis of labelled apelin-36. All multiply charged peaks correspond to $^{13}C/^{15}N$ NMR isotope-enriched apelin-36 (see Table 2.3) (m/z range = 4433.0 – 4434.6 amu; expected mass of 100% $^{13}C/^{15}N$ labelled apelin-36 is 4444 amu).

Chapter 3: Studying the Extracellular Face of the AR

3.1 Introduction

This chapter reports functional characterization of the AR, with a focus on the extracellular (EC) face and the involvement of this region in apelin binding. As discussed in chapter 1, the N-terminus of the AR contributes significantly to the GPCR's affinity for apelin. In particular, removal of the second 10 residues of the N-terminus causes a dramatic reduction in apelin binding affinity (increased K_d), and mutation of key acidic residues E20A and D23A has a similar effect [94]. In addition, it is likely that the extracellular loops (ELs) are involved in apelin binding and AR activation, based on the precedent for their functional importance in other GPCRs [93; 95; 96; 97; 98; 100; 101], as well as their uniqueness as non-conserved regions, and because of their surface location and consequent accessibility to the cationic peptide apelin.

In order to study the EC face of the receptor, the chosen method was to combine site-directed mutagenesis of the AR with functional assays in human embryonic kidney (HEK)293A cell culture. Following transient transfection of a pcDNA 3.1 expression vector containing the wild-type (WT) or mutated receptor gene, AR activation in response to apelin was monitored by measuring the activation (phosphorylation) of ERK (ERK → pERK) downstream of the activated GPCR. The quantification of downstream ERK phosphorylation has been reported

many times as a measure of GPCR activation [102]. Although this event occurs several stages downstream of receptor activation and is therefore not a direct measure of GPCR function, it still provides a valid and semi-quantifiable endpoint to monitor activation. To date, for the AR in particular, a number of studies have made use of this assay [48; 76; 78; 91; 103; 104]. In these studies and the one reported here, visualization of the activated ERK was achieved using western blotting.

In combining site-directed mutagenesis of the EC face with ERK activation assays, the principle is that if a given mutation reduces or enhances AR activation in response to apelin, the amino acid in question must be important for the normal function of the receptor. By mutating residues along the EC face, and observing the effects on AR function, it should be possible to identify key residues involved in apelin binding and AR activation. Thus characterizing the AR-apelin interaction will inform future functional/structural studies of the receptor, and help in the design of novel ligands to modulate this physiologically and pathologically important receptor.

Regarding the choice of which EC face residues to mutate, selections were made based on both previous literature and our own hypotheses about potentially functionally important residues (Figure 3.1). Thus, mutants E20A and D23A were selected based on their previously established importance for apelin binding [94]. Applying the principle that other negatively charged residues might be involved in binding the cationic apelin peptide, residues D92 and D94 in EL1 and E174, E194, and E198 in EL2 were mutated to alanine. Based on the previous finding that TM residues W152, F255, and W259 were important for AR activation by apelin [90],

and in view of the steric and electronic properties of aromatic amino acids, residues F97 and F100 (EL1) and Y182, Y185, and W197 (EL2) were also substituted with alanine. Finally, residues P96, G98, and T99 in EL1 were mutated based on the potential functional relevance, respectively, of their rigidity, flexibility, and hydrophobicity. In addition to these mutated residues, there remain several residues, in particular the negatively charged and aromatic D172, D184, and W195 in EL2, as well as residues in EL3 and potential disulfide forming cysteines. These residues have not yet been mutated, but their functional characterization remains a goal of this project.

The results and discussion that follow report functional data for the WT AR and the aforementioned 16 mutants of the N-terminus and ELs, and discuss the implications of these findings on our understanding of the AR-apelin interaction. In addition, a report is given of the successful activation of the AR by the recombinant apelin-36, the production and purification of which was discussed in chapter 2. Lastly, this chapter addresses some limitations of the ERK activation assay, outlines additional data that need to be gathered, and suggests alternative methodologies that should be considered for future study of mutant AR activation.

3.2 Materials and Methods

3.2.1 Materials

pcDNA 3.1 vector containing the N-terminally triple haemagglutinin-tagged AR (3xHA-AR) gene was purchased from the Missouri University of Science and

Technology cDNA resource center (Rolla, MO). Phusion polymerase and reaction buffer were purchased from New England Biolabs (NEB; Whitby, ON); dNTPs and DNA primers for mutagenesis of the 3xHA-AR gene were purchased from Biobasic Inc. (Markham, ON). Cell culture dishes were purchased from Corning (Tewksbury, MA). Fetal bovine serum (FBS) was purchased from Invitrogen (Burlington, ON). Primary antibodies for ERK (rabbit polyclonal) and pERK (pTyr204; mouse monoclonal) were purchased from Santa-Cruz (Dallas, TX). Non-cross-reactive Dylight 549-conjugated donkey anti-rabbit and Dylight 649-conjugated donkey anti-mouse secondary antibodies were purchased from Rockland (Gilbertsville, PA). The apelin-13 administered to AR-transfected HEK293A cells was produced in-house (Nathan Weatherbee-Martin, BScH) by solid-phase peptide synthesis and purified by RP-HPLC using protocols detailed previously [85]. Laemmli sample buffer for SDS-PAGE and nitrocellulose membrane were purchased from Bio-Rad (Mississauga, ON). BLUeye prestained protein ladder was purchased from FroggaBio (Toronto, ON). Other reagents for SDS-PAGE were purchased from Fisher Scientific (Ottawa, ON). Dulbecco's Modified Eagle's Medium (DMEM), penicillin-streptomycin solution, Protein A Sepharose beads, and all other chemicals were purchased from Sigma-Aldrich (Oakville, ON).

3.2.2 Site-Directed Mutagenesis of the AR

The WT 3xHA-AR gene was mutated according to the guidelines of the Quikchange (Stratagene, Wilmington, DE) mutagenesis protocol. Thus, mutually complementary forward and reverse primers were designed containing codon

mismatches with the AR gene at the site of amino acid substitution. These central mismatched regions were flanked by regions complementary to the AR gene. Subsequently, thermocycling reactions were performed using Phusion polymerase (New England Biolabs), allowing generation of mutated circular plasmids from the template WT AR pcDNA 3.1 vector. Alanine single point mutations in the AR N-terminus (E20A and D23A), and along EL1 (D92A, D94A, P96A, F97A, G98A, T99A, F100A) were prepared by David Langelaan, PhD. EL1 mutant C102S was prepared by Ryan Holstead, BScH. Alanine single point mutations along EL2 (E174A, E194A, Y182A, Y185A, E194A, W197A, E198A) were prepared by myself. All constructs were confirmed by sequencing (Genewiz Inc, South Plainfield, NJ). The primer sequences and thermocycling reaction conditions used for mutagenesis are listed in Tables 3.1 and 3.2, respectively.

3.2.3 Cell Culture, AR Gene Transfection, Apelin Stimulation, and Preparation of Lysates

Human Embryonic Kidney (HEK) 293A cells were subcultured in 10 cm dishes and grown in DMEM containing penicillin and streptomycin (500 units/L) supplemented with 10% Fetal Bovine Serum (FBS). At ~70% confluence, cells were transfected by addition of 500 μL of a serum-free DMEM solution containing 10 μg of the AR-coding pcDNA 3.1 plasmid and 100 μg of polyethylenimine (PEI). Cells were incubated with the transfection mixture for 24 hours, at which time the medium was aspirated and refreshed with serum-free DMEM (no FBS). After an additional 24 hours, plates of cells were stimulated with apelin-13. For initial

experiments, plates were treated in pairs constituting stimulated (1 μM, apelin-13) and non-stimulated (DMEM, no apelin), respectively, for 4 minutes. For dose-response experiments, plates were treated with a range of apelin concentrations (10^{-11} M – 10^{-6} M) and compared to a non-stimulated sample. Immediately after stimulation, the medium was aspirated and cells were harvested with 1.5 mL cold phosphate buffered saline into microcentrifuge tubes and centrifuged (13 000x*g*, 1 min, 4 ˚C). Cell pellets were treated with 6 μL DNase I (10 mg/mL) then resuspended in 150 μL radioimmunoprecipitation assay (RIPA) buffer with added protease inhibitor cocktail (50 mM Tris/HCl, pH 7.5, 10 mM $MgCl_2$, 150 mM NaCl, 0.5% sodium deoxycholate, 1% Nonidet P-40, 0.1% SDS, Complete Protease inhibitors (Roche, Laval, QC)). To aid in separation of a protein fraction free from cellular debris, 30 μL of a suspension of Protein A Sepharose beads (100mg/mL) in RIPA containing bovine serum albumin (BSA) were added to each sample; the samples were vortexed, and allowed to nutate at 4 ˚C for 20 minutes. Finally, lysates were centrifuged (13 000x*g*, 15 min, 4 ˚C) and the supernatant protein fractions were collected and added to 150 μL of 2x Laemmli sample buffer. Samples were again allowed to nutate at 4 ˚C for 5-10 minutes, after which they were either heated at 65 ˚C for 10 min to prepare for SDS-PAGE loading, or kept at -20˚C for future analysis.

3.2.4 Resolution of Lysate Proteins by SDS-PAGE and Western Blotting Analysis

Lysates were resolved by SDS-PAGE at 200 V for 40 minutes. Protein was then transferred from the gels onto nitrocellulose membranes by electrophoresis at 115 V for 60 minutes. Each membrane was blocked for one hour in 25 mL of tris-buffered saline (TBS) containing 2 % BSA (weight by volume), and then incubated in 5 mL blocking buffer containing primary antibodies for ERK (polyclonal rabbit, 1:1000) and pERK (monoclonal mouse, 1:500) at 4 ˚C overnight. Membranes were washed, and fluorophore-conjugated secondary antibodies (Dylight 549, donkey anti-rabbit, 1:2000; and Dylight 649, donkey anti-mouse, 1:1000) were applied in 5 mL blocking buffer for 1 hour. Membranes were again washed, dried, and then imaged by fluorescent excitation and detection using a VersaDoc imaging system (Bio-Rad). Digital images were analyzed using Bio-Rad's Image Lab software.

3.2.5 Statistical analysis

AR activation data were compared using statistical analysis in Graphpad's Prism 6 software. Activation data collected for the AR EC face mutants in response to 1 μM apelin-13 were compared using a one-way analysis of variance (ANOVA) test, with α equal to 0.05. P values for differing levels of significance are given in the corresponding figure captions. Apelin-13 dose-response data from individual experiments were plotted as "fold increase in pERK" versus "log[apelin-13]", and fit to a sigmoidal curve defined by the equation,

$$y = \frac{(E_{max} - 1)x}{EC_{50}} + 1$$

wherein y represents the fold increase in pERK value; x represents the log[apelin-13] value; E_{max} is the maximal pERK response, or the maximum y-axis value

approached by the curve; and EC_{50} is the half-maximal effective concentration, or the x-axis value corresponding to the point where the slope of the curve is steepest. The addition of "1" as a second term reflects the 1-fold increase in response to zero apelin-13, and this value was constrained to 1 in the fitting of experimental data. EC_{50} and E_{max} values were derived from the individual dose-response curve fits, and average EC_{50} and E_{max} values were determined from the means of at least three independent experiments. Experimental EC_{50} and E_{max} values of all constructs were compared to the apelin-13-activated WT AR using unpaired t tests, and differences were judged significant in cases where the P value was less than 0.1.

3.3 Results And Discussion

3.3.1 Functional Characterization of Mutants of the EC Face of the AR

Site-directed mutagenesis of the 3xHA-AR EL2 was successful, as confirmed by DNA sequencing (Genewiz; South Plainfield, NJ) and the function of these mutants, as well as those of the N-terminus and EL1 (pictured in Figure 3.1), was probed in HEK293A cells. All AR constructs were derived from an N-terminally haemagglutinin-tagged AR (3xHA-AR), allowing for future verification of cell-surface localization of the WT and mutated receptors. The mutants were evaluated in comparison to the WT AR based on their ability to activate downstream ERK signalling in response to apelin-13. For these initial studies, a dose of 1 μM apelin-13 was administered for 4 minutes to cells expressing the WT or mutant AR. This dose and time-course were selected based on a precedent set by previous studies of AR

activation, which have shown that 1 μM apelin-13 induces maximal ERK phosphorylation (E_{max}) downstream of the AR, and that this maximal effect occurs between 3 and 5 minutes post-stimulation [76; 78; 103]. A dose and time-course promoting maximal activation were selected with the aim of inducing the strongest possible pERK signal. Moreover, a previous study demonstrated that mutations to the AR N-terminus caused changes in the activation of $G\alpha_q$ that were detectible in response to a maximal dose of 3 μM apelin-36 [94].

3.3.1.1 Functional Characterization of N-terminal Mutants E20A and D23A

Figure 3.2 shows the activation data collected for the N-terminal mutants E20A and D23A. As mentioned earlier, these mutants were previously shown to have greatly reduced binding affinity for apelin-13 [94]. In addition, when HEK293 cells stably expressing the WT, E20A, or D23A AR were treated with 3 μM apelin-36, both mutants showed significantly reduced downstream Ca^{2+} mobilization in response to the ligand, with D23A in particular showing effectively no response [94]. However, when our transiently transfected cells were treated with 1 μM apelin-13, both mutants induced ERK phosphorylation at levels equivalent to the WT AR (Figure 3.2). By contrast, negative control cells transfected with the angiotensin II receptor type 1 (AT_1R) showed no ERK phosphorylation in response to apelin-13.

Strikingly, no difference in ERK activation was observed for these mutants, despite their previously reported loss of affinity for apelin-13, and their reduced Ca^{2+} signalling in response to apelin-36. As introduced in chapter 1, the AR can

couple to both $G\alpha_i$ and $G\alpha_q$, with the former being the primary mediator of ERK activation downstream of the AR [76], and the latter being responsible for Ca^{2+} mobilization and other related effects [46]. Therefore, one explanation for the unattenuated ERK signalling of the E20A and D23A mutants is that mutation of these residues produces a receptor that is biased towards $G\alpha_i$ and away from $G\alpha_q$. This would be explained along the following lines: the E20A and D23A mutations reduce the affinity of the AR for apelin. This lower-affinity apelin-AR interaction still activates the receptor, but the "active" conformation it stabilizes is different (or simply shorter-lived) than the conformation adopted by the WT AR upon apelin-binding. Importantly, this new "active" conformation favours $G\alpha_i$ interactions at the expense of $G\alpha_q$ interactions. As a result, the coupling of the mutated AR to $G\alpha_i$ remains intact and apparently unattenuated, while the coupling to $G\alpha_q$ is reduced or completely abrogated.

On the other hand, it may be that both $G\alpha_i$ and $G\alpha_q$ coupling are attenuated, but that this effect is more evident for the $G\alpha_q$ pathway at the high apelin doses (1 and 3 μM) in question. This would likely be the case if $G\alpha_i$ signalling is typically the more prominent route of AR signalling, with $G\alpha_q$ signalling being present only at high concentrations of ligand or in response to long-lived, high affinity apelin-AR interactions. In this case the reduced apelin-affinity conferred by the E20A and D23A mutations would affect $G\alpha_q$ signalling "first", before attenuation of the $G\alpha_i$-mediated ERK cascade would be observed. In this model, the latter $G\alpha_i$-mediated signalling could still proceed even if the AR adopted an "active" conformation only

very briefly, which would be the rule for the E20A and D23A mutants because their affinity for apelin is so far below the WT.

Finally, it should be noted that the previous Ca^{2+} mobilization studies involved treatment with apelin-36 [94], whereas our ERK activation measurements were made in response to apelin-13. Though in general, it seems likely that AR mutations would have similar effects on apelin-13- and apelin-36-induced signalling, the fact that different isoforms were being administered prevents the results from being directly comparable.

3.3.1.2 Functional Characterization of EL1 mutants

For most of the EL1 mutants, similar behaviour was observed. In fact, none of the mutations, with the exception of C102S, had any detectable effect on apelin-induced ERK phosphorylation – all these mutants mediated the same response as the WT receptor (Figure 3.3). EL1 is the region of the EC face that is most highly conserved between the AR and the AT_1R, so it is perhaps not surprising that these residues would not have a significant role in the binding affinity/specificity of the AR for apelin vs. angiotensin II. That is, given that angiotensin II does not activate the AR, it makes sense that amino acids shared by both the AR and the AT_1R would not contribute significantly to the affinity and specificity of apelin for the AR. Other, less-conserved residues on the EC face may be more likely to contribute to the specificity of the apelin-AR interaction.

However, the effect of the C102S mutation – slightly increased ERK activation – is perhaps less intuitive. Close to the membrane interface between EL1 and TM3,

C102 is a widely conserved residue among class A and B GPCRs that commonly forms a disulfide with another conserved cysteine (C181) in EL2 (illustrated in Figure 3.1). For example, in the case of the AT_1R, disruption of this disulfide reduces the affinity of the GPCR for Ang II by ~10 fold, whereas binding of a non-peptidic agonist, EXP-985, is completely ablated. If both this disulfide and another between the N-terminus and EL3 are disrupted, the binding of Ang II by the AT_1R is completely ablated [105]. The case for the AR may be similar – that is, disruption of the C102-C181 disulfide may partially reduce apelin binding, yet still allow AR activation at high concentrations of apelin; conversely, simultaneous mutation of both C102 and C19 or C281 may totally prevent apelin binding and AR activation. On the other hand, in other GPCRs, disruption of this disulfide between El1/TM3 and EL2 has led to constitutive activation of the receptor in the absence of ligand, suggesting that the role of this disulfide is to constrain the receptor in an inactive conformation, with EL2 acting as a negative regulator. When the disulfide is broken, EL2 gains conformational flexibility, decreasing the energy barrier between the inactive and active conformations [106]. From our initial experiments, the meaning of the slightly increased C102S-mediated ERK activation is unclear. Further study of this and other mutants of putative disulfide-forming residues will help to clarify its role.

3.3.1.3 Functional Characterization of EL2 mutants

Finally, characterization of the EL2 mutants (Figure 3.4) revealed a few noteworthy effects. Namely, mutants E174A, W197A, and E198A all showed

reduced ERK phosphorylation in response to apelin-13. Of these three, E174A had the strongest effect, the effect of E198A was less significant, and W197A had the least significant effect on activation. The involvement of these EL2 residues makes sense in principle. In particular, E174 and E198, like the functionally critical E20 and D23 in the N-terminus, are negatively charged residues which likely interact with the highly cationic apelin peptide, and may be involved in the initial attraction of apelin to the AR, its proper positioning, and/or the entry of its C-terminus past the EC face and into the AR binding pocket. Similarly, the aromatic W197A, like the key aromatic residues buried in the AR binding pocket (W152, F255, W259) [90], may, by virtue of its steric and/or electronic properties, interact with aromatic or other residues on apelin. Thus W197 too could play a role in allowing or directing the entry of apelin into the transmembrane binding site.

These three mutations in EL2 were the only ones found to cause a reduction in maximal ERK activation. It will be necessary to verify the normal cell surface expression of these mutants, to confirm that this reduction is indeed the result of an altered apelin-AR interaction, and not due to retention of the mutated receptors inside the cell. This verification can be performed using on-cell ELISAs (enzyme-linked immunosorbent assays; also known as On-cell westerns™ (Li-Cor)) to calculate the ratio of 3xHA antigen present at the cell surface of unpermeabilized cells versus the total 3xHA antigen present in detergent-permeabilized cells.

3.3.2 Effect of Apelin-13 Concentration on Detection of Altered ERK Activation.

Thus, the apelin-induced ERK activation assays highlighted a few residues – E174, W197, and E198 in EL2 – which, because of the reduced activation mediated by their respective mutants, may be functionally important for the AR-apelin interaction. However, only these three of the 16 mutants characterized had an attenuated response to apelin-13. Nor was their response completely abrogated, but rather reduced by a partial, though significant, amount – indicating that none of these residues, individually, is critical to the AR's functional response to apelin.

Moreover, the characterization of the N-terminal mutants E20A and D23A, whose ERK response was completely intact, despite their greatly reduced affinity for apelin [94], led us to question the use of a single, relatively high apelin concentration in our ability to detect altered ERK activation. In interpreting this finding, it is helpful to consider apelin binding and AR activation with respect to the pharmacological parameters: affinity (K_d), efficacy, potency (EC_{50}), and maximal effect (E_{max}) [107]. Receptor-ligand affinity, or K_d, is measured in units of concentration, and reflects the concentration of ligand at which half the receptor binding sites are occupied by ligand. Thus a smaller K_d reflects tighter binding, and *vice versa.* However, strong affinity alone does not lead to receptor activation; the bound ligand must also have efficacy, or the ability, once bound, to activate the receptor. Thus at a given concentration, two ligands may have the same K_d, yet if one has higher efficacy, receptor activation, and therefore the magnitude of downstream effects, will be greater. Potency, described in terms of the half-maximal effective concentration (EC_{50}) of ligand, is a combination of affinity and efficacy, and indicates the concentration of a ligand required to induce 50% of the maximal downstream

response. This maximal downstream response, for a given functional readout (*e.g.* ERK phosphorylation), is referred to as the E_{max}. Importantly, the E_{max} may or may not vary when the receptor is mutated to alter the affinity or efficacy, and thus the potency, of the receptor-ligand pair.

All of these parameters together highlight the interrelationship of a number of factors that, for our purposes, culminate in the signal – ERK phosphorylation – by which we quantify AR activation. These include the ligand concentration; the concentration of receptors at the cell membrane; and the cellular machinery available to transduce the GPCR signal downstream *via* second effectors, desensitize cells by receptor internalization and recycling/degradation, and so on. Considering this, it becomes clear that even if a given mutation reduces the GPCR-ligand affinity (thus reducing ligand potency), it may not necessarily reduce the maximal downstream response (E_{max}) for a given functional readout. Thus, at a high enough dose of apelin, even though a certain mutation of the AR EC face may significantly affect apelin affinity/potency, such effects will not be detectible by our experimental methods, should the E_{max} for ERK phosphorylation remain unaltered

For example, a study by Conner *et al.* (2007), in which the residues in EL2 of the vasopressin receptor ($V_{1a}R$) were systematically mutated to alanine, identified several mutants with drastically (~200 to 2300-fold) reduced affinity for the peptide vasopressin (VP) [95]. The authors also collected dose-response data for these low-affinity mutants, evaluating their ability to mediate $G\alpha_q$-coupled IP_3 production. Strikingly, they observed that while the potencies of VP at these mutant receptors were reduced (EC_{50} values ranging from ~7 to 40-fold above the WT), the

maximal VP_1R-mediated IP_3 production (E_{max}) of the mutants was unaffected, relative to the WT.

These are important residues at the VP_1R EC face, contributing to ligand affinity and potency, and potentially directing the ligand towards the binding site, which are nevertheless not required for receptor activation. Their loss does not prevent G-protein coupling or β-arrestin recruitment, and, when the ligand is present at a high enough concentration, their presence or absence makes no difference to the maximal signalling response that is produced. Conversely, it should be noted that there might be residues in a GPCR, the alteration of which renders the GPCR incapable of being activated by any concentration of ligand [95; 108]. In contrast to these "functionally critical" residues, some EC face residues – including perhaps E20A and D23A of the AR, and others – may contribute greatly to the affinity and potency of the GPCR-ligand interaction, yet not be required for the functional coupling of the receptor to downstream signalling pathways.

3.3.2.1 Apelin-13 Dose-Response for the WT AR and Several Mutants

All this being said, it is clear that the apelin concentration with which the AR-transfected cells are treated can have a major impact on whether or not mutation-induced changes in AR signalling will be detectable. Namely, a high enough concentration may induce the same maximal response (E_{max}) regardless of changes in the ability of apelin to activate the mutated AR. Thus, to evaluate the effect of varying apelin-13 dose on AR activation, and to determine experimentally the E_{max} and EC_{50} values, a series of dose-response experiments was carried out for the WT AR, and for the mutants E20A, D23A, and E174A.

Figure 3.5 shows four independent replicates of the apelin-13 dose-response of WT AR-mediated ERK activation (details of individual fits shown in Table 3.3). From the average of the ligand concentration required to produce half the maximal pERK response, an experimental EC_{50} of 0.4 nM ± 0.1 nM was determined (Table 3.4). Evidently, this EC_{50} is several orders of magnitude lower than the 1 μM dose used in the WT and mutant AR activation experiments reported above. As mentioned previously, this 1 μM dose was selected based on the precedent set by previous AR activation studies monitoring ERK phosphorylation, wherein 1 μM was the most commonly administered dose [76; 78; 91; 103]. Some of these functional studies characterized only the WT AR – raising the possibility that the high apelin concentration in question might be less well suited to the detection of differences between AR mutants. However, our laboratory previously used this assay to identify several mutants of the AR transmembrane domain 1 (TM1) with significantly reduced ERK signalling, even at a 1 μM dose of apelin-17 [91]. Likewise, Zhou *et al.* demonstrated reduced Ca^{2+} mobilization by the E20A and D23A mutants, even while administering 3 μM apelin-36 [94]. Thus, there is precedent to show that altered AR-mediated ERK signalling can be detected even at apelin doses well above the EC_{50}.

Nevertheless, based on our results and the principles discussed above, it seemed likely that the high dose of apelin-13 administered thus far could explain the discrepancy between the reduced affinity of the E20A and D23A mutants and their apparently unaffected mediation of ERK activation. Moreover, other mutants, such as the EL2 mutant E174A, might be affected more severely than our 1 μM apelin-induced ERK activation data could detect. Therefore, dose-response data were

gathered for these three mutants, the results of which are presented in Tables 3.3 and 3.4 and Figures 3.6, 3.7, and 3.8.

As Table 3.4 shows, none of the three mutants in question mediated a reduced maximal ERK response (E_{max}) to apelin-13. However, the potency of apelin-13 was significantly reduced ($P < 0.1$) at E20A (EC_{50} = 1.3 ± 0.2 nM), D23A (EC_{50} = 12 ± 1 nM), and E174A (EC_{50} = 11 ± 6 nM), releative to the WT AR (EC_{50} = 0.4 ± 0.1 nM). These results serve to confirm that mutations at the EC face of a GPCR can alter the affinity (K_d) and potency (EC_{50}) of a ligand without altering the E_{max}, which will be reached at a high enough dose of ligand, despite the increased K_d and EC_{50}. They also corroborate previous findings regarding the reduced affinity and activation of mutants E20A and D23A [94], showing that despite having an unaltered E_{max} for pERK production, the response to apelin of these mutants was nevertheless attenuated. Likewise, they confirm our initial finding that residue E174 has an important role in the apelin-AR interaction and in AR activation. The importance of this latter residue supports our hypothesis that negatively charged residues on the AR EC face can interact with apelin – strengthening the affinity and specificity of apelin for the AR, and contributing to the potency of this cationic peptide. This also confirms the need for dose-response characterization of additional EC face mutants – in particular W197A and E198A, which mediated reduced ERK activation in response to 1 μM apelin-13, and of additional mutants of EL2 and EL3 still to be prepared.

The finding that the potency of apelin-13 at mutant D23A was more significantly reduced than at E20A, relative to the WT AR, was not unexpected.

Previous functional characterization of E20A and D23A found that, of the two mutations, D23A caused a greater loss of affinity for apelin; moreover, while the Ca^{2+} mobilization of D23A was completely abrogated, that of E20A was still partially intact, though attenuated [94]. Thus, the finding that D23A has more severely reduced pERK activation is consistent with previous literature.

3.3.2.2 Confirmation of Apelin-36 Bioactivity: Dose-Response at the WT AR

Chapter 2 described the production and purification of recombinant apelin-36 from *E. coli.* To verify that the purified peptide was bioactive, apelin-36 dose-response experiments were performed in HEK293 cells expressing the WT AR (Figure 3.9). The results show that the recombinantly expressed apelin-36 is a functional activator of the AR. These experiments yielded a calculated EC_{50} of 3 ± 2 nM (Table 3.4). Although, due to a large associated error, this value does not differ significantly from the EC_{50} of apelin-13, qualitatively it appears that the apelin-36 EC_{50} is higher. Moreover, this is to be expected based on previous studies comparing the AR-mediated cellular responses to these two peptides, which observe a lower potency for apelin-36 versus apelin-13 [32; 76; 79]. The lack of a statistically significant difference between the EC_{50} values of apelin-13 and apelin-36 at the WT AR can be attributed in part to the limited resolution of our ERK activation assay. In particular replicates #1 and #3 of the apelin-36 dose-response experiments differ by one to two orders of magnitude from replicates #2 and #4. This resulted in a large standard error that would likely be reduced with further experimental replicates. Thus, whereas the mean values appear different, the large standard error

prevents us from concluding that apelin-36 is significantly less potent than apelin-13.

3.3.2.3 Conclusions Drawn from AR Dose-Response Experiments

The results reported above identify several key residues on the EC face of the AR that are involved in apelin binding and AR activation. They also highlight an important difference between ligand affinity and efficacy. Namely, reduced ligand affinity does not necessarily correspond to reduced receptor activation. To use a relevant example, we know from previous literature [32; 76] that the binding affinity of apelin-36 is stronger than that of apelin-13. Yet perhaps because of this, the lower-affinity apelin-13 is the more potent activator of certain downstream signalling pathways [32; 76]. This has been rationalized because the high-affinity apelin-36-AR interaction causes formation of a stable complex with β-arrestin, leading to prolonged intracellular retention of the AR. By contrast, the low-affinity apelin-13-AR interaction is transient, permitting fast dissociation from β-arrestin and recycling to the cell surface, hence the greater potency of apelin-13 [79].

Considering such an example, it seems logical that a further reduction in affinity (induced by mutation of the EC face), might not adversely affect AR activation. Yet, while the affinities and potencies of apelin-13 and -36 are inversely correlated, there are clearly cases when the reduced binding affinity of a ligand correlates with reduced potency. Such appears to be the case for the mutants E20A, D23A, and E174A (noting, though, that this can only be conclusively stated for E20A and D23A, as no affinity data have been gathered for E174A). In any case, it is clear that the maximal activation (E_{max}) of a given pathway need not be affected, even in

the presence of mutations causing significant reductions in ligand affinity and potency.

3.3.3 Caveats Concerning the Study of Exogenous Proteins in Cell Culture

The study of GPCR function in HEK cells, with ERK in particular as a downstream readout, warrants a few remarks and caveats. The study of transfected proteins in cell culture, despite taking place in a living system, is generally referred to as *in vitro* methodology. This is to distinguish it from truly *in vivo* systems, the observation of which is considered far more relevant to the actual physiology and biochemistry of complex organisms. Thus, our experimental system is artificial in a few important ways. Firstly, cell lines are genetically abnormal – the most evident manifestation of which is their immortality, or property of proliferating indefinitely, rather than ceasing proliferation (becoming senescent) as other cells eventually do. Secondly, the addition of exogenous genes in the form of DNA vectors can lead to production of exogenous protein at levels far above normal physiological expression. Although highly expressed exogenous proteins can provide a stronger signal for a given functional readout, and likewise reduce the potential impact of background signal from endogenous proteins, we must be aware that their presence in such quantities affects not only their own function, but that of all components of the cell, either directly or indirectly. Nevertheless the transient transfection/over-expression system is versatile and provides a way to observe the behaviour, not only of wild-type proteins, but also of mutated forms that do not exist endogenously, and compare their properties. For the HEK293A line in particular, there is precedent

for studying GPCR activation in these cells, and no endogenous expression of the AR has been detected, making them a suitable choice for studying AR function [109].

3.3.4 Limitations in the Quantification of pERK Western Blots

As indicated above, the densitometry of western blots reported here had certain limitations in sensitivity and reproducibility. Several factors contribute to these limitations and are discussed below.

In our case, quantified bands were normalized as effectively as possible within a given blot. For example, all quantified pERK bands (visualized with one fluorescent antibody) were divided by the corresponding total ERK bands (visualized with a second fluorescent antibody). In this way we could account for variations in the total amount of protein loaded into the wells of SDS-PAGE, as total cellular ERK should not vary between the various apelin-stimulated and non-stimulated samples. Likewise, for a given experiment, all activation data were analyzed as "fold-increase in pERK" values, in that all apelin-stimulated samples (whether for a single 1 μM dose or for a range of concentrations) were divided by the corresponding non-stimulated sample. This analysis of activation data as "fold-increase" ratios (as opposed to absolute values) was necessary because experiment-to-experiment (blot-to-blot) variations in the antibody signal visualized on a membrane prevent the derivation of absolute values of protein levels from the blots. Alternatively, measurements can be normalized against a reference "housekeeping protein," assumed to remain constant between control and treated samples; however, these rely on the levels of reference protein being unaltered between samples under experimental conditions, which is not always the case [110].

Moreover, relative variations in the density of the reference bands do not necessarily correspond to the same relative changes in reference protein level [111]. Thus normalization against a reference housekeeping protein is prone to similar variations in specific and background signal and densitometric quantification as the "fold-increase" ratiometric method.

In any case, while normalization was performed, and the method of quantification was valid in principle, issues of poor signal-to-noise, in combination with a limited dynamic range of signal, led to challenges in quantifying the blots, and in turn to significant variability between experiments. Ultimately, comparison of all samples to the "non-stimulated" (NS) sample proved to be one of the most problematic aspects of quantification. In a sense, this practice makes the NS sample the single most important value on the blot – at least for E_{max} values and the y-axis scale of pERK fold-increases – because the magnitude of all other values depends on it. At the same time, this value, by definition, should have the weakest pERK signal of any sample on the western blot, because no apelin is added to induce ERK phosphorylation. The result is that this important NS sample is also the most prone to being obscured or buried by the background signal, and such variations can lead to large fluctuations in its relative magnitude.

Put another way, if this weak NS sample could be said to have a 100% pERK signal on a given day, another day it might have only a 50% signal due to a (relatively small) increase in the overall background signal on the membrane. This increased background would also affect the other, apelin-stimulated lanes, but the relative impact on these lanes would be much less, because they would have had a

much higher pERK intensity to begin with. The net result of this would be a significant inflation of the "fold-increase in pERK" values (y-axis), causing the E_{max} values for this particular experiment to be substantially higher than usual (*e.g.* Figure 3.9, panels b and c). Fortunately, the EC_{50} values (x-axis) would not be affected. A corresponding opposite effect would be observed if, for a given experiment, the NS signal was 50% stronger than usual – which could occur due to lower background fluorescence on the membrane, or if natural cellular variations caused the baseline quantity of pERK to be slightly higher than usual. Overall the principle is that a "small" absolute change has little relative effect on the magnitude of a large value, but the same change has a much bigger relative effect on the magnitude of a small value.

In addition to the variation arising from low signal-to-noise ratios, our western blotting was limited by the relatively narrow linear dynamic range (LDR) of pERK signals detected using our fluorescent secondary antibodies. In most cases, stimulation of the WT AR with a high (1 μM) dose of apelin led to a maximal increase in pERK to ~4-fold above the basal level. Although in some cases densitometry yielded maximal values as high as 10- or 12-fold, these are more likely artifacts of the quantification process described above than values representing true increases. This being said, pERK typically ranged from the 1-fold change defined for the NS sample, to a ~4-fold change associated with maximal stimulation. Naturally, this limited dynamic range, in combination with the substantial variability between experiments, made it difficult to precisely determine the apelin dose at which maximal activation was reached, limiting the precision of experimental EC_{50} values.

The cause of this limited LDR could be either cellular (cells quickly reach maximal ERK activation, saturating the signalling pathway so that no more ERK phosphorylation occurs) or technical (antibody-conjugated fluorophores quickly reach saturation when bound to a large enough quantity of pERK, so that greater quantities of pERK cannot be detected), or a combination of both. In our antibody detection system, fluorescent, rather than chemiluminescent, secondary antibodies were used. Fluorescent detection has been shown to have tenfold greater quantifiable LDR than chemiluminescent detection, at the cost of two- to fourfold lower sensitivity [112]. As such, the -fold pERK increases derived from fluorescence should more accurately represent actual changes in protein concentration within the cell, but their lower sensitivity will limit detection of smaller amounts of protein (*e.g.* the NS sample, with its weak pERK signal). If ligand-induced activation is evaluated by comparison to the NS sample, the obscuring of this important signal by background fluorescence may outweigh the improved LDR of fluorescent detection. In any case, both chemiluminescence and fluorescence have their advantages and disadvantages, which should be considered when designing new experiments.

3.3.5 Conclusions and Future Directions

The findings reported above provide activation data for the WT AR, as well as 17 mutants of the N-terminus and ELs. In addition, they demonstrate the activity of the recombinant apelin-36, the production of which was discussed in chapter 2. The data collected for the WT AR and all mutants at a 1 μM dose of apelin-13 led to identification of several significant differences in AR-mediated ERK activation. To determine the impact of apelin-13 concentration on our ability to detect differences

in AR activation, dose-response experiments were performed for the WT AR and the mutants E20A, D23A, and E174A. The results of these experiments identify key residues on the EC face, demonstrate the influence of ligand dose in detection of such differences, and also illustrate some limitations of our ERK assay, with respect to both dynamic range and variability between experiments. These limitations in sensitivity and reproducibility, in combination with the time-consuming, low-throughput nature of conventional western blotting, make it practical to consider alternative methods that could be used in future to characterize AR signalling, both for the WT and mutant receptors.

In-cell ELISAs (enzyme-linked immunosorbent assays; also known as In-cell westerns™) provide a high-throughput alternative to conventional western blotting, wherein cells are seeded, stimulated, probed with antibodies, and analyzed, all within a 96-well microplate. A particular advantage of these assays is that antibodies are added directly to the cells in the microplate, circumventing the need for time-consuming cell lysis, SDS-PAGE, and membrane transfer. In addition, the microplate format allows for the simultaneous analysis of many more samples than conventional western blotting allows. A disadvantage of this method is that cellular proteins are never resolved by size prior to addition of antibodies, and so issues of antibody non-specificity must be thoroughly avoided in order to obtain valid results [113].

Bioluminescence resonance energy transfer (BRET) assays also provide a versatile alternative for studying the activation of GPCRs. BRET relies on the use of an enzymatically tagged donor protein and a fluorescently tagged acceptor protein.

The donor enzyme, *renilla* luciferase (Rluc), catalyzes the oxidation of a substrate called coelanterazine, resulting in light emission (bioluminescence) at a particular wavelength. The excitation spectrum of the acceptor fluorophore is such that, if it is close enough to the donor, it will be excited by the energy of the donor through a phenomenon known as resonance energy transfer (RET). This RET is highly distance dependent, dropping off rapidly at distances greater than 10 nm, and thus BRET provides a reliable and quantifiable measure of the co-localization of two proteins [114].

Though the potential applications of BRET extend well beyond monitoring GPCR activation, there are a number of useful donor/acceptor configurations that may be used for this purpose. For example, by fusing enhanced green fluorescent protein (EGFP) to the C-terminus of a GPCR, and Rluc to β-arrestin, the ligand-induced recruitment of β-arrestin can be monitored. Because the BRET assay involves less sample preparation and the measurements are made in "real-time" (while the cells are still living), it can also provide information about the time-course of protein-protein interactions. Thus, for example, in the case of the AR, the short-lived β-arrestin interaction induced by apelin-13 (fast recycling) should be discernable from the long-lived one induced by apelin-36 (slow recycling). BRET assays can also be designed to monitor the subcellular localization of the GPCR. For example, the Rluc donor can be fused to proteins known to localize at the plasma membrane (*e.g.* KRas) or at early endosomes (*e.g.* Rab5a) or recycling endosomes (*e.g.* Rab4, Rab11) [115; 116]. The GPCR's relative presence at the cell surface and

within the cell can then be quantified, and this distribution can be monitored over time and in response to stimulation with various ligands.

Thus, other assays such as BRET and in-cell ELISAs would provide alternative ways to monitor the activation of the WT and mutant AR. The main criteria to consider in choosing between alternative methods should be the sensitivity and reproducibility of the techniques, as well as the quantity of samples that can be analyzed simultaneously, and the amount of time required to conduct the experiments (*i.e.* high- or low-throughput). In these regards, both BRET and in-cell ELISAs provide advantages over the traditional western blotting used until now. Of the two methods, in-cell ELISAs against pERK provide a higher-throughput alternative, because of their 96-well microplate format. On the other hand, they carry similar issues of antibody signal, with the additional caveat that proteins are not resolved by size, and so non-specific binding of antibodies is especially problematic. By contrast, BRET is relatively lower-throughput, but it does not depend on antibodies. BRET assays are also versatile, because different protein-protein interactions may be characterized; moreover, the measurement of these interactions is typically much more direct than quantification of ERK activation, which occurs distantly downstream of GPCR activation in the signal cascade.

Table 3.1 Mutagenic primer sequences used for site-directed mutagenesis of the AR.

Amino acid substitution	Forward primer sequence	Reverse primer sequence
E174A	ACCACCGGGGACTTGGCAA ACACCACTAAGGTG	CACCTTAGTGGTCTTTGCCA AGTCCCCGGTGGT
Y182A	ACTAAGGTGCAGTGCGCAA TGGACTACTCCATG	CATGGAGTAGTCCATTGCGC ACTGCACCTTAGT
Y185A	CAGTGCTACATGGACGCTT CCATGGTGGCCACT	AGTGGCCACCATGGAAGCGT CCATGTAGCACTG
E194A	GCCACTGTGAGCTCAGCTT GGGCCTGGGAGGTG	CACCTCCCAGGCCCAAGCTG AGCTCACAGTGGC
W197A	AGCTCAGAGTGGGCCGCTG AGGTGGGCCTTGGG	CCCAAGGCCCACCTCAGCGG CCCACTCTGAGCT
E198A	TCAGAGTGGGCCTGGGCAG TGGGCCTTGGGGTC	GACCCCAAGGCCCACTGCCC AGGCCCACTCTGA

Table 3.2 The reaction composition and thermocycling conditions used for PCR amplification of apelin-36.

Reaction composition	
Total volume (μL)	50
Buffer	1x Phusion HF buffer
Template DNA (ng)	50
[Primers] (μM)	0.5
Final [Mg^{2+}] (mM)	2
[DNTPs] (μM)	200
Polymerase type and amount	Phusion polymerase, 1 unit
Cycling conditions	
Initial denaturation	98 °C, 30 sec
Number of cycles	25
Melting step	98 °C, 10 sec
Annealing step	60 °C, 30 sec
Extension step	72 °C, 3.5 min
Final Extension	72 °C, 7 min

Table 3.3 EC_{50}, E_{max}, and R^2 values derived from sigmoidal curve fits of individual dose-response experiments at the WT AR and mutants E20A, D23A, and E174A (see figures 3.5 to 3.9). Values were derived using Graphpad's Prism 6 software according to the methods outlined in section 3.2.5.

Receptor/ligand	EC_{50} (nM)	E_{max}	R^2
WT AR/Ap13			
# 1	0.09	2.9	0.71
# 2	0.37	2.8	0.84
# 3	0.72	4.9	0.97
# 4	0.39	2.6	0.92
E20A AR/Ap13			
# 1	1.25	3.1	0.88
# 2	1.70	3.2	0.81
# 3	0.94	1.9	0.79
D23A AR/Ap13			
# 1	10.15	1.5	0.15
# 2	13.96	2.2	0.77
# 3	11.47	2.2	0.93
E174A AR/Ap13			
# 1	21.82	1.9	0.70
# 2	0.001	1.4	0.40
# 3	11.30	2.9	0.99
WT AR/Ap36			
# 1	0.12	2.2	0.93
# 2	3.94	11.5	0.88
# 3	0.07	9.7	0.85
# 4	6.91	2.7	0.94

Table 3.4 Mean EC_{50} and E_{max} values for the WT AR and mutants E20A, D23A, and E174A, derived from apelin dose-response experiments. EC_{50} and E_{max} values represent the means from three independent dose-response experiments, and were calculated using GraphPad's Prism 6 software. EC_{50} and E_{max} values were compared by unpaired t tests (significance when $P < 0.1$) also performed in Prism 6 according to the methods described in section 3.2.5. Ranges of error represent standard error.

Receptor	**Ligand**	**EC_{50} (nM)**	**EC_{50} differs significantly from WT/Ap13?**	**E_{max}**	**E_{max} differs significantly from WT/Ap13?**
WT AR	apelin-13	0.4 ± 0.1	N/A	3 ± 1	N/A
E20A AR	apelin-13	1.3 ± 0.2	Yes	2.7 ± 0.4	No
D23A AR	apelin-13	12 ± 1	Yes	2.0 ± 0.2	No
E174A AR	apelin-13	11 ± 6	Yes	2.0 ± 0.5	No
WT AR	apelin-36	3 ± 2	No	7 ± 2	No

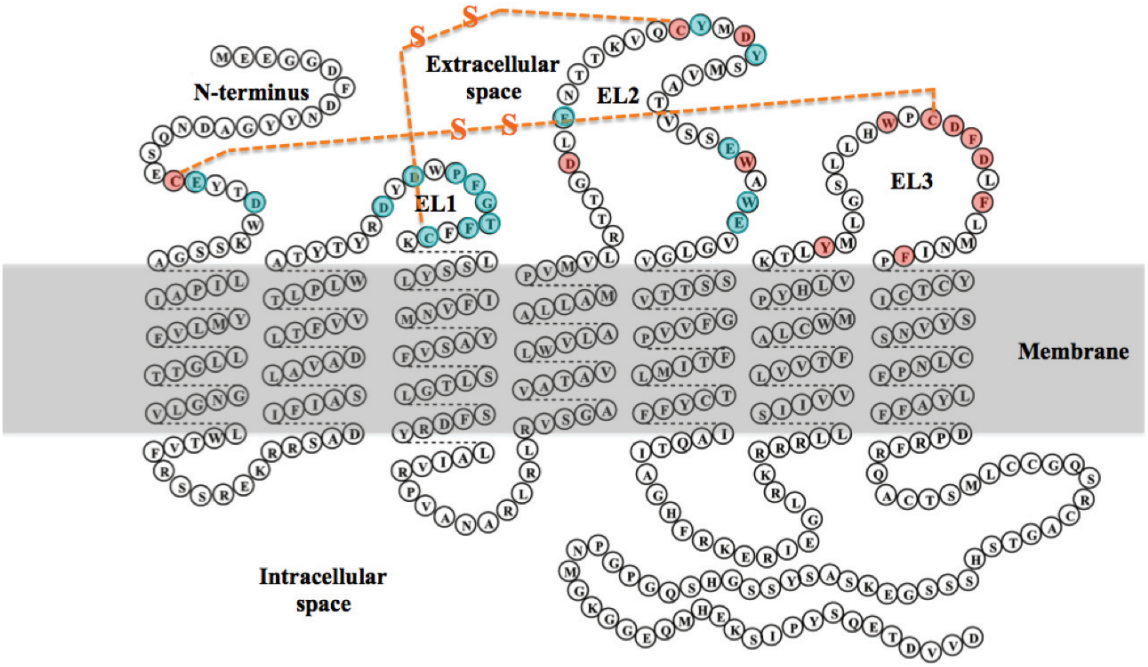

Figure 3.1 Schematic "snake-plot" representation of the AR, depicting the N-terminal, EL1, and EL2 residues that were mutated for receptor activation studies. Residues highlighted in teal were mutated to alanine, and the mutants were functionally characterized. Residues highlighted in red are those to be characterized in future studies. The orange dotted lines represent putative disulfide bonds. Original AR snake-plot created by Aditya Pandey.

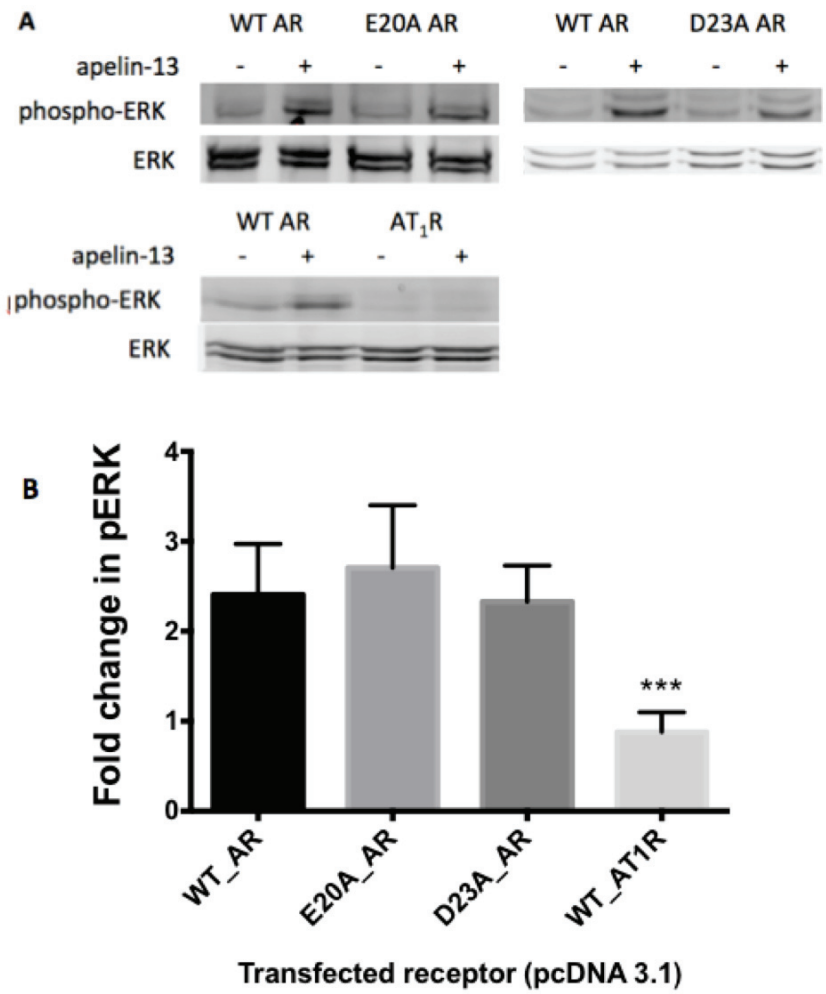

Figure 3.2 Functional analysis of 3xHA-AR N-terminal mutants. For the WT AR, N-terminal mutants, and the WT AT_1R (negative control), the fold change in (apelin-13-induced) ERK phosphorylation was determined (B). Representative western blots for each receptor are shown in (A). Cells were treated with 1 μm apelin-13 for 4 minutes. Error bars indicate standard error, determined from the mean of three or more experiments (n >= 3). * indicates significant difference from the WT AR (***=$p<0.001$). Bar graphs were produced using Graphpad's Prism 6 software.

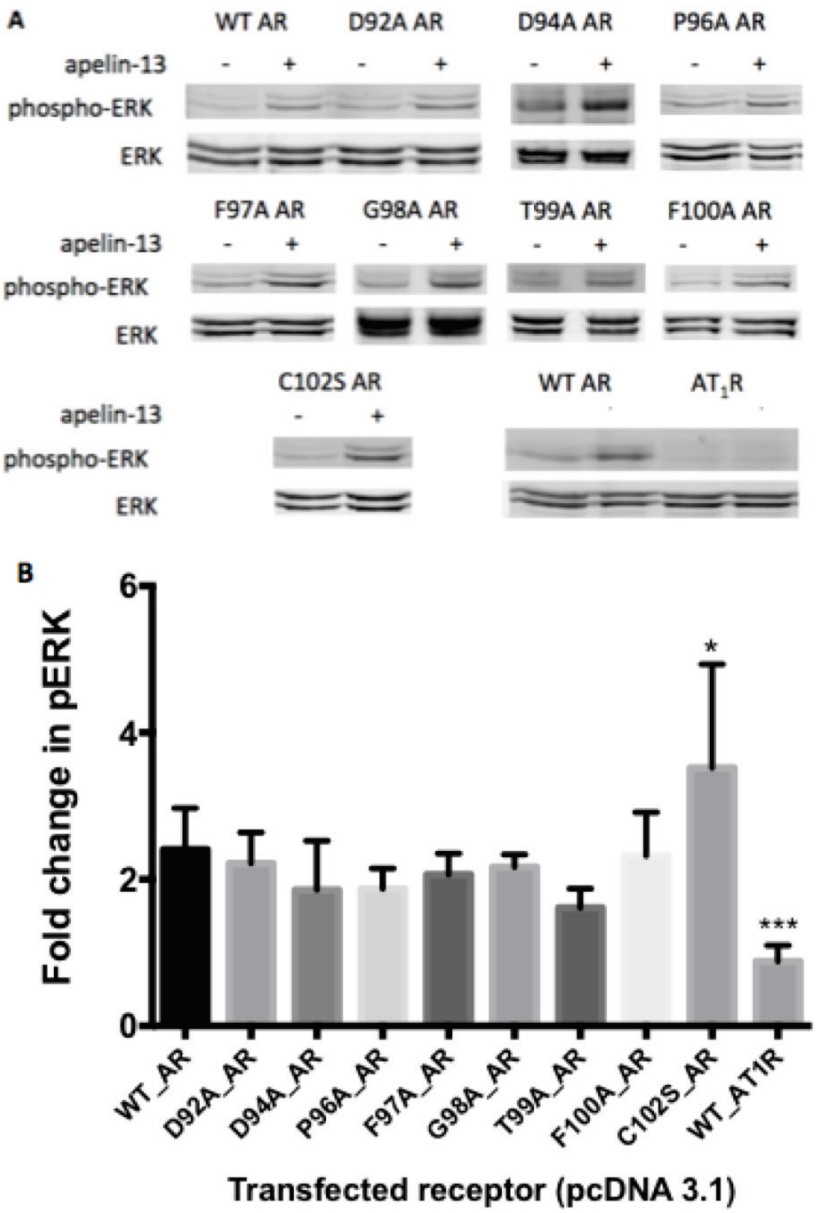

Figure 3.3 Functional analysis of 3xHA-AR ELl mutants. For the WT AR, EL1 mutants, and the WT AT_1R (negative control), the fold change in (apelin-13-induced) ERK phosphorylation was determined (B). Representative western blots for each receptor are shown in (A). Cells were treated with 1 μm apelin-13 for 4 minutes. Error bars indicate standard error, determined from the mean of three or more experiments (n >= 3). * indicates significant difference from the WT AR (*=p<0.05; ***=p<0.001). Bar graphs were produced using Graphpad's Prism 6 software.

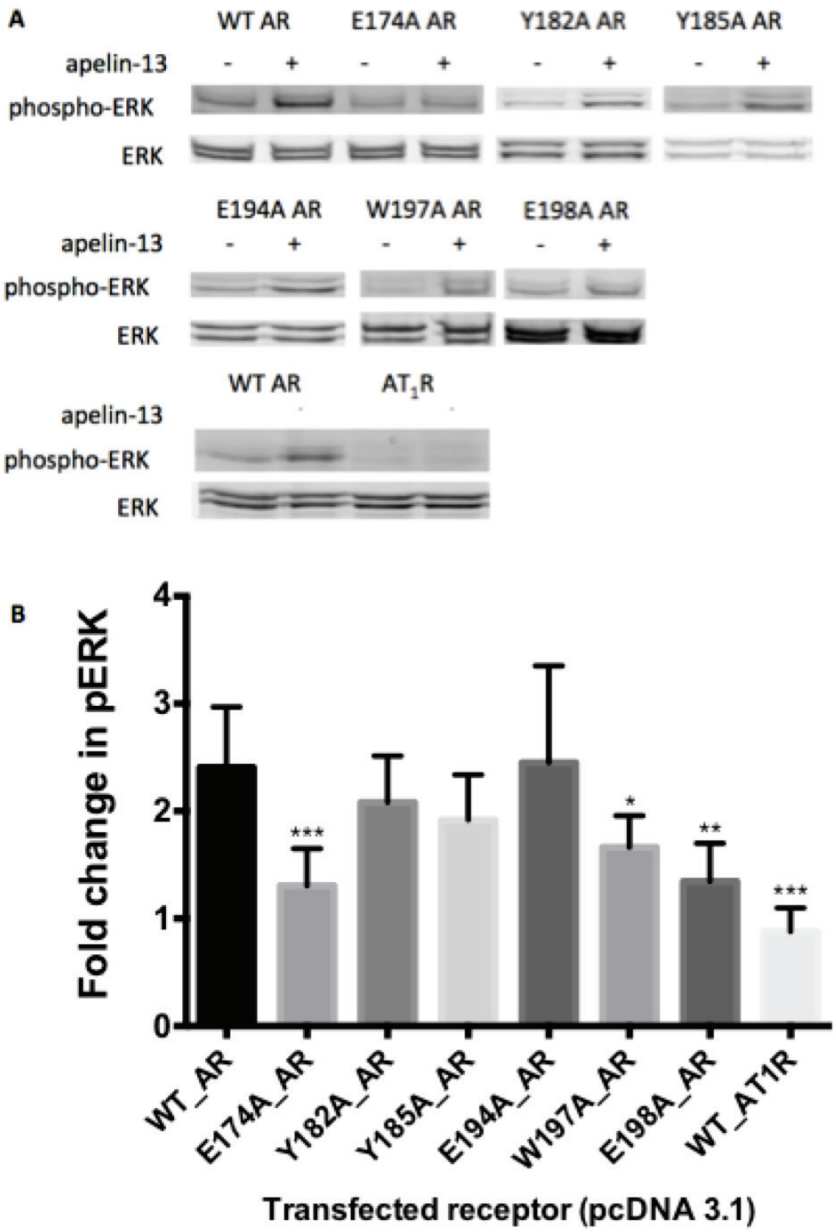

Figure 3.4 Functional analysis of 3xHA-AR EL2 mutants. For the WT AR, EL2 mutants, and the WT AT_1R (negative control), the fold change in (apelin-13-induced) ERK phosphorylation was determined (B). Representative western blots for each receptor are shown in (A). Cells were treated with 1 μm apelin-13 for 4 minutes. Error bars indicate standard error, determined from the mean of three or more experiments (n >= 3). * indicates significant difference from the WT AR (*=p<0.05; **=p<0.01; ***=p<0.001). Bar graphs were produced using Graphpad's Prism 6 software.

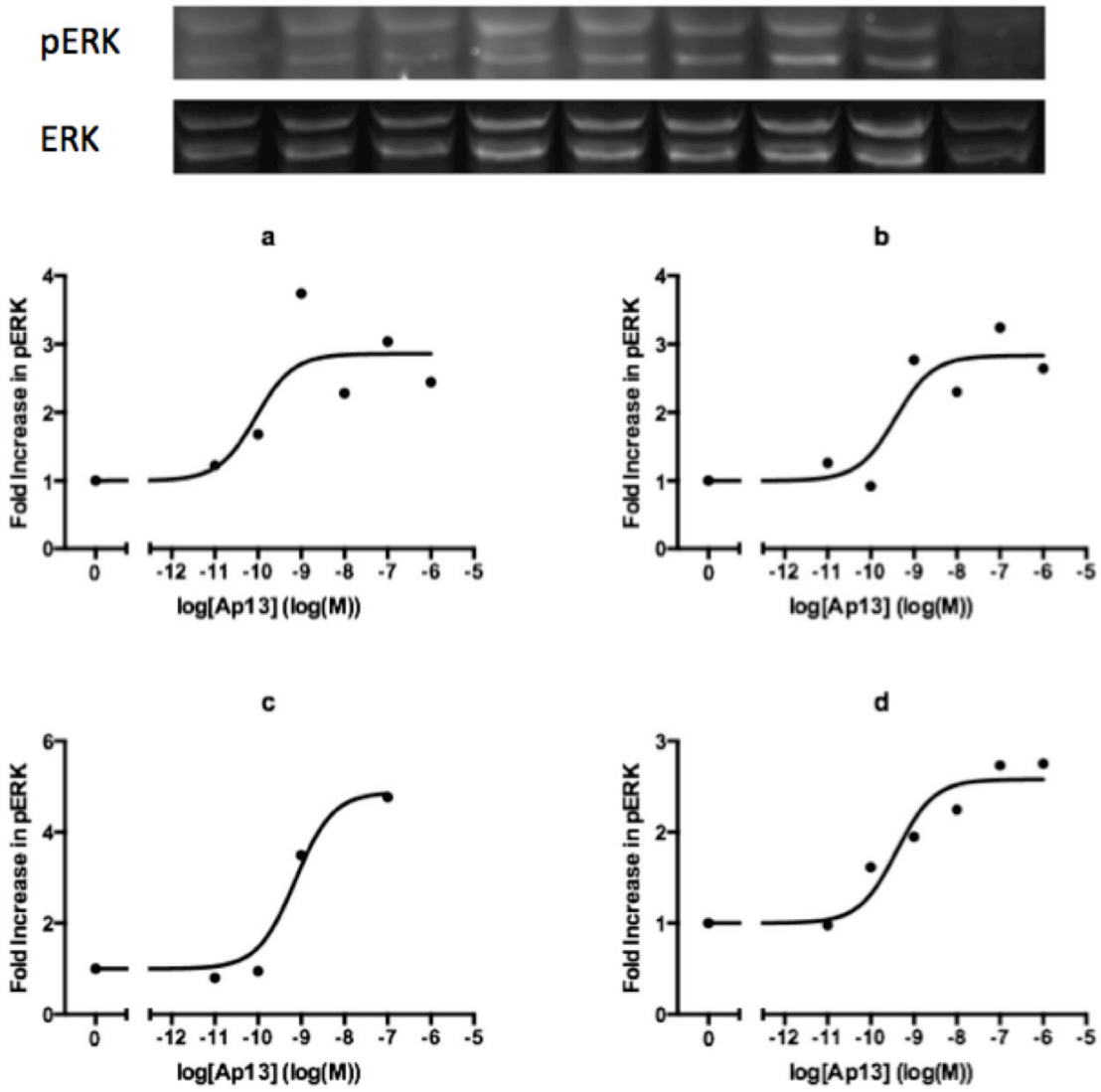

Figure 3.5 Dose-response experiments for apelin-13-induced ERK activation mediated by the WT 3xHA-AR. ERK activation is reported as the fold change in (apelin-13-induced) ERK phosphorylation. Cells were treated with varying concentrations of apelin-13 (10^{-11} M – 10^{-6} M) for 4 minutes. A representative western blot is shown above. Dose-response plots were produced using Graphpad's Prism 6 software, with the zero-dose baseline response plotted in a non-logarithmic form.

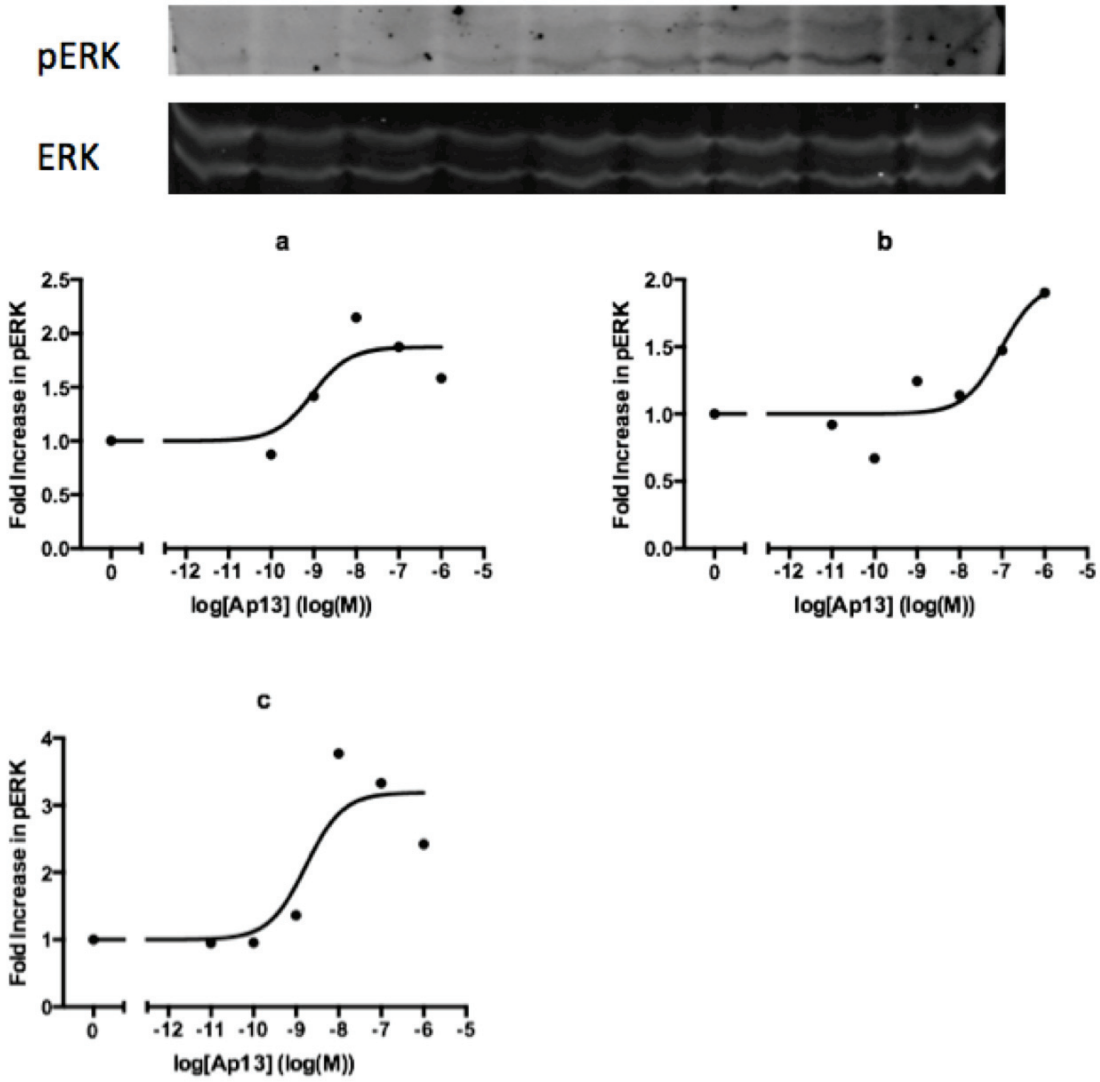

Figure 3.6 Dose-response experiments for apelin-13-induced ERK activation mediated by the E20A 3xHA-AR mutant. ERK activation is reported as the fold change in (apelin-13-induced) ERK phosphorylation. Cells were treated with varying concentrations of apelin-13 (10^{-11} M – 10^{-6} M) for 4 minutes. A representative western blot is shown above. Dose-response plots were produced using Graphpad's Prism 6 software, with the zero-dose baseline response plotted in a non-logarithmic form.

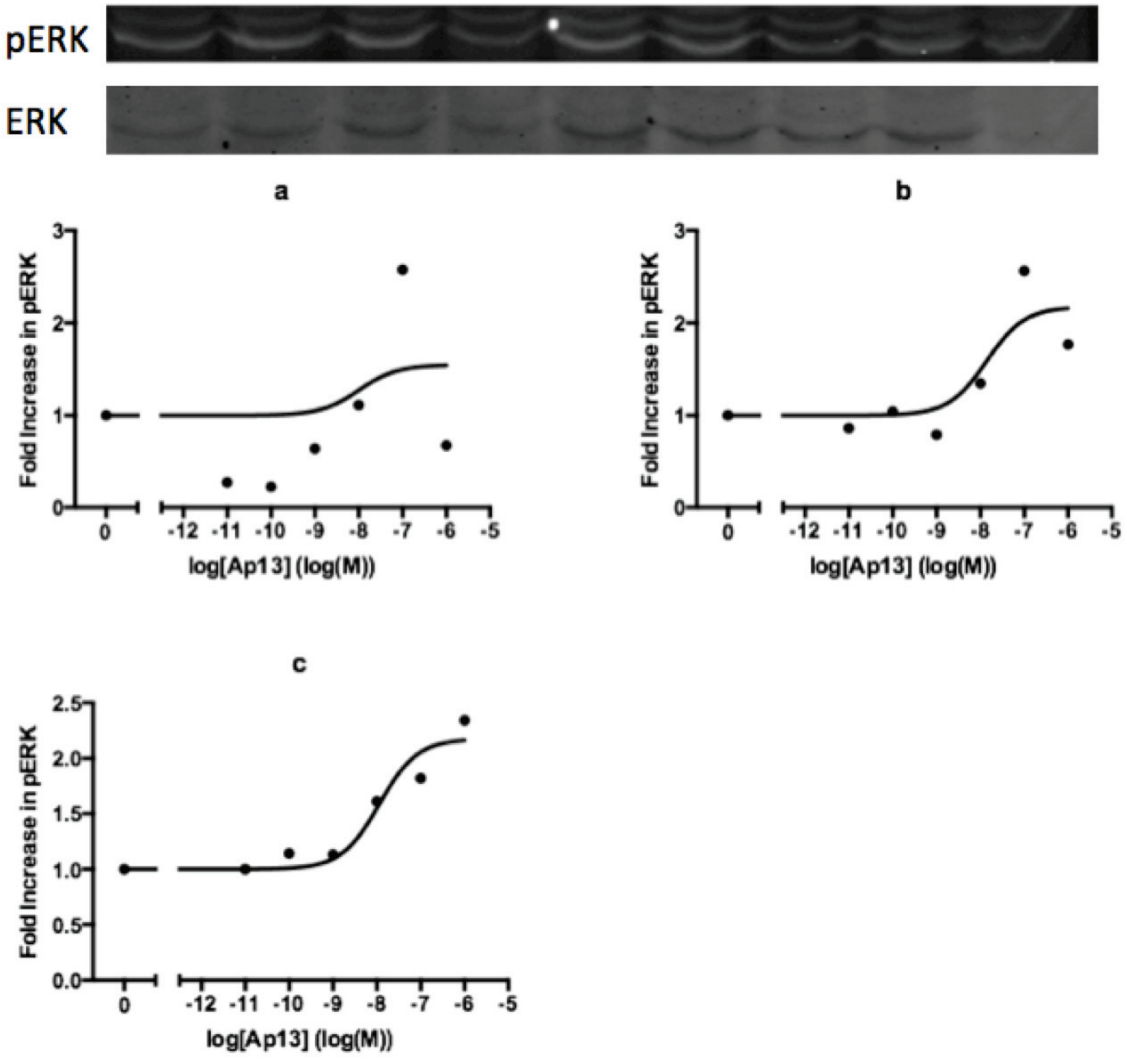

Figure 3.7 Dose-response experiments for apelin-13-induced ERK activation mediated by the D23A 3xHA-AR mutant. ERK activation is reported as the fold change in (apelin-13-induced) ERK phosphorylation. Cells were treated with varying concentrations of apelin-13 (10^{-11} M – 10^{-6} M) for 4 minutes. A representative western blot is shown above. Dose-response plots were produced using Graphpad's Prism 6 software, with the zero-dose baseline response plotted in a non-logarithmic form.

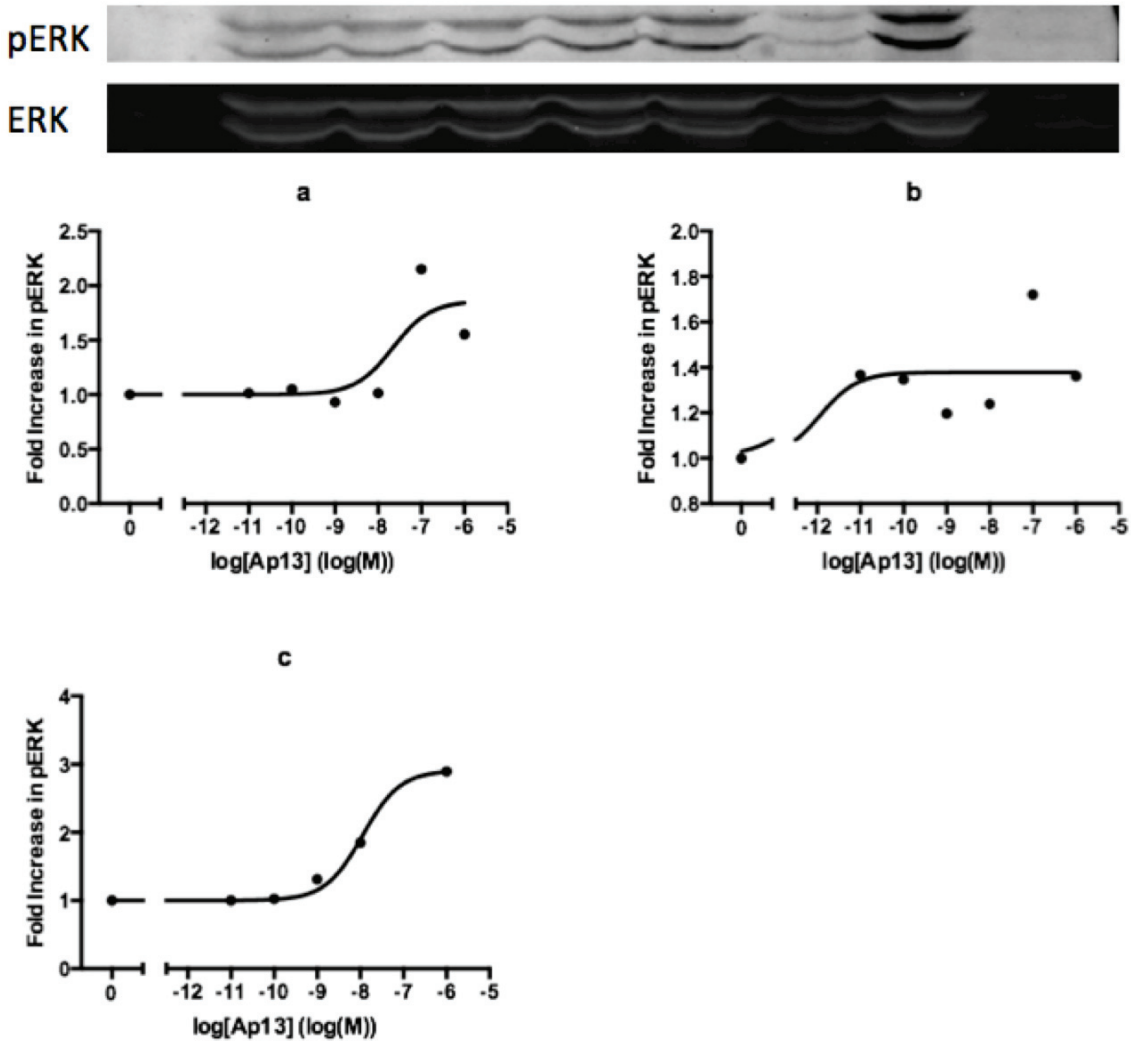

Figure 3.8 Dose-response experiments for apelin-13-induced ERK activation mediated by the E174A 3xHA-AR mutant. ERK activation is reported as the fold change in (apelin-13-induced) ERK phosphorylation. Cells were treated with varying concentrations of apelin-13 (10^{-11} M – 10^{-6} M) for 4 minutes. A representative western blot is shown above. Dose-response plots were produced using Graphpad's Prism 6 software, with the zero-dose baseline response plotted in a non-logarithmic form.

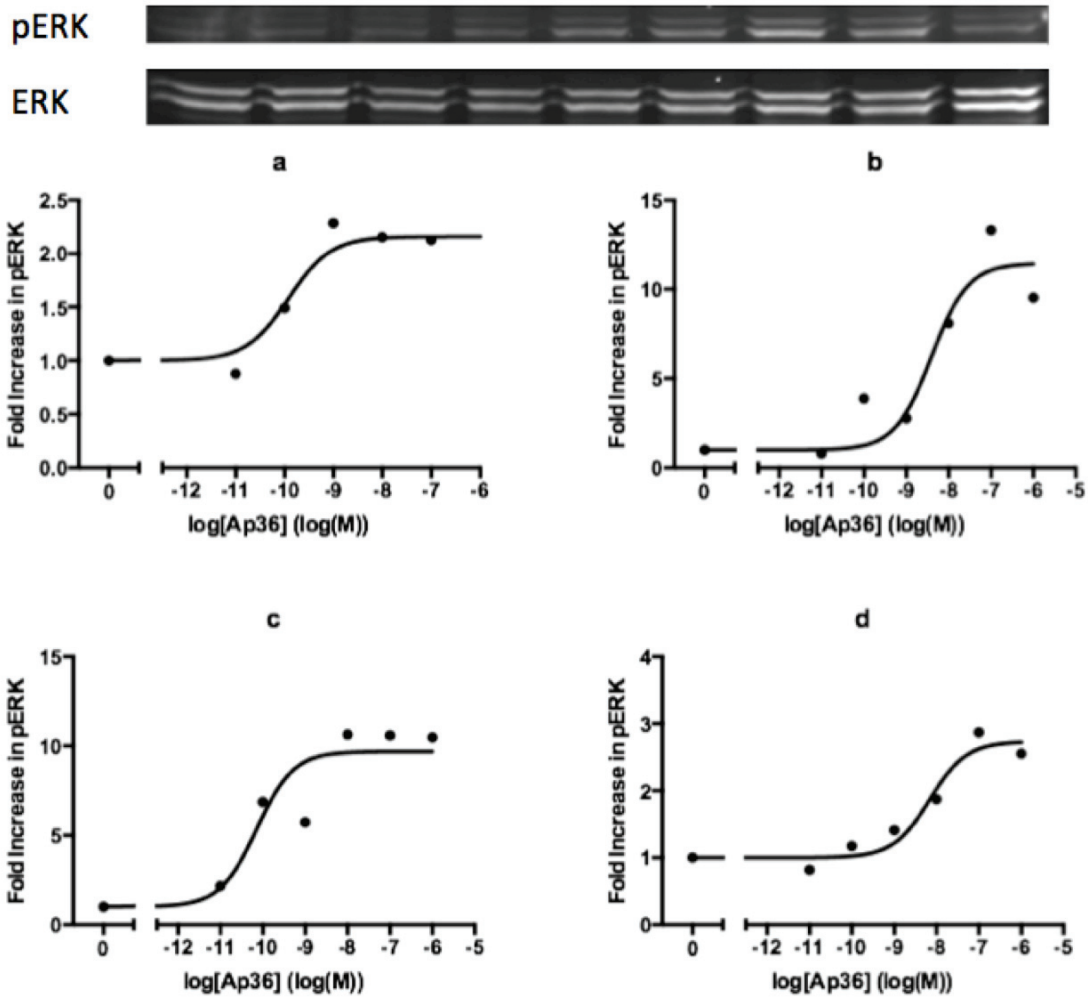

Figure 3.9 Dose-response experiments for apelin-36-induced ERK activation mediated by the WT 3xHA-AR. ERK activation is reported as the fold change in (apelin-36-induced) ERK phosphorylation. Cells were treated with varying concentrations of apelin-36 (10^{-11} M – 10^{-6} M) for 4 minutes. A representative western blot is shown above. Dose-response plots were produced using Graphpad's Prism 6 software, with the zero-dose baseline response plotted in a non-logarithmic form.

Chapter 4: Conclusion

4.1 Summary of Findings

The aim of this research has been the functional characterization of residues at the EC face of the AR, by means of site-directed mutagenesis and analysis of WT and mutant receptor activation. In addition to these assays, recombinant apelin-36 was produced and purified, and shown to be a functional activator of the AR. The protocol for *E. coli* expression of apelin-36 as a SUMO-fusion protein, which can be efficiently and inexpensively cleaved and purified, can be applied to produce other peptides, in particular the remaining apelin isoforms, as well as the various toddler peptides.

The activation studies performed for the WT and mutant receptors yielded insights about the relative activity of the mutants, as well the importance of ligand concentration in detecting mutation-induced effects. In particular, they revealed that mutation of D23 in the N-terminus and E174 in EL2 produced receptors with attenuated pERK responses to apelin-13, albeit without affecting the E_{max} for ERK activation. Initial high-dose studies also indicated that residues W197 and E198 might be important for apelin binding and AR activation. Moreover, a mutant of residue C102 at the C-terminal edge of EL1, which likely forms a conserved disulfide to C181 in EL2, appeared to mediate slightly increased ERK activation, marking this residue, along with other potential disulfide-forming cysteines on the EC face, as important for future characterization. In addition to the identification of these key amino acids, performing these assays also helped to establish some technical and

conceptual limitations of using ERK activation and western blotting as a functional readout of GPCR activation.

4.2 Future Directions

It is timely here to reiterate the validity of studying the EC face of the AR in order to understand its activation by apelin. As described previously, the residues in this region are both the most highly variable and most incompletely characterized within GPCRs. They are also highly dynamic, and their positions at the cell surface, protruding from the membrane, make them probable points of first contact for GPCR ligands diffusing through the extracellular space. For the AR in particular, its interaction with the highly cationic peptide apelin is likely mediated, at least in part, by anionic and other residues in the ELs and N-terminus. Indeed, the results presented herein support this hypothesis, and it is likely that additional residues in the ELs mediate important interactions with apelin.

In future, the use of more sensitive, quantitative, and higher throughput assays will help us identify such functionally important residues and study the effects of altering them. Techniques based on BRET will make it possible to track the subcellular localization of the AR, monitoring interactions with plasma membrane or endosomal markers, or with β-arrestins and G-proteins in real time. Likewise, by labelling the AR N-terminus with a fluorescent protein, Förster resonance energy transfer (FRET) can be used to measure the binding of fluorophore-labelled apelin or toddler/ELABELA isoforms at the EC face, allowing direct characterization of various AR mutants. These techniques will also provide more direct and versatile

ways to compare the signalling properties of the various apelin and toddler isoforms. This final point in particular marks an important area of future AR research, which will help us understand subtle differences in AR activation, and aid in the rational design of novel therapeutics targeting the AR.

Bibliography

[1] de Mendoza, A., Sebe-Pedros, A., and Ruiz-Trillo, I. 2014. The Evolution of the GPCR Signaling System in Eukaryotes: Modularity, Conservation, and the Transition to Metazoan Multicellularity. Genome Biol Evol **6**(3): 606-619. doi: 10.1093/gbe/evu038.

[2] Vassilatis, D.K., Hohmann, J.G., Zeng, H., Li, F., Ranchalis, J.E., Mortrud, M.T., Brown, A., Rodriguez, S.S., Weller, J.R., Wright, A.C., Bergmann, J.E., and Gaitanaris, G.A. 2003. The G protein-coupled receptor repertoires of human and mouse. Proc Natl Acad Sci U S A **100**(8): 4903-4908. doi: 10.1073/pnas.0230374100.

[3] Takeda, S., Kadowaki, S., Haga, T., Takaesu, H., and Mitaku, S. 2002. Identification of G protein-coupled receptor genes from the human genome sequence. FEBS Lett **520**(1-3): 97-101.

[4] Fredriksson, R., Lagerstrom, M.C., Lundin, L.G., and Schioth, H.B. 2003. The G-protein-coupled receptors in the human genome form five main families. Phylogenetic analysis, paralogon groups, and fingerprints. Mol Pharmacol **63**(6): 1256-1272. doi: 10.1124/mol.63.6.1256.

[5] Kroeze, W.K., Sheffler, D.J., and Roth, B.L. 2003. G-protein-coupled receptors at a glance. J Cell Sci **116**(Pt 24): 4867-4869. doi: 10.1242/jcs.00902.

[6] Perez, D.M. 2003. The evolutionarily triumphant G-protein-coupled receptor. Mol Pharmacol **63**(6): 1202-1205. doi: 10.1124/mol.63.6.1202.

[7] Overington, J.P., Al-Lazikani, B., and Hopkins, A.L. 2006. How many drug targets are there? Nat Rev Drug Discov **5**(12): 993-996. doi: 10.1038/nrd2199.

[8] Luttrell, L.M., and Kenakin, T.P. 2011. Refining efficacy: allosterism and bias in G protein-coupled receptor signaling. Methods Mol Biol **756**: 3-35. doi: 10.1007/978-1-61779-160-4_1.

[9] Yao, X.J., Velez Ruiz, G., Whorton, M.R., Rasmussen, S.G., DeVree, B.T., Deupi, X., Sunahara, R.K., and Kobilka, B. 2009. The effect of ligand efficacy on the formation and stability of a GPCR-G protein complex. Proc Natl Acad Sci U S A **106**(23): 9501-9506. doi: 10.1073/pnas.0811437106.

[10] Neves, S.R., Ram, P.T., and Iyengar, R. 2002. G protein pathways. Science **296**(5573): 1636-1639. doi: 10.1126/science.1071550.

[11] Kimple, A.J., Bosch, D.E., Giguere, P.M., and Siderovski, D.P. 2011. Regulators of G-protein signaling and their Galpha substrates: promises and challenges in their use as drug discovery targets. Pharmacol Rev **63**(3): 728-749. doi: 10.1124/pr.110.003038.

[12] Clapham, D.E., and Neer, E.J. 1997. G protein beta gamma subunits. Annu Rev Pharmacol Toxicol **37**: 167-203. doi: 10.1146/annurev.pharmtox.37.1.167.

[13] Kozasa, T., Jiang, X., Hart, M.J., Sternweis, P.M., Singer, W.D., Gilman, A.G., Bollag, G., and Sternweis, P.C. 1998. p115 RhoGEF, a GTPase activating protein for Galpha12 and Galpha13. Science **280**(5372): 2109-2111.

[14] Simonds, W.F. 1999. G protein regulation of adenylate cyclase. Trends Pharmacol Sci **20**(2): 66-73.

[15] Kammermeier, P.J., Ruiz-Velasco, V., and Ikeda, S.R. 2000. A voltage-independent calcium current inhibitory pathway activated by muscarinic agonists in rat sympathetic neurons requires both Galpha q/11 and Gbeta gamma. J Neurosci **20**(15): 5623-5629.

[16] Rhee, S.G. 2001. Regulation of phosphoinositide-specific phospholipase C. Annu Rev Biochem **70**: 281-312. doi: 10.1146/annurev.biochem.70.1.281.

[17] Lutz, S., Shankaranarayanan, A., Coco, C., Ridilla, M., Nance, M.R., Vettel, C., Baltus, D., Evelyn, C.R., Neubig, R.R., Wieland, T., and Tesmer, J.J. 2007. Structure of Galphaq-p63RhoGEF-RhoA complex reveals a pathway for the activation of RhoA by GPCRs. Science **318**(5858): 1923-1927. doi: 10.1126/science.1147554.

[18] Kimple, A.J., Soundararajan, M., Hutsell, S.Q., Roos, A.K., Urban, D.J., Setola, V., Temple, B.R., Roth, B.L., Knapp, S., Willard, F.S., and Siderovski, D.P. 2009. Structural determinants of G-protein alpha subunit selectivity by regulator of G-protein signaling 2 (RGS2). J Biol Chem **284**(29): 19402-19411. doi: 10.1074/jbc.M109.024711.

[19] Ahmed, S.M., and Angers, S. 2013. Emerging non-canonical functions for heterotrimeric G proteins in cellular signaling. J Recept Signal Transduct Res **33**(3): 177-183. doi: 10.3109/10799893.2013.795972.

[20] Luttrell, L.M., and Gesty-Palmer, D. 2010. Beyond desensitization: physiological relevance of arrestin-dependent signaling. Pharmacol Rev **62**(2): 305-330. doi: 10.1124/pr.109.002436.

[21] Luttrell, L.M., and Lefkowitz, R.J. 2002. The role of beta-arrestins in the termination and transduction of G-protein-coupled receptor signals. J Cell Sci **115**(Pt 3): 455-465.

[22] Luttrell, L.M., and Miller, W.E. 2013. Arrestins as regulators of kinases and phosphatases. Prog Mol Biol Transl Sci **118**: 115-147. doi: 10.1016/b978-0-12-394440-5.00005-x.

[23] Violin, J.D., and Lefkowitz, R.J. 2007. Beta-arrestin-biased ligands at seven-transmembrane receptors. Trends Pharmacol Sci **28**(8): 416-422. doi: 10.1016/j.tips.2007.06.006.

[24] Ahn, S., Shenoy, S.K., Wei, H., and Lefkowitz, R.J. 2004. Differential kinetic and spatial patterns of beta-arrestin and G protein-mediated ERK activation by the angiotensin II receptor. J Biol Chem **279**(34): 35518-35525. doi: 10.1074/jbc.M405878200.

[25] Nelson, G., Hoon, M.A., Chandrashekar, J., Zhang, Y., Ryba, N.J., and Zuker, C.S. 2001. Mammalian sweet taste receptors. Cell **106**(3): 381-390.

[26] Sun, X., Iida, S., Yoshikawa, A., Senbonmatsu, R., Imanaka, K., Maruyama, K., Nishimura, S., Inagami, T., and Senbonmatsu, T. 2011. Non-activated APJ suppresses the angiotensin II type 1 receptor, whereas apelin-activated APJ acts conversely. Hypertens Res **34**(6): 701-706. doi: 10.1038/hr.2011.19.

[27] Kenakin, T. 2011. Functional selectivity and biased receptor signaling. J Pharmacol Exp Ther **336**(2): 296-302. doi: 10.1124/jpet.110.173948.

[28] Deupi, X. 2014. Relevance of rhodopsin studies for GPCR activation. Biochim Biophys Acta **1837**(5): 674-682. doi: 10.1016/j.bbabio.2013.09.002.

[29] Kim, T.H., Chung, K.Y., Manglik, A., Hansen, A.L., Dror, R.O., Mildorf, T.J., Shaw, D.E., Kobilka, B.K., and Prosser, R.S. 2013. The role of ligands on the equilibria between functional states of a G protein-coupled receptor. J Am Chem Soc **135**(25): 9465-9474. doi: 10.1021/ja404305k.

[30] Deupi, X., and Kobilka, B.K. 2010. Energy landscapes as a tool to integrate GPCR structure, dynamics, and function. Physiology (Bethesda) **25**(5): 293-303. doi: 10.1152/physiol.00002.2010.

[31] O'Dowd, B.F., Heiber, M., Chan, A., Heng, H.H., Tsui, L.C., Kennedy, J.L., Shi, X., Petronis, A., George, S.R., and Nguyen, T. 1993. A human gene that shows identity with the gene encoding the angiotensin receptor is located on chromosome 11. Gene **136**(1-2): 355-360.

[32] Tatemoto, K., Hosoya, M., Habata, Y., Fujii, R., Kakegawa, T., Zou, M.X., Kawamata, Y., Fukusumi, S., Hinuma, S., Kitada, C., Kurokawa, T., Onda, H., and Fujino, M. 1998. Isolation and characterization of a novel endogenous peptide ligand for the human APJ receptor. Biochem Biophys Res Commun **251**(2): 471-476. doi: 10.1006/bbrc.1998.9489.

[33] Shin, K., Pandey, A., Liu, X.Q., Anini, Y., and Rainey, J.K. 2013. Preferential apelin-13 production by the proprotein convertase PCSK3 is implicated in obesity. FEBS Open Bio **3**: 328-333. doi: 10.1016/j.fob.2013.08.001.

[34] Kleinz, M.J., and Davenport, A.P. 2005. Emerging roles of apelin in biology and medicine. Pharmacol Ther **107**(2): 198-211. doi: 10.1016/j.pharmthera.2005.04.001.

[35] Reaux, A., Gallatz, K., Palkovits, M., and Llorens-Cortes, C. 2002. Distribution of apelin-synthesizing neurons in the adult rat brain. Neuroscience **113**(3): 653-662.

[36] Azizi, M., Iturrioz, X., Blanchard, A., Peyrard, S., De Mota, N., Chartrel, N., Vaudry, H., Corvol, P., and Llorens-Cortes, C. 2008. Reciprocal regulation of plasma apelin and vasopressin by osmotic stimuli. J Am Soc Nephrol **19**(5): 1015-1024. doi: 10.1681/asn.2007070816.

[37] Maguire, J.J., Kleinz, M.J., Pitkin, S.L., and Davenport, A.P. 2009. [Pyr1]apelin-13 identified as the predominant apelin isoform in the human heart: vasoactive mechanisms and inotropic action in disease. Hypertension **54**(3): 598-604. doi: 10.1161/hypertensionaha.109.134619.

[38] Said El Messari, X.I., Celine Fassot, Nadia De Mota, Darren Roesch and Catherine Llorens-Cortes. 2004. Functional dissociation of apelin receptor signaling and endocytosis: implications for the effects of apelin on arterial blood pressure. Journal of Neurochemistry(90): 1290-1301.

[39] Yuji Kawamata, Y.H., Shoji Fukusumi, Masaki Hosoya, Ryo Fujii, Shuji Hinuma, Naoki Nishizawa, Chieko Kitada, Haruo Onda, Osamu Nishimura, Masahiko Fujino. 2001. Molecular properties of apelin: tissue distribution and receptor binding. Biochimica et Biophysica Acta **1538**: 162-171.

[40] Kawamata, Y., Habata, Y., Fukusumi, S., Hosoya, M., Fujii, R., Hinuma, S., Nishizawa, N., Kitada, C., Onda, H., Nishimura, O., and Fujino, M. 2001. Molecular properties of apelin: tissue distribution and receptor binding. Biochim Biophys Acta **1538**(2-3): 162-171.

[41] O'Carroll, A.M., Lolait, S.J., Harris, L.E., and Pope, G.R. 2013. The apelin receptor APJ: journey from an orphan to a multifaceted regulator of homeostasis. J Endocrinol **219**(1): R13-35. doi: 10.1530/joe-13-0227.

[42] Pitkin, S.L., Maguire, J.J., Bonner, T.I., and Davenport, A.P. 2010. International Union of Basic and Clinical Pharmacology. LXXIV. Apelin receptor nomenclature, distribution, pharmacology, and function. Pharmacol Rev **62**(3): 331-342. doi: 10.1124/pr.110.002949.

[43] Masri, B., Knibiehler, B., and Audigier, Y. 2005. Apelin signalling: a promising pathway from cloning to pharmacology. Cell Signal **17**(4): 415-426. doi: 10.1016/j.cellsig.2004.09.018.

[44] Pauli, A., Norris, M.L., Valen, E., Chew, G.L., Gagnon, J.A., Zimmerman, S., Mitchell, A., Ma, J., Dubrulle, J., Reyon, D., Tsai, S.Q., Joung, J.K., Saghatelian, A., and Schier, A.F. 2014. Toddler: an embryonic signal that promotes cell movement via Apelin receptors. Science **343**(6172): 1248636. doi: 10.1126/science.1248636.

[45] Chng, S.C., Ho, L., Tian, J., and Reversade, B. 2013. ELABELA: a hormone essential for heart development signals via the apelin receptor. Dev Cell **27**(6): 672-680. doi: 10.1016/j.devcel.2013.11.002.

[46] Szokodi, I., Tavi, P., Foldes, G., Voutilainen-Myllyla, S., Ilves, M., Tokola, H., Pikkarainen, S., Piuhola, J., Rysa, J., Toth, M., and Ruskoaho, H. 2002. Apelin, the novel endogenous ligand of the orphan receptor APJ, regulates cardiac contractility. Circ Res **91**(5): 434-440.

[47] Ashley, E.A., Powers, J., Chen, M., Kundu, R., Finsterbach, T., Caffarelli, A., Deng, A., Eichhorn, J., Mahajan, R., Agrawal, R., Greve, J., Robbins, R., Patterson, A.J., Bernstein, D., and Quertermous, T. 2005. The endogenous peptide apelin potently improves cardiac contractility and reduces cardiac loading in vivo. Cardiovasc Res **65**(1): 73-82. doi: 10.1016/j.cardiores.2004.08.018.

[48] Scimia, M.C., Hurtado, C., Ray, S., Metzler, S., Wei, K., Wang, J., Woods, C.E., Purcell, N.H., Catalucci, D., Akasaka, T., Bueno, O.F., Vlasuk, G.P., Kaliman, P., Bodmer, R., Smith, L.H., Ashley, E., Mercola, M., Brown, J.H., and Ruiz-Lozano, P. 2012. APJ acts as a dual receptor in cardiac hypertrophy. Nature **488**(7411): 394-398. doi: 10.1038/nature11263.

[49] Zhang, Z., Yu, B., and Tao, G.Z. 2009. Apelin protects against cardiomyocyte apoptosis induced by glucose deprivation. Chin Med J (Engl) **122**(19): 2360-2365.

[50] Wang, W., McKinnie, S.M., Patel, V.B., Haddad, G., Wang, Z., Zhabyeyev, P., Das, S.K., Basu, R., McLean, B., Kandalam, V., Penninger, J.M., Kassiri, Z., Vederas, J.C., Murray, A.G., and Oudit, G.Y. 2013. Loss of Apelin exacerbates myocardial infarction adverse remodeling and ischemia-reperfusion injury: therapeutic potential of synthetic Apelin analogues. J Am Heart Assoc **2**(4): e000249. doi: 10.1161/jaha.113.000249.

[51] Zhang, Q., Yao, F., Raizada, M.K., O'Rourke, S.T., and Sun, C. 2009. Apelin gene transfer into the rostral ventrolateral medulla induces chronic blood pressure elevation in normotensive rats. Circ Res **104**(12): 1421-1428. doi: 10.1161/circresaha.108.192302.

[52] Lee, D.K., Cheng, R., Nguyen, T., Fan, T., Kariyawasam, A.P., Liu, Y., Osmond, D.H., George, S.R., and O'Dowd, B.F. 2000. Characterization of apelin, the ligand for the APJ receptor. J Neurochem **74**(1): 34-41.

[53] Lee, D.K., Saldivia, V.R., Nguyen, T., Cheng, R., George, S.R., and O'Dowd, B.F. 2005. Modification of the terminal residue of apelin-13 antagonizes its hypotensive action. Endocrinology **146**(1): 231-236. doi: 10.1210/en.2004-0359.

[54] Reaux, A., De Mota, N., Skultetyova, I., Lenkei, Z., El Messari, S., Gallatz, K., Corvol, P., Palkovits, M., and Llorens-Cortes, C. 2001. Physiological role of a novel neuropeptide, apelin, and its receptor in the rat brain. J Neurochem **77**(4): 1085-1096.

[55] Tatemoto, K., Takayama, K., Zou, M.X., Kumaki, I., Zhang, W., Kumano, K., and Fujimiya, M. 2001. The novel peptide apelin lowers blood pressure via a nitric oxide-dependent mechanism. Regul Pept **99**(2-3): 87-92.

[56] Cheng, X., Cheng, X.S., and Pang, C.C. 2003. Venous dilator effect of apelin, an endogenous peptide ligand for the orphan APJ receptor, in conscious rats. Eur J Pharmacol **470**(3): 171-175.

[57] Dai, L., Smith, P.M., Kuksis, M., and Ferguson, A.V. 2013. Apelin acts in the subfornical organ to influence neuronal excitability and cardiovascular function. J Physiol **591**(Pt 13): 3421-3432. doi: 10.1113/jphysiol.2013.254144.

[58] Kagiyama, S., Fukuhara, M., Matsumura, K., Lin, Y., Fujii, K., and Iida, M. 2005. Central and peripheral cardiovascular actions of apelin in conscious rats. Regul Pept **125**(1-3): 55-59. doi: 10.1016/j.regpep.2004.07.033.

[59] Charles, C.J., Rademaker, M.T., and Richards, A.M. 2006. Apelin-13 induces a biphasic haemodynamic response and hormonal activation in normal conscious sheep. J Endocrinol **189**(3): 701-710. doi: 10.1677/joe.1.06804.

[60] Boucher, J., Masri, B., Daviaud, D., Gesta, S., Guigne, C., Mazzucotelli, A., Castan-Laurell, I., Tack, I., Knibiehler, B., Carpene, C., Audigier, Y., Saulnier-Blache, J.S., and Valet, P. 2005. Apelin, a newly identified adipokine up-regulated by insulin and obesity. Endocrinology **146**(4): 1764-1771. doi: 10.1210/en.2004-1427.

[61] Sorhede Winzell, M., Magnusson, C., and Ahren, B. 2005. The apj receptor is expressed in pancreatic islets and its ligand, apelin, inhibits insulin secretion in mice. Regul Pept **131**(1-3): 12-17. doi: 10.1016/j.regpep.2005.05.004.

[62] Chen, H., Zheng, C., Zhang, X., Li, J., Li, J., Zheng, L., and Huang, K. 2011. Apelin alleviates diabetes-associated endoplasmic reticulum stress in the pancreas of Akita mice. Peptides **32**(8): 1634-1639. doi: 10.1016/j.peptides.2011.06.025.

[63] Yue, P., Jin, H., Aillaud, M., Deng, A.C., Azuma, J., Asagami, T., Kundu, R.K., Reaven, G.M., Quertermous, T., and Tsao, P.S. 2010. Apelin is necessary for the maintenance of insulin sensitivity. Am J Physiol Endocrinol Metab **298**(1): E59-67. doi: 10.1152/ajpendo.00385.2009.

[64] Attane, C., Foussal, C., Le Gonidec, S., Benani, A., Daviaud, D., Wanecq, E., Guzman-Ruiz, R., Dray, C., Bezaire, V., Rancoule, C., Kuba, K., Ruiz-Gayo, M., Levade, T., Penninger, J., Burcelin, R., Penicaud, L., Valet, P., and Castan-Laurell, I. 2012. Apelin treatment increases complete Fatty Acid oxidation, mitochondrial oxidative capacity, and biogenesis in muscle of insulin-resistant mice. Diabetes **61**(2): 310-320. doi: 10.2337/db11-0100.

[65] Higuchi, K., Masaki, T., Gotoh, K., Chiba, S., Katsuragi, I., Tanaka, K., Kakuma, T., and Yoshimatsu, H. 2007. Apelin, an APJ receptor ligand, regulates body adiposity and favors the messenger ribonucleic acid expression of uncoupling proteins in mice. Endocrinology **148**(6): 2690-2697. doi: 10.1210/en.2006-1270.

[66] Brailoiu, G.C., Dun, S.L., Yang, J., Ohsawa, M., Chang, J.K., and Dun, N.J. 2002. Apelin-immunoreactivity in the rat hypothalamus and pituitary. Neurosci Lett **327**(3): 193-197.

[67] Roberts, E.M., Pope, G.R., Newson, M.J., Landgraf, R., Lolait, S.J., and O'Carroll, A.M. 2010. Stimulus-specific neuroendocrine responses to osmotic challenges in apelin receptor knockout mice. J Neuroendocrinol **22**(4): 301-308. doi: 10.1111/j.1365-2826.2010.01968.x.

[68] Taheri, S., Murphy, K., Cohen, M., Sujkovic, E., Kennedy, A., Dhillo, W., Dakin, C., Sajedi, A., Ghatei, M., and Bloom, S. 2002. The effects of centrally administered apelin-13 on food intake, water intake and pituitary hormone release in rats. Biochem Biophys Res Commun **291**(5): 1208-1212. doi: 10.1006/bbrc.2002.6575.

[69] Clarke, K.J., Whitaker, K.W., and Reyes, T.M. 2009. Diminished metabolic responses to centrally-administered apelin-13 in diet-induced obese rats fed a high-fat diet. J Neuroendocrinol **21**(2): 83-89. doi: 10.1111/j.1365-2826.2008.01815.x.

[70] Cox, C.M., D'Agostino, S.L., Miller, M.K., Heimark, R.L., and Krieg, P.A. 2006. Apelin, the ligand for the endothelial G-protein-coupled receptor, APJ, is a potent angiogenic factor required for normal vascular development of the frog embryo. Dev Biol **296**(1): 177-189. doi: 10.1016/j.ydbio.2006.04.452.

[71] Kalin, R.E., Kretz, M.P., Meyer, A.M., Kispert, A., Heppner, F.L., and Brandli, A.W. 2007. Paracrine and autocrine mechanisms of apelin signaling govern embryonic and tumor angiogenesis. Dev Biol **305**(2): 599-614. doi: 10.1016/j.ydbio.2007.03.004.

[72] Picault, F.X., Chaves-Almagro, C., Projetti, F., Prats, H., Masri, B., and Audigier, Y. 2014. Tumour co-expression of apelin and its receptor is the basis of an autocrine loop involved in the growth of colon adenocarcinomas. Eur J Cancer **50**(3): 663-674. doi: 10.1016/j.ejca.2013.11.017.

[73] Choe, H., Farzan, M., Konkel, M., Martin, K., Sun, Y., Marcon, L., Cayabyab, M., Berman, M., Dorf, M.E., Gerard, N., Gerard, C., and Sodroski, J. 1998. The orphan seven-transmembrane receptor apj supports the entry of primary T-cell-line-tropic and dualtropic human immunodeficiency virus type 1. J Virol **72**(7): 6113-6118.

[74] Zou, M.X., Liu, H.Y., Haraguchi, Y., Soda, Y., Tatemoto, K., and Hoshino, H. 2000. . FEBS Lett **473**(1): 15-18.

[75] Newson, M.J., Pope, G.R., Roberts, E.M., Lolait, S.J., and O'Carroll, A.M. 2013. Stress-dependent and gender-specific neuroregulatory roles of the apelin receptor in the hypothalamic-pituitary-adrenal axis response to acute stress. J Endocrinol **216**(1): 99-109. doi: 10.1530/joe-12-0375.

[76] Masri, B., Morin, N., Pedebernade, L., Knibiehler, B., and Audigier, Y. 2006. The apelin receptor is coupled to Gi1 or Gi2 protein and is differentially desensitized by apelin fragments. J Biol Chem **281**(27): 18317-18326. doi: 10.1074/jbc.M600606200.

[77] Kang, Y., Kim, J., Anderson, J.P., Wu, J., Gleim, S.R., Kundu, R.K., McLean, D.L., Kim, J.D., Park, H., Jin, S.W., Hwa, J., Quertermous, T., and Chun, H.J. 2013. Apelin-APJ signaling is a critical regulator of endothelial MEF2 activation in cardiovascular development. Circ Res **113**(1): 22-31. doi: 10.1161/circresaha.113.301324.

[78] Masri, B., Lahlou, H., Mazarguil, H., Knibiehler, B., and Audigier, Y. 2002. Apelin (65-77) activates extracellular signal-regulated kinases via a PTX-sensitive G protein. Biochem Biophys Res Commun **290**(1): 539-545. doi: 10.1006/bbrc.2001.6230.

[79] Lee, D.K., Ferguson, S.S., George, S.R., and O'Dowd, B.F. 2010. The fate of the internalized apelin receptor is determined by different isoforms of apelin mediating differential interaction with beta-arrestin. Biochem Biophys Res Commun **395**(2): 185-189. doi: 10.1016/j.bbrc.2010.03.151.

[80] Evans, N.A., Groarke, D.A., Warrack, J., Greenwood, C.J., Dodgson, K., Milligan, G., and Wilson, S. 2001. Visualizing differences in ligand-induced beta-arrestin-GFP interactions and trafficking between three recently characterized G protein-coupled receptors. J Neurochem **77**(2): 476-485.

[81] El Messari, S., Iturrioz, X., Fassot, C., De Mota, N., Roesch, D., and Llorens-Cortes, C. 2004. Functional dissociation of apelin receptor signaling and endocytosis: implications for the effects of apelin on arterial blood pressure. J Neurochem **90**(6): 1290-1301. doi: 10.1111/j.1471-4159.2004.02591.x.

[82] Zhou, N., Fan, X., Mukhtar, M., Fang, J., Patel, C.A., DuBois, G.C., and Pomerantz, R.J. 2003. Cell-cell fusion and internalization of the CNS-based, HIV-1 co-receptor, APJ. Virology **307**(1): 22-36.

[83] Zhen, E.Y., Higgs, R.E., and Gutierrez, J.A. 2013. Pyroglutamyl apelin-13 identified as the major apelin isoform in human plasma. Anal Biochem **442**(1): 1-9. doi: 10.1016/j.ab.2013.07.006.

[84] Mesmin, C., Fenaille, F., Becher, F., Tabet, J.C., and Ezan, E. 2011. Identification and characterization of apelin peptides in bovine colostrum and milk by liquid chromatography-mass spectrometry. J Proteome Res **10**(11): 5222-5231. doi: 10.1021/pr200725x.

[85] Langelaan, D.N., Bebbington, E.M., Reddy, T., and Rainey, J.K. 2009. Structural insight into G-protein coupled receptor binding by apelin. Biochemistry **48**(3): 537-548. doi: 10.1021/bi801864b.

[86] Langelaan, D.N., and Rainey, J.K. 2009. Headgroup-dependent membrane catalysis of apelin-receptor interactions is likely. J Phys Chem B **113**(30): 10465-10471. doi: 10.1021/jp904562q.

[87] Macaluso, N.J., and Glen, R.C. 2010. Exploring the 'RPRL' motif of apelin-13 through molecular simulation and biological evaluation of cyclic peptide analogues. ChemMedChem **5**(8): 1247-1253. doi: 10.1002/cmdc.201000061.

[88] Macaluso, N.J., Pitkin, S.L., Maguire, J.J., Davenport, A.P., and Glen, R.C. 2011. Discovery of a competitive apelin receptor (APJ) antagonist. ChemMedChem **6**(6): 1017-1023. doi: 10.1002/cmdc.201100069.

[89] Murza, A., Parent, A., Besserer-Offroy, E., Tremblay, H., Karadereye, F., Beaudet, N., Leduc, R., Sarret, P., and Marsault, E. 2012. Elucidation of the structure-activity relationships of apelin: influence of unnatural amino acids on binding, signaling, and plasma stability. ChemMedChem **7**(2): 318-325. doi: 10.1002/cmdc.201100492.

[90] Iturrioz, X., Gerbier, R., Leroux, V., Alvear-Perez, R., Maigret, B., and Llorens-Cortes, C. 2010. By interacting with the C-terminal Phe of apelin, Phe255 and Trp259 in helix VI of the apelin receptor are critical for internalization. J Biol Chem **285**(42): 32627-32637. doi: 10.1074/jbc.M110.127167.

[91] Langelaan, D.N., Reddy, T., Banks, A.W., Dellaire, G., Dupre, D.J., and Rainey, J.K. 2013. Structural features of the apelin receptor N-terminal tail and first transmembrane segment implicated in ligand binding and receptor trafficking. Biochim Biophys Acta **1828**(6): 1471-1483. doi: 10.1016/j.bbamem.2013.02.005.

[92] Deupi, X., and Standfuss, J. 2011. Structural insights into agonist-induced activation of G-protein-coupled receptors. Curr Opin Struct Biol **21**(4): 541-551. doi: 10.1016/j.sbi.2011.06.002.

[93] Palczewski, K., Kumasaka, T., Hori, T., Behnke, C.A., Motoshima, H., Fox, B.A., Le Trong, I., Teller, D.C., Okada, T., Stenkamp, R.E., Yamamoto, M., and Miyano, M. 2000. Crystal structure of rhodopsin: A G protein-coupled receptor. Science **289**(5480): 739-745.

[94] Zhou, N., Zhang, X., Fan, X., Argyris, E., Fang, J., Acheampong, E., DuBois, G.C., and Pomerantz, R.J. 2003. The N-terminal domain of APJ, a CNS-based coreceptor for HIV-1, is essential for its receptor function and coreceptor activity. Virology **317**(1): 84-94.

[95] Conner, M., Hawtin, S.R., Simms, J., Wootten, D., Lawson, Z., Conner, A.C., Parslow, R.A., and Wheatley, M. 2007. Systematic analysis of the entire second extracellular loop of the V(1a) vasopressin receptor: key residues, conserved throughout a G-protein-coupled receptor family, identified. J Biol Chem **282**(24): 17405-17412. doi: 10.1074/jbc.M702151200.

[96] Cherezov, V., Rosenbaum, D.M., Hanson, M.A., Rasmussen, S.G., Thian, F.S., Kobilka, T.S., Choi, H.J., Kuhn, P., Weis, W.I., Kobilka, B.K., and Stevens, R.C. 2007. High-resolution crystal structure of an engineered human beta2-adrenergic G protein-coupled receptor. Science **318**(5854): 1258-1265. doi: 10.1126/science.1150577.

[97] Fraser, C.M. 1989. Site-directed mutagenesis of beta-adrenergic receptors. Identification of conserved cysteine residues that independently affect ligand binding and receptor activation. J Biol Chem **264**(16): 9266-9270.

[98] Warne, T., Serrano-Vega, M.J., Baker, J.G., Moukhametzianov, R., Edwards, P.C., Henderson, R., Leslie, A.G., Tate, C.G., and Schertler, G.F. 2008. Structure of a beta1-adrenergic G-protein-coupled receptor. Nature **454**(7203): 486-491. doi: 10.1038/nature07101.

[99] Panavas, T., Sanders, C., and Butt, T.R. 2009. SUMO fusion technology for enhanced protein production in prokaryotic and eukaryotic expression systems. Methods Mol Biol **497**: 303-317. doi: 10.1007/978-1-59745-566-4_20.

[100] Chien, E.Y., Liu, W., Zhao, Q., Katritch, V., Han, G.W., Hanson, M.A., Shi, L., Newman, A.H., Javitch, J.A., Cherezov, V., and Stevens, R.C. 2010. Structure of the human dopamine D3 receptor in complex with a D2/D3 selective antagonist. Science **330**(6007): 1091-1095. doi: 10.1126/science.1197410.

[101] Wu, B., Chien, E.Y., Mol, C.D., Fenalti, G., Liu, W., Katritch, V., Abagyan, R., Brooun, A., Wells, P., Bi, F.C., Hamel, D.J., Kuhn, P., Handel, T.M., Cherezov, V., and Stevens, R.C. 2010. Structures of the CXCR4 chemokine GPCR with small-molecule and cyclic peptide antagonists. Science **330**(6007): 1066-1071. doi: 10.1126/science.1194396.

[102] Eishingdrelo, H., and Kongsamut, S. 2013. Minireview: Targeting GPCR Activated ERK Pathways for Drug Discovery. Curr Chem Genomics Transl Med **7**: 9-15. doi: 10.2174/2213988501307010009.

[103] Masri, B., Morin, N., Cornu, M., Knibiehler, B., and Audigier, Y. 2004. Apelin (65-77) activates p70 S6 kinase and is mitogenic for umbilical endothelial cells. Faseb j **18**(15): 1909-1911. doi: 10.1096/fj.04-1930fje.

[104] Bai, B., Tang, J., Liu, H., Chen, J., Li, Y., and Song, W. 2008. Apelin-13 induces ERK1/2 but not p38 MAPK activation through coupling of the human apelin receptor to the Gi2 pathway. Acta Biochim Biophys Sin (Shanghai) **40**(4): 311-318.

[105] Ohyama, K., Yamano, Y., Sano, T., Nakagomi, Y., Hamakubo, T., Morishima, I., and Inagami, T. 1995. Disulfide bridges in extracellular domains of angiotensin II receptor type IA. Regul Pept **57**(2): 141-147.

[106] Peeters, M.C., van Westen, G.J., Li, Q., and AP, I.J. 2011. Importance of the extracellular loops in G protein-coupled receptors for ligand recognition and receptor activation. Trends Pharmacol Sci **32**(1): 35-42. doi: 10.1016/j.tips.2010.10.001.

[107] Strange, P.G. 2008. Agonist binding, agonist affinity and agonist efficacy at G protein-coupled receptors. Br J Pharmacol **153**(7): 1353-1363. doi: 10.1038/sj.bjp.0707672.

[108] Han, X., Tachado, S.D., Koziel, H., and Boisvert, W.A. 2012. Leu128(3.43) (l128) and Val247(6.40) (V247) of CXCR1 are critical amino acid residues for g protein coupling and receptor activation. PLoS One **7**(8): e42765. doi: 10.1371/journal.pone.0042765.

[109] Thomas, P., and Smart, T.G. 2005. HEK293 cell line: a vehicle for the expression of recombinant proteins. J Pharmacol Toxicol Methods **51**(3): 187-200. doi: 10.1016/j.vascn.2004.08.014.

[110] Wu, L., Hu, X., Tang, H., Han, Z., and Chen, Y. 2014. Valid application of western blotting. Mol Biol Rep **41**(5): 3517-3520. doi: 10.1007/s11033-014-3215-5.

[111] Pitre, A., Pan, Y., Pruett, S., and Skalli, O. 2007. On the use of ratio standard curves to accurately quantitate relative changes in protein levels by Western blot. Anal Biochem **361**(2): 305-307. doi: 10.1016/j.ab.2006.11.008.

[112] Gingrich, J.C., Davis, D.R., and Nguyen, Q. 2000. Multiplex detection and quantitation of proteins on western blots using fluorescent probes. Biotechniques **29**(3): 636-642.

[113] Moerke, N.J., and Hoffman, G.R. 2011. Development of in-cell Western assays using far-red fluorophores. Curr Protoc Chem Biol **3**(1): 39-52. doi: 10.1002/9780470559277.ch100153.

[114] Lohse, M.J., Nuber, S., and Hoffmann, C. 2012. Fluorescence/bioluminescence resonance energy transfer techniques to study G-protein-coupled receptor activation and signaling. Pharmacol Rev **64**(2): 299-336. doi: 10.1124/pr.110.004309.

[115] Jensen, D.D., Halls, M.L., Murphy, J.E., Canals, M., Cattaruzza, F., Poole, D.P., Lieu, T., Koon, H.W., Pothoulakis, C., and Bunnett, N.W. 2014. Endothelin-converting enzyme-1 and beta-arrestins exert spatiotemporal control of substance P-induced inflammatory signals. J Biol Chem. doi: 10.1074/jbc.M114.578179.

[116] Holmes, K.D., Babwah, A.V., Dale, L.B., Poulter, M.O., and Ferguson, S.S. 2006. Differential regulation of corticotropin releasing factor 1alpha receptor endocytosis and trafficking by beta-arrestins and Rab GTPases. J Neurochem **96**(4): 934-949. doi: 10.1111/j.1471-4159.2005.03603.x.